



**US Army Corps  
of Engineers®**  
Engineer Research and  
Development Center



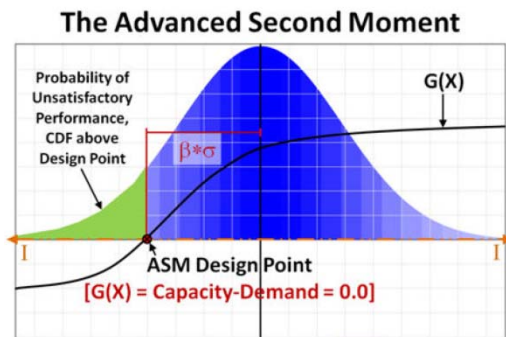
Navigation Systems Research Program

# Simulation and Advanced Second Moment Reliability Analyses of Pile Groups Using CPGA-R

Formulation, User's Guide, and Example Problems

Robert M. Ebeling, Barry C. White, and Moira T. Fong

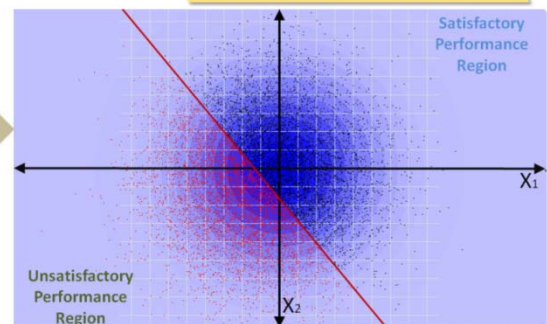
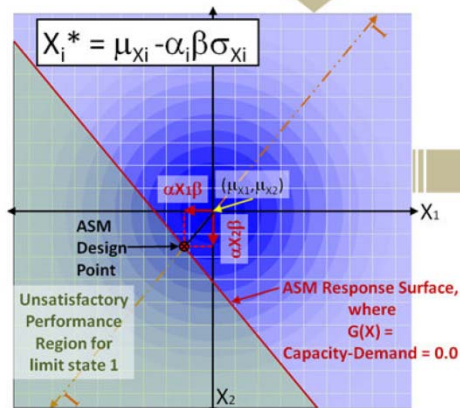
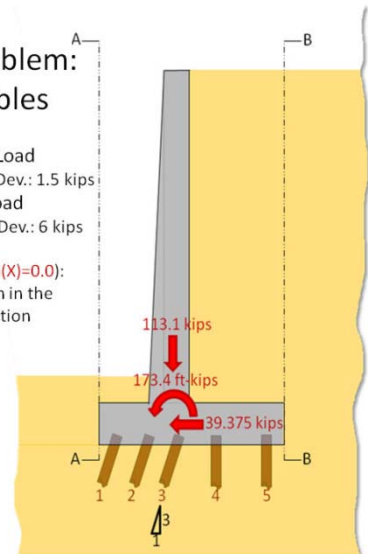
September 2013



Example Problem:  
Two Variables

X1-Horizontal Load  
Mean: 39.375 kips Std.Dev.: 1.5 kips  
X2-Vertical Load  
Mean: 113.1 kips Std.Dev.: 6 kips

Limit state (where  $G(X)=0.0$ ):  
0.25 inch deflection in the  
horizontal direction



Importance Sampling using Latin Hypercube and Based Around The Advanced Second Moment Design Point

**The US Army Engineer Research and Development Center (ERDC)** solves the nation's toughest engineering and environmental challenges. ERDC develops innovative solutions in civil and military engineering, geospatial sciences, water resources, and environmental sciences for the Army, the Department of Defense, civilian agencies, and our nation's public good. Find out more at [www.erdclibrary.army.mil](http://www.erdclibrary.army.mil).

To search for other technical reports published by ERDC, visit the ERDC online library at <http://acwc.sdp.sirsi.net/client/default>.

# **Simulation and Advanced Second Moment Reliability Analyses of Pile Groups Using CPGA-R**

Formulation, User's Guide, and Example Problems

Robert M. Ebeling, Barry C. White, and Moira T. Fong

*Information Technology Laboratory  
US Army Engineer Research and Development Center  
3909 Halls Ferry Road  
Vicksburg, MS 39180-6199*

Final report

Approved for public release; distribution is unlimited.

Prepared for Headquarters, US Army Corps of Engineers  
Washington, DC 20314-1000

Under Work Unit LB182K

## Abstract

More than 50% of the US Army Corps of Engineers' locks and their approach walls have continued past their economic lifetimes. As these structures wear out, they must be retrofitted, replaced, or upgraded with a lock extension. Innovative designs must be considered for Corps hydraulic structures, particularly flexible approach walls, and new tools for evaluating these designs must be developed.

The Computer-Aided Structural Engineering (CASE) computer program CPGA performs basic pile group analyses using Saul's method. It is intended to be a simple program to aid in the rapid pile group analysis/design of the Corps hydraulic structures that are founded on groups of piles. The analysis uses the stiffness method, with the pile cap assumed to be rigid and the piles assumed to be linearly elastic. Soil resistance to pile movement may be included.

Probabilistic data generated during a reliability analysis of Corps hydraulic structures is formally used in risk and reliability engineering for major rehabilitation studies. Reliability studies deal with the demand on a system and the capacity of the system to respond to that demand. Both the demand and capacity can contain uncertainty, so the interaction of demand and capacity also will be uncertain. A reliability index can be determined for the uncertain interaction, and the probability of unsatisfactory performance can be determined from the reliability index.

This report deals with the extension of CPGA to include the generation of probabilistic data and application of risk-based methods to the analysis of the Corps pile group-founded hydraulic structures. The software is named CPGA-R, with the R referring to the new reliability analysis capability. CPGA-R uses both Advanced Second Moment (ASM) and Importance Sampling Simulation reliability analyses techniques.

**DISCLAIMER:** The contents of this report are not to be used for advertising, publication, or promotional purposes. Citation of trade names does not constitute an official endorsement or approval of the use of such commercial products. All product names and trademarks cited are the property of their respective owners. The findings of this report are not to be construed as an official Department of the Army position unless so designated by other authorized documents.

**DESTROY THIS REPORT WHEN NO LONGER NEEDED. DO NOT RETURN IT TO THE ORIGINATOR.**

# Contents

<b>Abstract</b> .....	<b>ii</b>
<b>Figures and Tables</b> .....	<b>v</b>
<b>Preface</b> .....	<b>ix</b>
<b>1 Introduction</b> .....	<b>1</b>
1.1 CPGA history .....	1
1.2 Revisiting RCPGA .....	6
1.3 Overview.....	6
1.4 Report contents .....	10
<b>2 Reliability Methods</b> .....	<b>12</b>
2.1 Variable space .....	12
2.2 Performance function.....	14
2.3 Probability of unsatisfactory performance .....	17
2.4 Monte Carlo and Latin Hypercube simulations.....	17
2.5 Advanced Second Moment (ASM) .....	21
2.5.1 ASM for uncorrelated, normal distributions .....	21
2.5.2 Dealing with non-normal distributions.....	26
2.5.3 Correlated random variables.....	27
2.5.4 ASM algorithm.....	28
2.5.5 ASM caveats.....	29
2.6 Importance Sampling.....	32
2.7 Specific CPGA information for running a reliability analysis .....	34
2.7.1 Introduction .....	34
2.7.2 Pile stiffness .....	36
2.7.3 Pile strength performance limits .....	37
<b>3 CPGA-R Graphical User Interface (GUI)</b> .....	<b>41</b>
3.1 Revisiting the CPGA GUI .....	41
3.2 GUI additions to support CPGA reliability analysis .....	43
3.2.1 Reliability Variable Input.....	46
3.2.2 Variable Correlation .....	51
3.2.3 Assign Limit States.....	52
3.3 GUI additions for saving and restoring reliability information .....	53
3.4 Performing a reliability run.....	55
<b>4 Testing CPGA-R</b> .....	<b>57</b>
4.1 CPGA-R.....	57
4.1.1 CPGA base input file .....	57
4.1.2 Reliability Test Run 1.....	63
4.1.3 Reliability Test Run 2.....	65

---

4.1.4	Reliability Test Run 3 .....	66
4.1.5	Reliability Test Run 4 .....	68
4.1.6	Visualizing ASM and simulation method results (Test Runs 5, 6, and 7).....	69
4.1.7	Difference in Latin Hypercube and Importance Sampling (Test Runs 8 and 9).....	74
4.1.8	Influence of correlating variables in CPGA-R.....	77
4.2	Understanding CPGA-R output formats.....	81
4.2.1	Advanced Second Moment (ASM) output.....	81
4.2.2	Latin Hypercube output and Importance Sampling with Latin Hypercube output.....	85
4.3	Inconsistencies for ASM calculations in 1997 RCPGA .....	86
<b>5</b>	<b>Summary, Conclusions, and Future Research .....</b>	<b>94</b>
5.1	Summary and conclusions.....	94
5.2	Future research .....	95
	<b>References.....</b>	<b>97</b>
	<b>Appendix A: Skin Friction and Tip Capacities of Piles .....</b>	<b>99</b>
	<b>Appendix B: CPGA-R Probability Density Function (PDF) Distributions and Their Properties .....</b>	<b>114</b>
	<b>Appendix C: .PGR File Format .....</b>	<b>119</b>
	<b>Report Documentation Page</b>	

# Figures and Tables

## Figures

Figure 1.1. Design of the Red River Lock and Dam 1 (USACE 1991). The Red River runs through Louisiana. ....	2
Figure 1.2. Pile forest at Red River Lock and Dam 1 (USACE 1991). ....	2
Figure 1.3. Pile layout for spillway at Melvin Price Lock and Dam in St. Louis, Missouri. ....	3
Figure 1.4. Lock and Dam 3 guide wall design (Mississippi River, near Red Wing, Minnesota). ....	3
Figure 1.5. Site information (geometry and loads) for a two-variable reliability analysis. ....	7
Figure 1.6. Finding an ASM design point (in variables $X_1$ and $X_2$ space). ....	9
Figure 1.7. Simulation runs determine the regions and probabilities of unsatisfactory performance. ....	10
Figure 2.1. 1D variable space with a normal PDF distribution and 2D variable space with normal PDF distributions for each variable axis. ....	13
Figure 2.2. (a) Untransformed and (b) transformed (standard normal) variable axes. ....	13
Figure 2.3. Capacity vs. demand related to the probability of unsatisfactory performance (after Nowak and Collins 2000, 2013). ....	15
Figure 2.4. A performance function for a single variable axis (untransformed and transformed). ....	15
Figure 2.5. A complex two-variable, $G(V)$ , function. ....	16
Figure 2.6. 2D variable space for Monte Carlo simulation. ....	18
Figure 2.7. Monte Carlo simulation samples for the previous 2D variable space evaluated with the performance function (black samples have $G(X) > 0.0$ , and red samples have $G(X) < 0.0$ ). ....	19
Figure 2.8. Creating a set of equal area bins in standard normal space. ....	19
Figure 2.9. Partitioning a 2D variable space for a Latin Hypercube selection of samples for two variables with normal distributions. ....	20
Figure 2.10. Using the normally distributed regions to assign samples according to the Latin Hypercube method for generating samples. ....	21
Figure 2.11. Using the reliability index ( $\beta$ ) to determine the probability and cumulative probability for an event. ....	23
Figure 2.12. In a two-variable space with a linear response surface, $\beta$ is the distance from the origin to a design point on the surface. ....	24
Figure 2.13. The directional cosines $\alpha$ combine to form the unit vector directed from the origin to the design point. ....	24
Figure 2.14. Finding the position of equivalent cumulative probability for a normal distribution as from a non-normal distribution (after Ang and Tang 1984). ....	27
Figure 2.15. Combining limit states creates a nonlinear ASM response surface. ....	30
Figure 2.16. (a and b) Two response surfaces, with Latin Hypercube samples; each have a $P_U < 0.5$ , but (c) combining the two creates $P_U > 0.5$ . ....	31

Figure 2.17. For sample $X_i$ , the distance to the original mean and the distribution mean can be determined and the probabilities computed. ....	32
Figure 2.18. An example of Importance Sampling giving better results than sampling about the original distribution. ....	35
Figure 2.19. The sampling distribution is centered at the ASM design point on the response surface. ....	35
Figure 3.1. Illustration of the new 3D input viewing features of CPGA-R. ....	42
Figure 3.2. The Pile Information addition to the CPGA-R GUI. ....	44
Figure 3.3. The CPGA-R window (with reliability input). ....	45
Figure 3.4. The Set Parameters menu. ....	45
Figure 3.5. The Reliability Input window. ....	45
Figure 3.6. The Select Piles for Assigning Variable Properties window for creating groups of pile variables. ....	48
Figure 3.7. Using the left mouse click-drag operation to select multiple piles. ....	48
Figure 3.8. Zooming to aid in the selection process. ....	49
Figure 3.9. The Selected Pile Variable Definition window. ....	50
Figure 3.10. Chosen properties and their distribution inputs. ....	51
Figure 3.11. Variables created with the selected piles. ....	51
Figure 3.12. The Assign Limit States window, with two limit states selected. ....	52
Figure 3.13. Selecting multiple piles for limit state assignment. ....	54
Figure 3.14. Setting the limit state for selected piles. ....	54
Figure 3.15. Updating the individual piles. ....	55
Figure 3.16. The reliability file options from the CPGA-R main menu. ....	55
Figure 3.17. CPGA-R Analyze options (with reliability options). ....	56
Figure 3.18. CPGA-R Reliability Output window. ....	56
Figure 4.1. Example problem of retaining wall on piles (after Hrennikoff 1950). ....	58
Figure 4.2. A simplified model of the Hrennikoff example. ....	59
Figure 4.3. Input and output details from the RCPGA Example1 analysis made by Ayyub et al. (1997). ....	61
Figure 4.4. Example 1 CPGA problem (after Ayyub et al. 1997). ....	61
Figure 4.5. Run 1 probabilistic variable input. ....	63
Figure 4.6. Run 1 limit state input. ....	64
Figure 4.7. Run 2 probabilistic variable input. ....	65
Figure 4.8. Run 2 limit state input. ....	66
Figure 4.9. Run 3 probabilistic variable input. ....	67
Figure 4.10. Run 3 limit state input. ....	67
Figure 4.11. Run 4 probabilistic variable input. ....	68
Figure 4.12. Run 4 limit state input. ....	69
Figure 4.13. Runs 5, 6, and 7 probabilistic variable input. ....	70
Figure 4.14. Run 5 limit state input. ....	70
Figure 4.15. Distribution of samples and results for Run 5 (using Latin Hypercube and Importance Sampling). ....	71



Figure 4.16. Run 6 limit state input.....	72
Figure 4.17. Distribution of samples and results for Run 6 (using Latin Hypercube and Importance Sampling). .....	72
Figure 4.18. Run 7 limit state input.....	73
Figure 4.19. Distribution of samples and results for Run 7 (using Latin Hypercube and Importance Sampling). .....	73
Figure 4.20. Runs 8 and 9 probabilistic variable input. ....	75
Figure 4.21. Runs 8 and 9 limit state input.....	75
Figure 4.22. Distribution of 10,000 samples and results for Runs 8 and 9 (using Latin Hypercube and Importance Sampling). .....	76
Figure 4.23. Distribution of 1,000 samples and results for Runs 8 and 9 (using Latin Hypercube and Importance Sampling). .....	76
Figure 4.24. Correlated variable input for Run 7 variables and limit states with a correlation factor of 0.85.....	77
Figure 4.25. Results from the run with a correlation factor of 0.85. ....	78
Figure 4.26. The spread and results of the simulation runs with a correlation factor of 0.85. ....	78
Figure 4.27. Using an inverse correlation factor (-0.85). ....	79
Figure 4.28. Results given an inverse correlation factor (-0.85). ....	79
Figure 4.29. The spread and results of the simulation runs with an inverse correlation factor (-0.85). ....	80
Figure A.1. Bearing capacity factor. ....	103
Figure A.2. (a) Values of $\alpha$ vs. undrained shear strength and (b) values of $\alpha_1\alpha_2$ applicable for long piles.....	104
Figure A.3. Unit side resistance for piles in sand vs. relative length (Mosher 1984). ....	111
Figure A.4. Unit tip resistance for piles in sand vs. relative length (Mosher 1984). ....	112
Figure B.1. Normal Distribution ( $\mu = -5, \sigma = 1$ ). ....	114
Figure B.2 Bounded Normal Distribution ( $\mu = -5, \sigma = 1, a = -6, b = -3$ ). ....	115
Figure B.3. Log-Normal Distribution ( $\mu = 5, \sigma = 3$ ). ....	116
Figure B.4. Bounded Log-Normal Distribution ( $\mu=5, \sigma=3, a=1, b=8$ ).....	116
Figure B.5. Uniform Distribution ( $a = 1, b = 5.5$ ). ....	117
Figure B.6. Triangular Distribution ( $a = 1, b = 10, c = 7$ ).....	117
Figure B.7. Right Triangular Distribution ( $a = 1, b = 10, c = 10$ ). ....	118
Figure B.8. Right Triangular Distribution ( $a = 1, b = 10, c = 1$ ). ....	118

## Tables

Table 2.1. Reliability index ( $\beta$ ) and probability of unsatisfactory performance ( $P_U$ ). ....	23
Table 4.1. Example input file. ....	62
Table 4.2. Results for example problem test runs. ....	64
Table 4.3. Examples of correlating pairs of variables and the effects on the probability of unsatisfactory performance. ....	80
Table 4.4. Results of CPGA-R with the Example 1 input from the RCPGA manual. ....	81

---

Table 4.5. Results of CPGA-R with Example 1 input for a Latin Hypercube run.....	86
Table 4.6. Results of CPGA-R with Example 1 input for an Importance Sampling run.....	86
Table 4.7. Reliability input for variables in the RCPGA software. ....	87
Table 4.8. Output from RCPGA ASM method.....	87
Table 4.9. Results of CPGA-R with Example 1 input from the RCPGA manual, modified to remove the pile translation variables. ....	90
Table A.1. Values of $\delta$ . ....	100
Table A.2. Values of $K$ . ....	101
Table A.3. Common values for corrected $K$ .....	101
Table A.4. S case shear strength. ....	105

## Preface

More than 50% of the Corps' locks and their approach walls have continued past their economic lifetimes. As these structures wear out, they must be retrofitted, replaced, or upgraded with a lock extension. Energy-absorbing flexible approach wall structural systems are being considered. They are less expensive to replace and provide extra protection for barge train traffic and personnel.

This technical report describes engineering methodologies for analyzing flexible approach wall systems founded on groups of piles and subjected to barge train impact loading. The computer program CPGA can perform an analysis/design of pile group-founded structures, including hydraulic ones that might experience impact loads tens of feet above the mudline. It can determine if a pile-founded hydraulic structure gives satisfactory performance. However, there is always some uncertainty in the demand and capacity of these structures. There are several reliability methodologies that can be used to compute the probability of unsatisfactory performance, given a method for determining unsatisfactory performance and with formal consideration of uncertainties in the demand and capacity of the structure.

This report introduces reliability methods and deals with an extension of CPGA to include the generation of probabilistic data and application of risk-based methods to the analysis of the Corps pile group-founded hydraulic structures. The software is called CPGA-R, with the R referring to the new reliability analysis capability. Both Advanced Second Moment (ASM) and Importance Sampling Simulation reliability analyses techniques are implemented within the program.

This report was authorized by Headquarters, US Army Corps of Engineers (HQUSACE), and was written from July to December 2012. It was published under the Navigation Systems Research Program, Work Unit "Flexible Approach Walls." At the time of publication, Jim Walker was the HQUSACE Navigation Business Line Manager. Funding to develop CPGA-R was provided by Reliability Model for Major Rehabilitation. Anjana Chudgar was the HQ Lead when it was initiated in FY12, and Richard Ludwitzke was Lead at the time of publication.

The Program Manager for the Navigation Systems Research Program was Charles Wiggins, Coastal and Hydraulics Laboratory (CHL), US Army Engineer Research and Development Center (ERDC). Jeff Lillycrop was Technical Director. The research was led by Dr. Robert M. Ebeling, Information Technology Laboratory (ITL), under the general supervision of Dr. Reed L. Mosher, Director, ITL; Dr. Kevin M. Barry, Acting Deputy Director, ITL; and Dr. Robert M. Wallace, Chief, Engineering and Informatic Systems Division (EISD), ITL. Dr. Ebeling was Principal Investigator of the “Flexible Approach Walls” work unit.

This report was written by Dr. Ebeling, Barry C. White, and Moira T. Fong, all of ITL. White and Fong are with the Computational Analysis Branch (CAB), of which Dr. Kevin Abraham was Acting Chief.

At the time of publication, COL Kevin J. Wilson was Commander, ERDC, and Dr. Jeffery P. Holland was Director.

# 1 Introduction

More than 50% of the US Army Corps of Engineers' (USACE) locks and approach walls have exceeded their economic lifetimes and, as these structures wear, they must be retrofitted, replaced, or upgraded with a lock extension. Energy-absorbing, flexible approach wall structural systems are being considered. The next-generation flexible structures are less expensive to replace and provide extra protection for barge train traffic and personnel.

This report describes engineering methodologies for analyzing flexible approach wall systems founded on groups of piles and subjected to barge train impact loading. The computer program CPGA can perform an analysis/design of pile group-founded structures, including hydraulic structures that might have impact loads applied tens of feet above the mudline. CPGA can determine if a pile-founded hydraulic structure gives satisfactory performance. However, there is always some uncertainty in the demand and capacity of these structures. Several reliability methodologies can compute the probability of unsatisfactory performance, given a method for determining unsatisfactory performance and formal consideration of uncertainties in the demand and capacity of the structure.

This report introduces reliability methods and deals with the extension of CPGA to include the generation of probabilistic data and application of risk-based methods to the analysis of the Corps pile group-founded hydraulic structures. The software is named CPGA-R, with the R referring to the new reliability analysis capability. CPGA-R uses both Advanced Second Moment (ASM) and Importance Sampling Simulation reliability analyses techniques.

## 1.1 CPGA history

Structural systems founded on pile groups are common features at Corps dams (Figures 1.1 and 1.2), spillways (Figure 1.3), and navigation structures (e.g., locks and upstream and downstream approach walls, as shown in Figure 1.4). The sheer number of piles used on dam and spillway projects can make the piles seem like an underground forest. This forest is the substructure that supports the hydraulic structure above.

A pile group founded on soil, or a bent/structural deck system that is supported above the mudline, transfers the load (e.g., due to barge impact) from its cap into the ground as a part of a substructural foundation system.

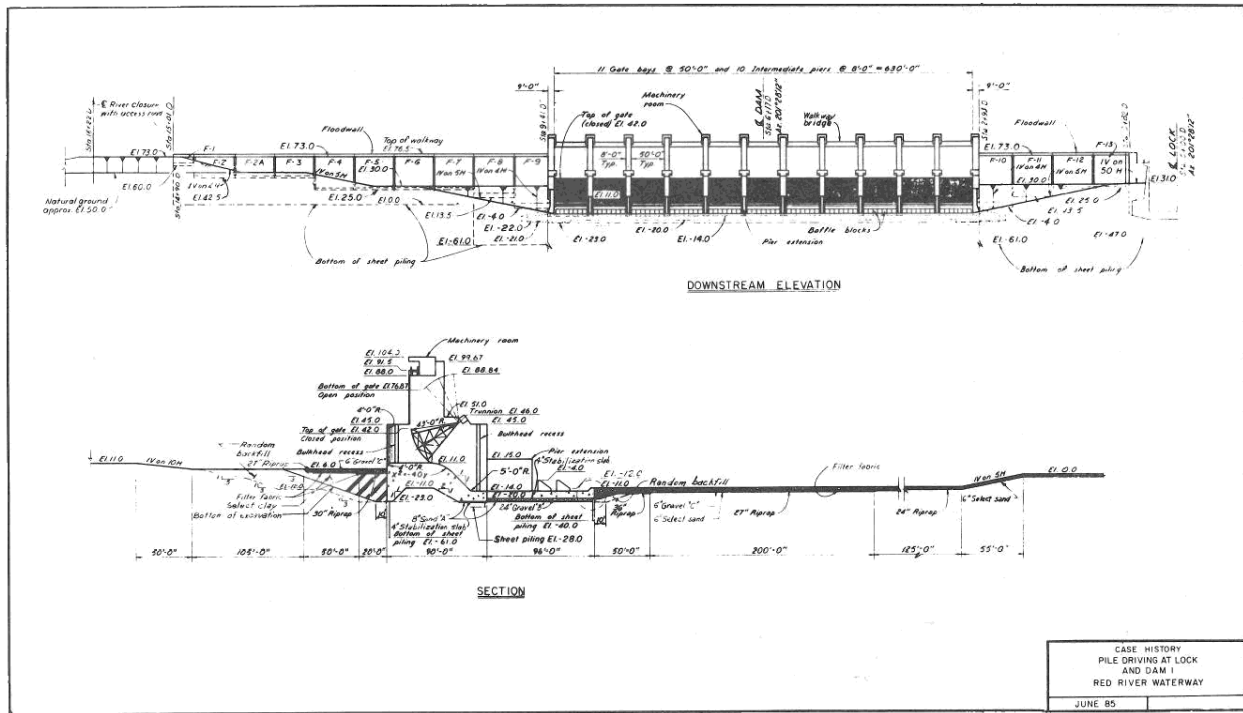


Figure 1.1. Design of the Red River Lock and Dam 1 (USACE 1991). The Red River runs through Louisiana.

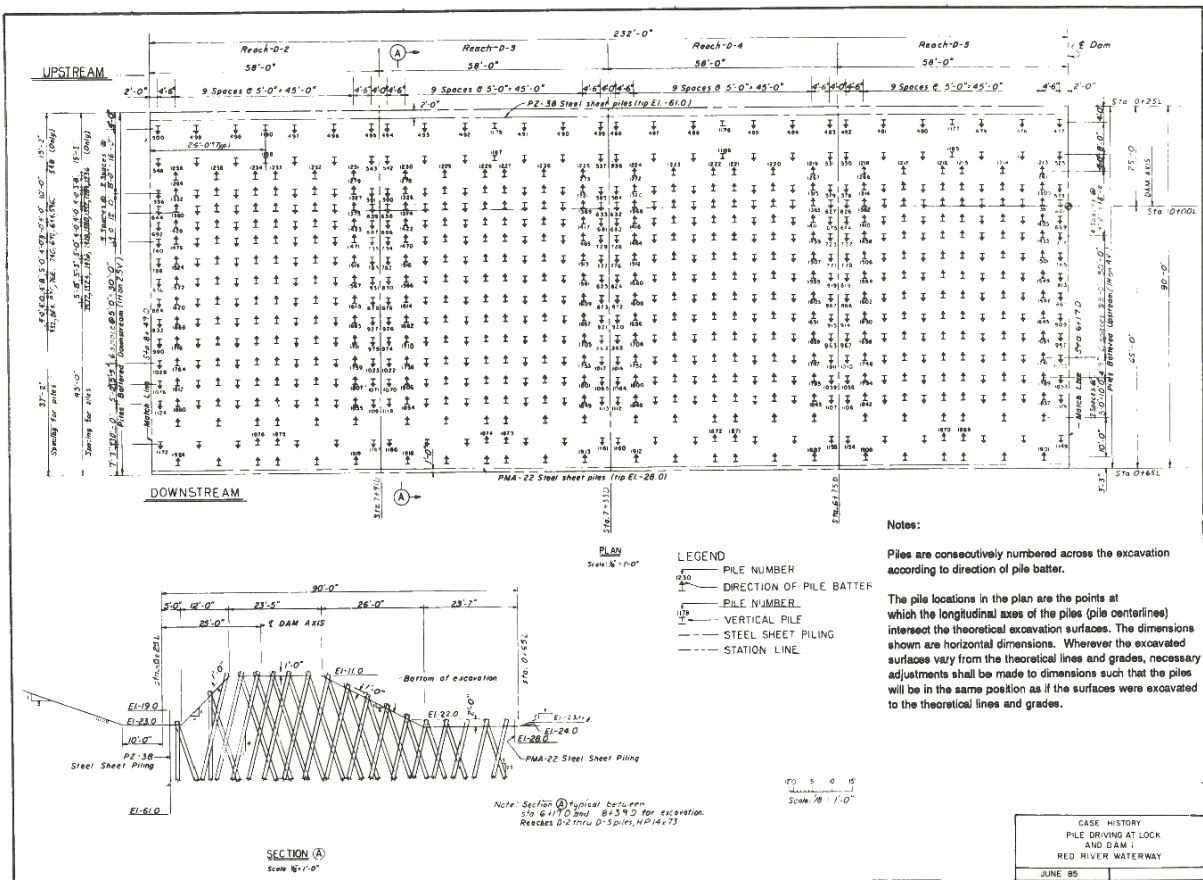


Figure 1.2. Pile forest at Red River Lock and Dam 1 (USACE 1991).



Figure 1.3. Pile layout for spillway at Melvin Price Lock and Dam in St. Louis, Missouri.



Figure 1.4. Lock and Dam 3 guide wall design (Mississippi River, near Red Wing, Minnesota).

Hartman et al. (1989) developed CPGA for assessing pile groups under user-defined loads and moments applied to the pile cap (or bent). CPGA can provide a strength evaluation of a pile foundation that includes both the individual piles and their rigid cap. The pile group cap is assumed to be nondeformable (i.e., rigid or inflexible). Each pile is represented by the calculated stiffness coefficients (Saul 1968). The stiffness coefficients of all piles are used to compose the stiffness matrix for the user-specified total pile group model. Pile cap displacements are calculated by multiplying the inverse of the pile group stiffness matrix by the set of user-specified applied loads. The user-specified static loads and/or moments are applied at the user-defined origin for this structure. CPGA calculates the equilibrium of forces by transforming the deformations of each pile into forces and moments acting at the pile top, then transforming those forces to the origin, and summing all the pile forces at the user-defined origin to match the load. The displacement of each pile head can be determined from the pile cap displacement. The force acting on each pile is equal to the pile stiffness multiplied by the pile head displacement. To determine unsatisfactory performance, the resultant forces can be compared to the user-defined allowable loads. To determine failure of the pile, axial loads and combined bending factors are identified at each pile.

Reliability studies deal with the demand on a system and the capacity of the system to respond to that demand. Both the demand and the capacity can be uncertain, therefore the interaction of demand and capacity also will be uncertain. A reliability index can be determined for this uncertain interaction, and the probability of unsatisfactory performance can be determined from this reliability index. Unsatisfactory performance is not only a catastrophic failure, but also any unacceptable deflection between expected and observed performance (Baecher and Christian 2003).

Limit states define the performance of a structural system. When a system exceeds a limit state, it has unsatisfactory performance. For instance, if a lock wall is moved too far from its initial, configured position, the moving parts connected to that lock wall (i.e., gates) might not be able to travel or align properly.

The limit states for CPGA can include the axial loads and bending factors introduced at each pile due to a load applied to a pile cap or due to pile cap displacement. The axial loads consider soil failures due to plunging or pull-out of the pile, depending on the direction of axial loading of the pile.



The combined bending and axial compression on the pile can lead to failure of the connection of a pile to the pile cap or hinging of the pile (e.g., near the mudline).

Reliability studies are performed to determine the probability of unsatisfactory performance ( $P_U$ ) of a structural system for a limit state or limit states affecting system performance. The reliability of the system is defined as the complement of the probability of unsatisfactory performance ( $1-P_U$ ) and is the probability of proper or satisfactory performance during which the structure behaves safely.

A 1991 Corps engineering manual (EM) discusses displacement limitations at the pile cap for proper operations at locks and dams. To maintain proper operation and integrity of the structure, the horizontal and vertical displacements resulting from applied loads should be limited (USACE 1991). For locks and dams, experience has shown that vertical deflections of 1/4 in. and lateral deflections of 1/4 to 1/2 in. represent long-term movements, although operational requirements might dictate tighter restrictions on deformations. These limitations should be maintained in the calculated pile head movements. The displacement guidance in the Corps EM needs to be adapted for use with next-generation, flexible approach walls. Specifically, barge train impact loadings of the impact beam or deck can occur tens of feet above the pile-to-soil foundation interface. The additional deflections that occur in these piles, where the pile extends above the ground surface, will need to be accounted for in the displacement criteria for flexible approach walls.

Published in 1997 was a US Army Engineer Waterways Experiment Station technical report (TR) about how to perform, using CPGA, a reliability study of a pile-based navigations structure. The TR outlined the structure of RCPGA, a software package for performing a reliability study of a CPGA model (Ayyub et al. 1997). It also defined the limits states required for the reliability study and methods for transforming distributions and correlated variables. The software that was to accompany the report was not released to the Computer-Aided Structural Engineering (CASE) library, but the results of runs made with the program were in the report. The results were extended in this report, and relevant sections of the 1997 report have been included.

At the beginning of this investigation, the goals were to include reliability methods for CPGA input models and to supply a set of routines that would be portable and easy to use for reliability studies relating to new and existing Corps engineering software such as programs in the CASE library.

CPGA does not consider the flexibility of a pile cap or the nonlinearity of soil behavior. This is especially true for pile shadowing, which is the result of pile forces acting through the soil to affect another pile in close proximity (as much as 8 pile diameters) (Ebeling et al. 2012).

## 1.2 Revisiting RCPGA

Ayyub et al. (1997) expanded CPGA to perform reliability analyses of Corps hydraulic structures (e.g., locks and dams), creating the software RCPGA. But RCPGA was not finalized nor added to the CASE library. Due to Corps district needs, this reliability capability has been reintroduced as a result of this new effort. The Ayyub et al. (1997) report served as a basis for the formulation. The authors of this report developed a set of software routines that uses the reliability formulations discussed in this report and implemented them with respect to the CPGA program. Ayyub et al. (1997) is the basis for this research and development effort. At the request of Headquarters, US Army Corps of Engineers (HQUSACE), the reliability formulation and numerical procedures developed were designed to be portable for use in new and existing Corps engineering applications such as CASE programs. This required additional research of reliability methods and an expansion of the procedure in Ayyub et al. (1997).

## 1.3 Overview

Reliability studies deal with the demand on a system and the capacity of the system to respond to that demand. Both the demand and the capacity can be uncertain, therefore the interaction of demand and capacity also will be uncertain. A reliability index can be determined for this uncertain interaction, and the probability of unsatisfactory performance can be determined from this reliability index. Keep in mind, unsatisfactory performance is not only a catastrophic failure resulting in the formation of a plastic hinge within the pile or at the pile-to-cap connection, but also is any unacceptable, excessive deflection of the pile cap.

Figure 1.5 shows a structure where two variables ( $X1$  and  $X2$ ) are introduced that vary the demand on the system. A single limit state is discussed in the figure, but the program will look for limit states for each pile as well as the specified limits at the pile cap. In fact, each component of the pile cap displacement can have a limitation for a reliability analysis.

## Example Problem: Two Variables

X1-Horizontal Load  
Mean: 39.375 kips Std.Dev.: 1.5 kips

X2-Vertical Load  
Mean: 113.1 kips Std.Dev.: 6 kips

Limit state (where  $G(X)=0.0$ ):  
0.25 inch deflection in the  
horizontal direction

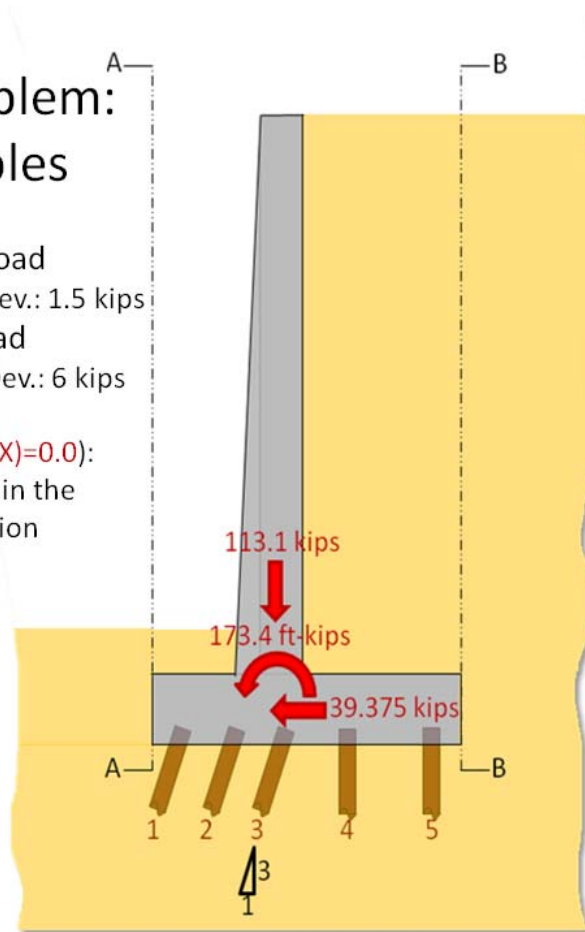


Figure 1.5. Site information (geometry and loads) for a two-variable reliability analysis.

The limit states for a pile group using CPGA-R include the axial loads and combined bending factors introduced at each pile for a load applied to a pile cap. The axial load factor for an individual pile considers soil failure due to plunging or pull-out of the pile. The combined bending and axial compression on the pile can lead to a structural failure anywhere within a pile. It is common for such a failure to occur at the pile's connection to its cap or at the hinging of the pile at the mudline.

The possible variables of the CPGA-R program are numerous and include the pile positions, angles, and batter; pile properties; pile design load strengths; unsupported buckling load calculation; soil modulus values; and loads acting on the pile structure. These variables are defined by their mean values and standard deviations along with a distribution type (e.g., normal, lognormal, triangular, and uniform). Uncertainties in all these variables are assessed by CPGA-R, and for all the user-specified limit states, to compute the probability of unsatisfactory performance ( $P_U$ ) of the structural system

for single or multiple limit states affecting system performance. It has been observed that multiple limit states can have a nonlinear additive effect on the determination of the value for the probability of unsatisfactory performance, which is an area measure, and must be considered accordingly.

Two reliability methods are Advanced Second Moment (ASM) and Importance Sampling Simulation.

ASM is a more traditional method used to estimate the probability of unsatisfactory performance ( $P_U$ ) by employing a numerical procedure to find the distance to the closest response surface to the mean values  $G(X)$ , defined as Capacity – Demand = 0, given by a statistical coefficient ( $\beta$ ), which is used to compute the value for  $P_U$  (Figure 1.6).  $\beta$  is the number of standard deviations the response surface is from the mean (i.e., centered in uniform normal distribution space) of all of the variables. In summary, the closest of the multiple limit state surfaces controls the value of  $\beta$  and, thus, the computed value for  $P_U$ . This value is accurate for a single, linear response state, but provides only an approximation for multiple limit states that combine to form a nonlinear response surface. For CPGA-R, most limits states are linear.

The Importance Sampling Simulation method is a more recent development. It uses a Latin Hypercube procedure to more accurately compute  $P_U$ , especially for cases involving nonlinear and/or multiple response surfaces. For each of the thousands of simulations, the Latin Hypercube method generates a CPGA-R input file with specific random values from each variable's distribution, assigned to the user-defined variables, and a CPGA-R analysis is performed on the resulting file. The simulation method computes  $P_U$  as equal to the number of simulations resulting in unsatisfactory performance (i.e.,  $G(X)$  of *Capacity – Demand*  $\leq 0.0$ ) divided by the total number of simulations (Figure 1.7). Importance Sampling takes weighted simulations about a point, using a normal distribution, closer to the response surface. The weighting of the simulation restores the probabilities of the original distributions, so Importance Sampling gives more accurate results with fewer simulation runs. The ASM method is used to provide a point at  $\beta$  distance from the actual mean, and this point acts as the mean for the weighted simulation distribution.

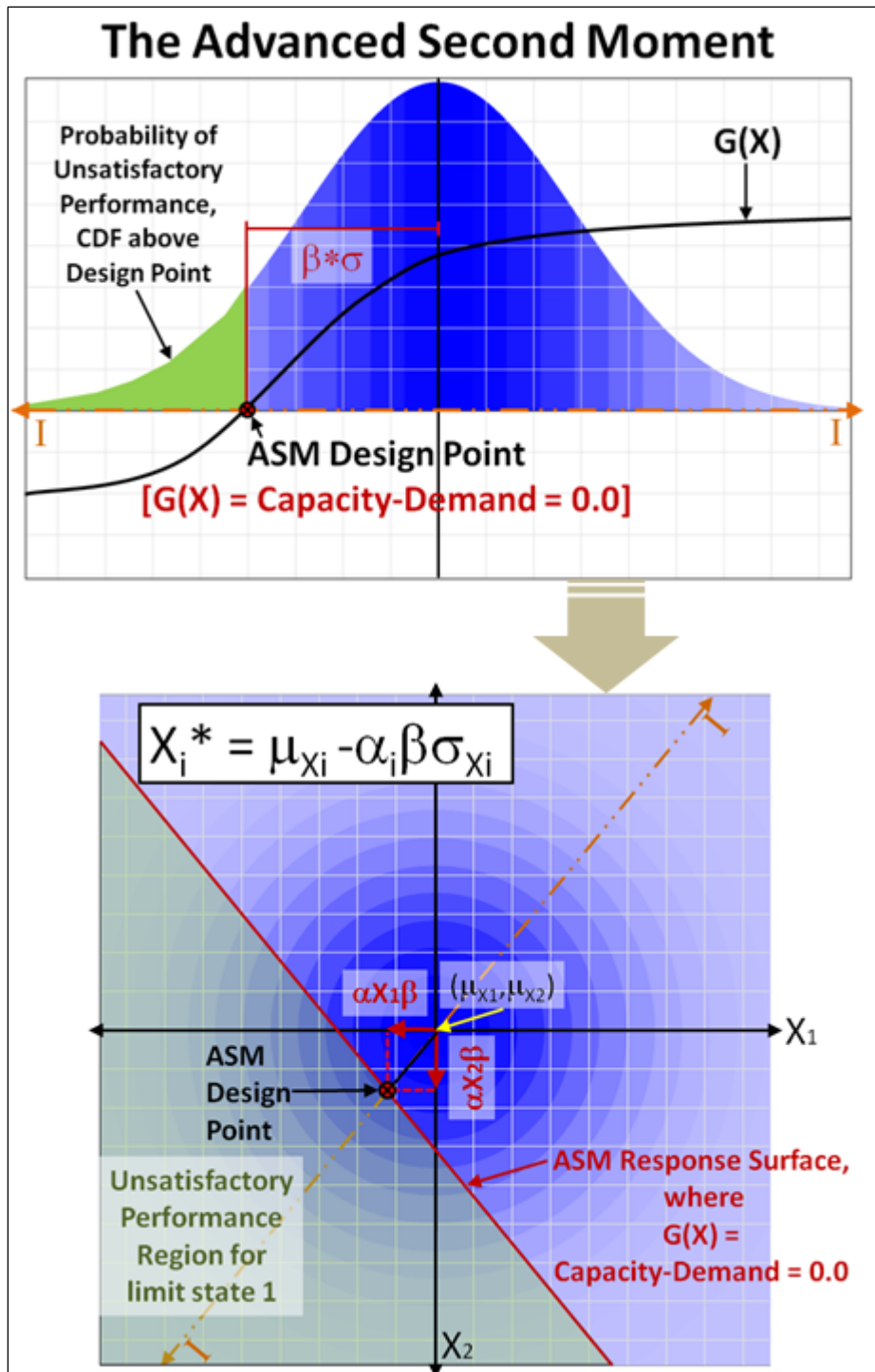


Figure 1.6. Finding an ASM design point (in variables X1 and X2 space).

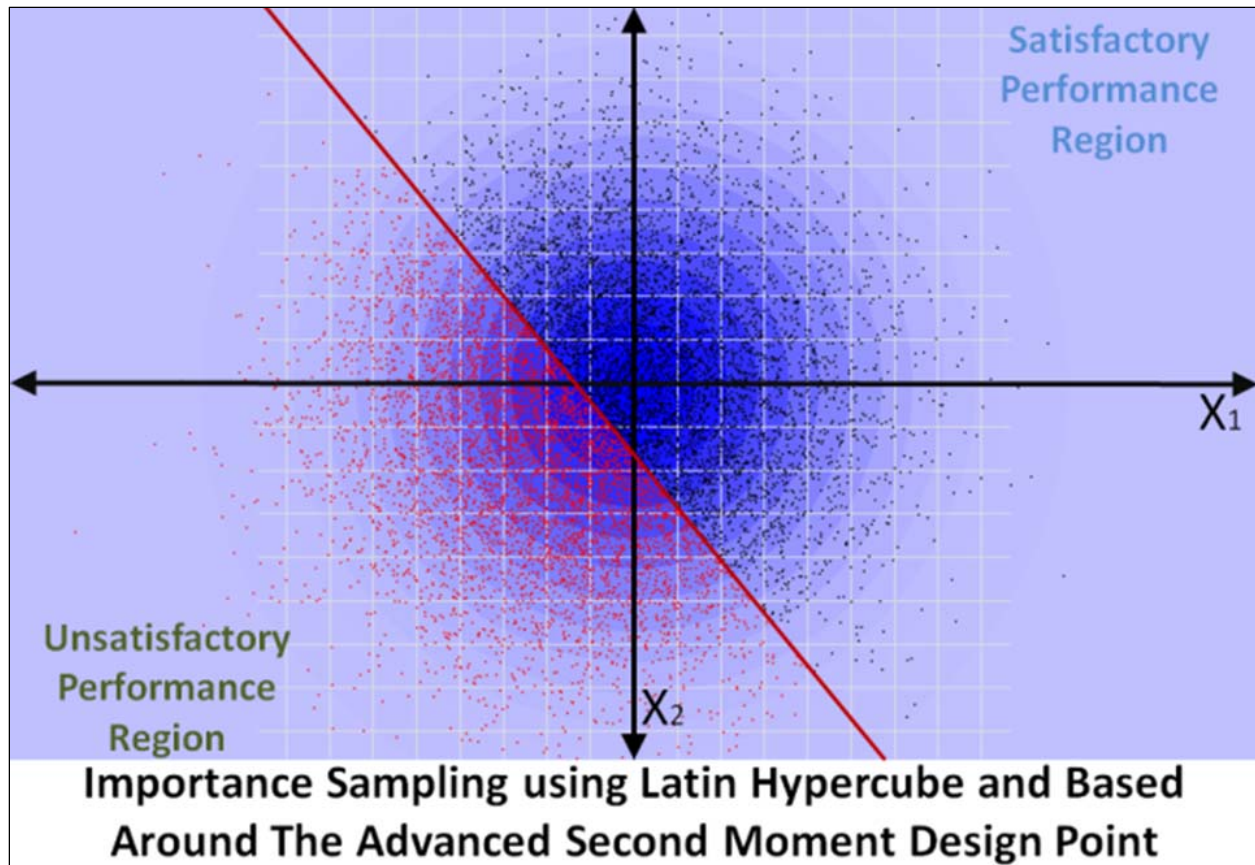


Figure 1.7. Simulation runs determine the regions and probabilities of unsatisfactory performance.

Notice that the multidimensional problem (2D case in Figure 1.6) has each axis normalized with an equivalent normal distribution so that the mean is at the origin and a standard deviation for a normal distribution is the unit distance. Given this condition, any line that passes through the origin, such as section I-I, follows a normal distribution and, given a distance from the origin ( $\beta$ ), the probability of unsatisfactory performance is the same. This is implied by the concentric bands of blue in the 2D example problem of Figures 1.6 and 1.7. These concentric bands reflect a normal distribution that is more commonly presented in the section I-I cut in the top image of Figure 1.6.

#### 1.4 Report contents

- Chapter 2 discusses simulation methods and the ASM formulation.
- Chapter 3 provides an overview of the CPGA-R graphical user interface (GUI).
- Chapter 4 compares CPGA-R results with those first presented in Ayyub et al. (1997) for example problems originally discussed by

Ayyub. Other example problems to highlight key findings also are presented and discussed.

- Chapter 5 features the summary, conclusions, and future research.
- Appendix A summarizes the calculation of skin friction and tip capacities of piles. These parameters have a large bearing on the individual capacity of piles.
- Appendix B discusses the probability density function (PDF) distributions used by CPGA-R and their properties. This discussion covers how the distributions are defined and the resulting probabilities are computed.
- Appendix C contains the specification of the pile group reliability file, a file that has an extension of .PGR.

## 2 Reliability Methods

### 2.1 Variable space

All reliability methods depend on a carefully constructed set of data that can vary and have implications on the performance of a system being studied. For the method discussed in this chapter, these data often differ according to a normal statistical distribution (e.g., pile positions possess an average center relative to the designated pile layout plan positions, but typically deviate during placement according to a normal distribution with a constant standard deviation). The normal distribution for an example using two independent variables is shown in Figure 2.1. If these two variables are not correlated, they are orthogonal and can be joined to form a multidimensional vector space in which each variable forms a different coordinate axis and, therefore, a direction vector. This state variable space,  $\bar{v}$ , can be changed with an affine<sup>1</sup> transformation so that the mean values for each variable are at the origin of the space and the unit distance is the standard deviation for each variable, describing the vector space  $\bar{x}$ , as shown in Figure 2.2. Any point in this vector space can be described by providing a value on each axis to form the vector  $\vec{X}$ , with one value for each variable.

The transformation of the normally distributed data for Axis 1 in the  $\bar{x}$  vector space is described as:

$$X_I = \frac{(v_I - \mu_{v_I})}{\sigma_{v_I}} \quad (2.1)$$

The complimentary transformation is given as:

$$v_I = (X_I * \sigma_{v_I}) + \mu_{v_I} \quad (2.2)$$

An important effect of this multidimensional space ( $\bar{x}$ ), composed of axes that are normalized so that the unit distance is one standard deviation and with values that are distributed using a standard normal distribution (Figure 2.1c), is that any point on a hyper-sphere centered at the origin and

---

<sup>1</sup> An affine transformation is a spatial transformation that preserves the linearity of line segments and the ratios of linear segments.



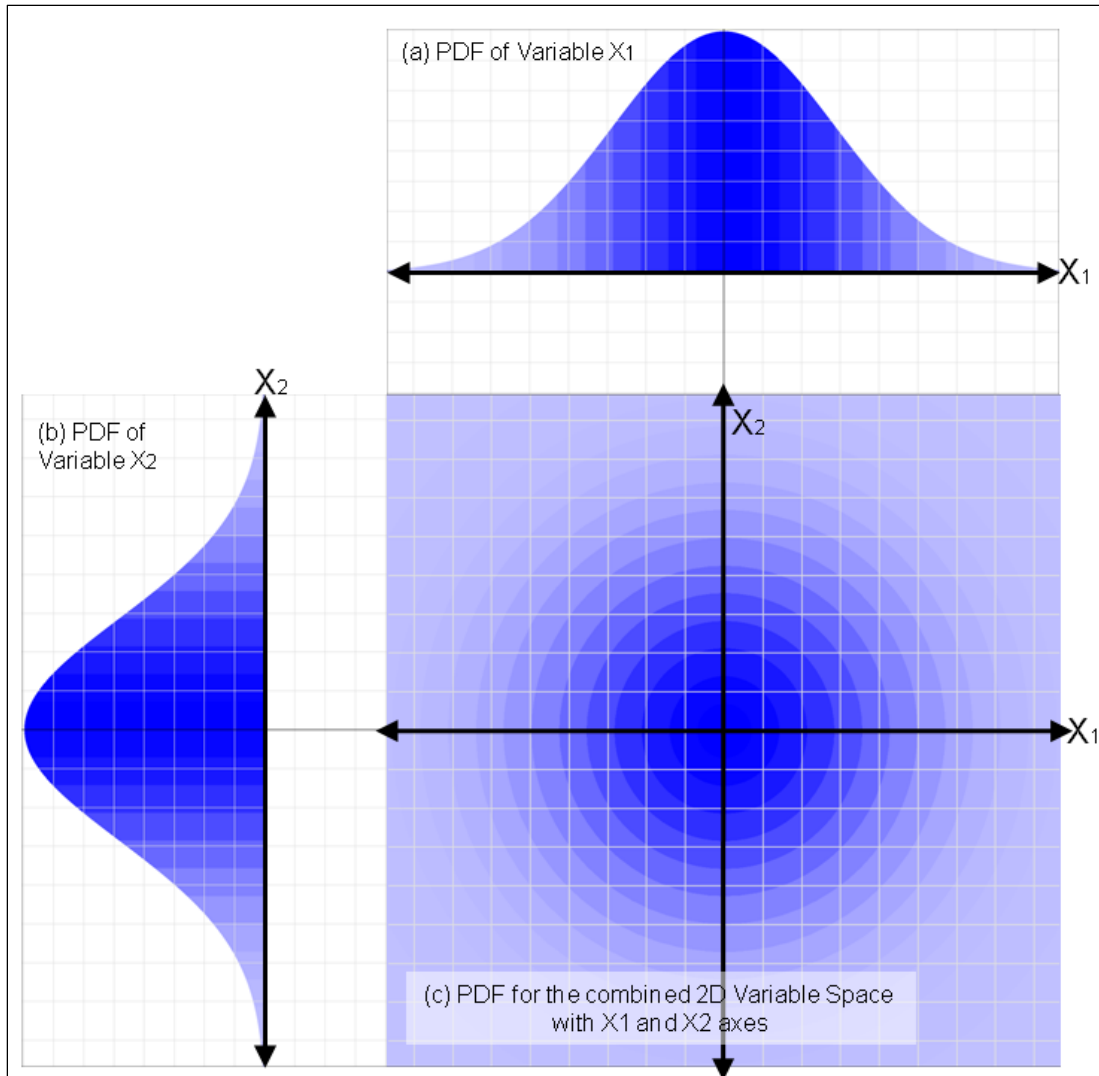


Figure 2.1. 1D variable space with a normal PDF distribution and 2D variable space with normal PDF distributions for each variable axis.

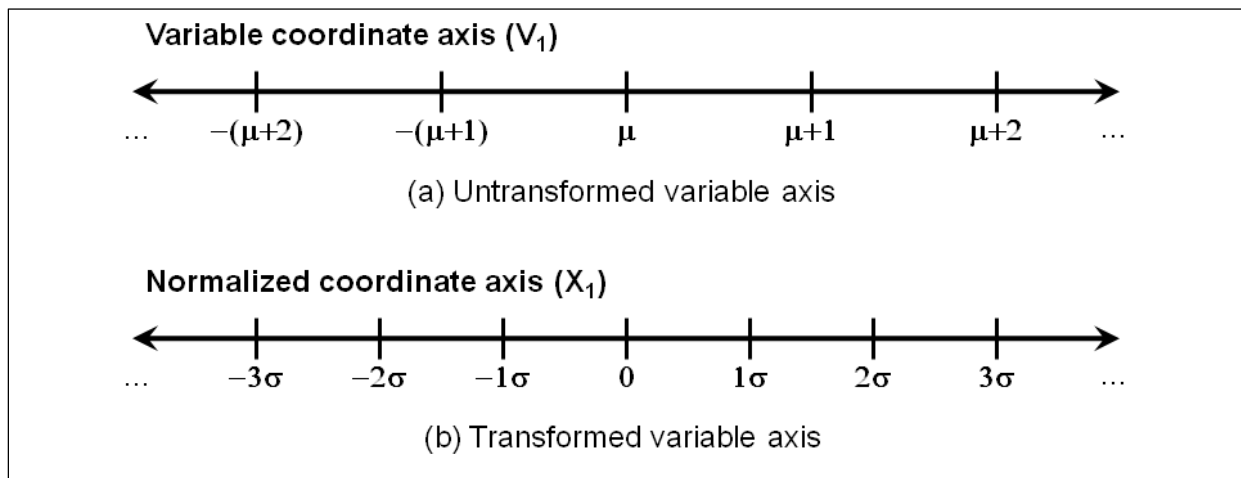


Figure 2.2. (a) Untransformed and (b) transformed (standard normal) variable axes.

with a certain radius will have the same probability of occurrence. This means the Euclidean distance of a point can be used to measure probability. This is represented in Figure 2.1c, where the background colors go from darker blue at the origin to lighter blue away from the origin in concentric bands that match the banding in the accompanying section cuts through the origin (Figure 2.1a and b).

## 2.2 Performance function

Reliability is based on the performance of a system as the variables in  $\bar{v}$  change. Therefore, it is important to know when the system fails. System failure will be discussed here, defining failure with respect to a CPGA analysis discussed later.

A limit state is the boundary between satisfactory and unsatisfactory performance of a structure (Nowak and Collins 2000, 2013). These limit states are further broken into ultimate limit states and serviceability limit states, depending on their severity. Ultimate limit states are related mostly to the system's loss of load-carrying capacity. For an individual pile, an ultimate limit state might involve exceeding the moment-carrying capacity, or plastic hinging of the pile. Serviceability limit states are related to gradual deterioration, comfort user, or maintenance cost. For a pile-founded structure, excess deformation, according to engineering standards, might be a serviceability limit state.

This limit state boundary is represented mathematically by a performance function that is positive for satisfactory performance of the structure, negative for unsatisfactory, and 0.0 at the limit state being investigated. The performance function can be defined with respect to the capacity of the structure,  $R$ , and the demand on the structure,  $Q$ . With respect to the capacity and demand, the performance function becomes:

$$g(R, Q) = R - Q \quad (2.3)$$

Using this definition of the performance function, satisfactory performance occurs when the capacity ( $R$ ) exceeds the demand ( $Q$ ), and unsatisfactory performance occurs when the demand ( $Q$ ) meets or exceeds the capacity ( $R$ ). The limit state occurs when the demand is balanced by the capacity. This can be related to the probabilities of whether the system performance is satisfactory or unsatisfactory (Figure 2.3).

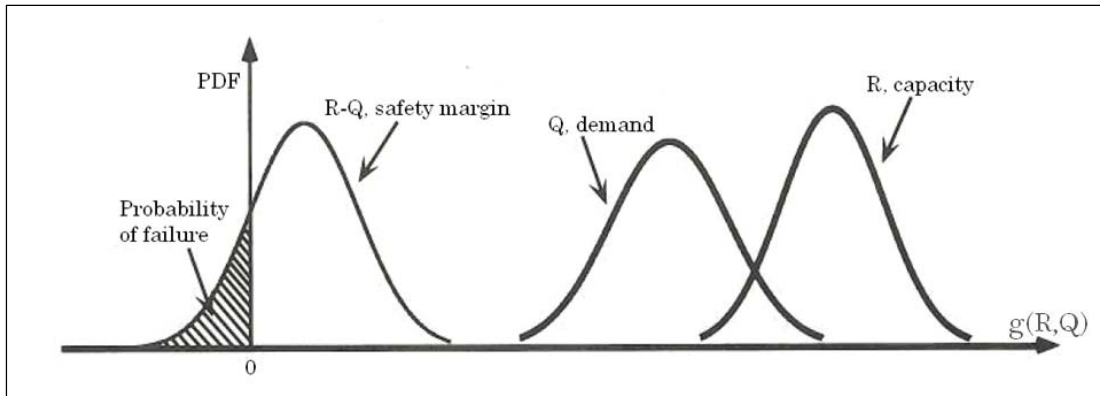


Figure 2.3. Capacity vs. demand related to the probability of unsatisfactory performance (after Nowak and Collins 2000, 2013).

The performance function is stretched or compressed when the 1D variable space is transformed between the physical space and the standard normal distribution space. Because an affine transformation is used, the function is translated and scaled linearly (Figure 2.4). For multiple dimensions, each axis might have a different scale, causing the response function to stretch and compress non-uniformly between dimensions, but the affine property is held (Figure 2.5).

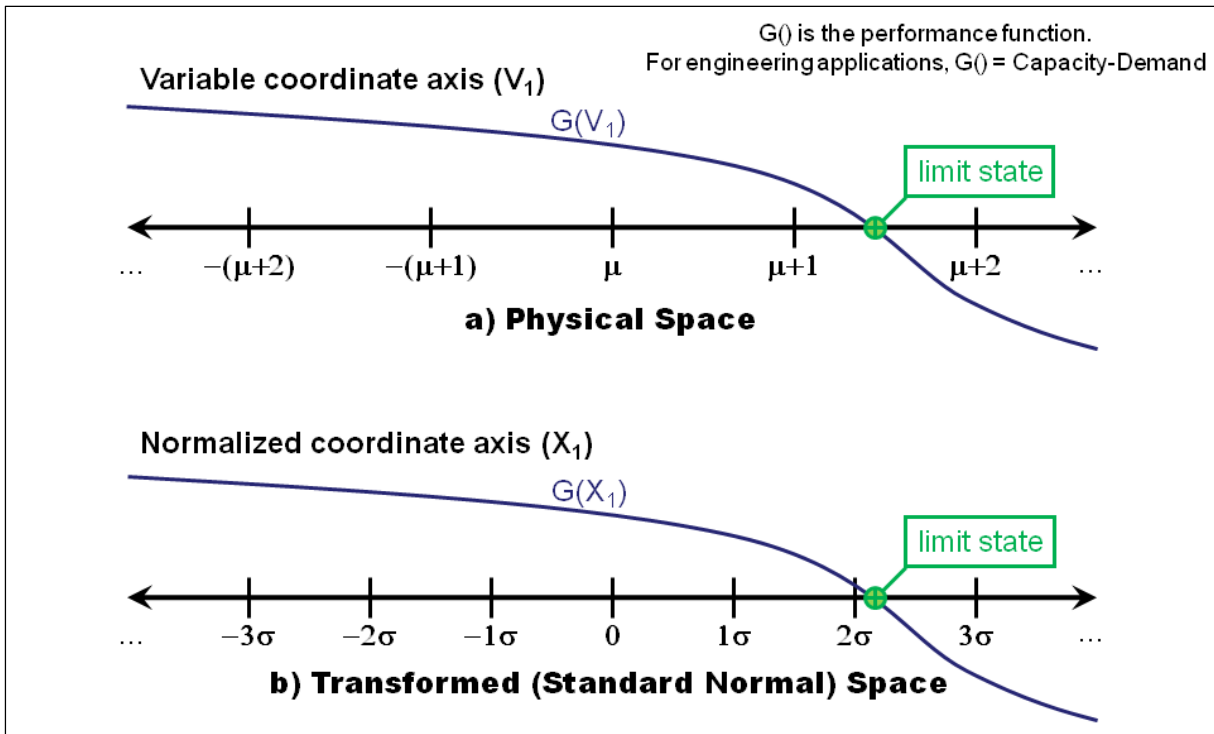


Figure 2.4. A performance function for a single variable axis (untransformed and transformed).

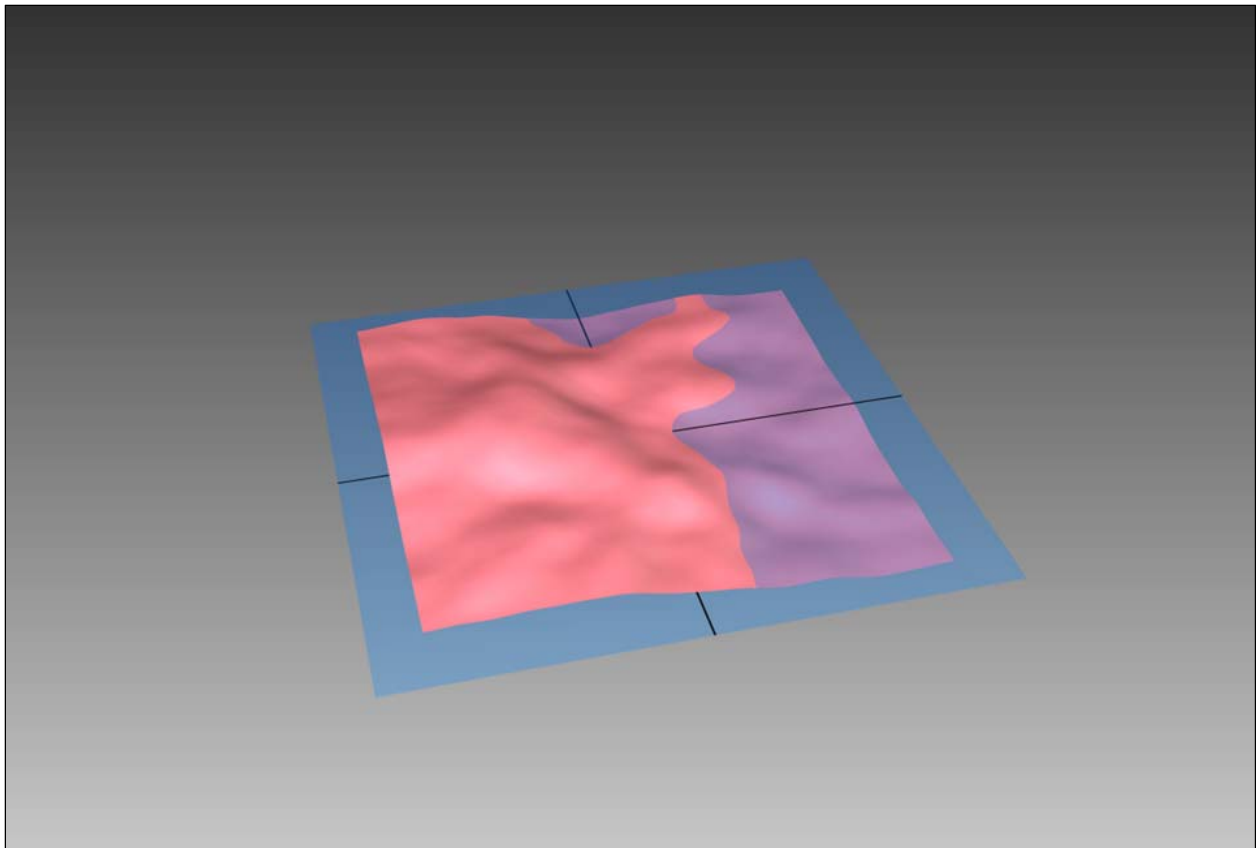


Figure 2.5. A complex two-variable,  $G(\vec{V})$ , function.

The state of the structure can be determined from a set of variables that describes a variable space ( $\vec{v}$ ). The variables in this space can affect the capacities as well as the demands on the structure. Given this variable space, it is possible to represent the performance function in the variable space as  $G(\vec{V})$ , where  $\vec{V}$  is the vector representation of a point in the vector space,  $\vec{v}$ . The performance function is still a representation of capacity vs. demand, and is represented as:

$$G(\vec{V}) = R - Q \quad (2.4)$$

Variables can be chosen that do not affect the capacity of the structure (e.g., the applied force in the  $X$  direction might not affect the capacity of the structural system in the  $Y$  direction). Likewise, variables can be chosen that do not affect the demand on the structure. The user must select a set of variables that affects either the capacity, demand, or both in order for the  $G(\vec{V})$  function to evaluate a limit state.

### 2.3 Probability of unsatisfactory performance

Given a limit state function based on variables  $G(\vec{V})$ , the probability of unsatisfactory performance can be given by:

$$P_u = P(R - Q < 0) = P(g(R, Q) < 0) = P(G(\vec{V}) < 0) \quad (2.5)$$

The probability of unsatisfactory performance ( $P_u$ ) can be estimated using simulation techniques (e.g., Monte Carlo, Latin Hypercube, Importance Sampling). The ASM method can be used to determine the most likely vector to occur at the limit state boundary, also called the response surface, defined as:

$$Z = G(\vec{V}) = 0 \quad (2.6)$$

This vector can pinpoint what variable conditions will cause unsatisfactory performance and provide a way of increasing estimation accuracy using Importance Sampling (to be discussed later).

### 2.4 Monte Carlo and Latin Hypercube simulations

Monte Carlo simulation estimates the probability of unsatisfactory performance by sampling the vector space ( $\vec{v}$ ) with a large number of sample points ( $\vec{V}_i$ ) randomly selected according to the distribution space. This estimation is accurate for:

$$P_u = \int f(x) p(x) dx \quad (2.7)$$

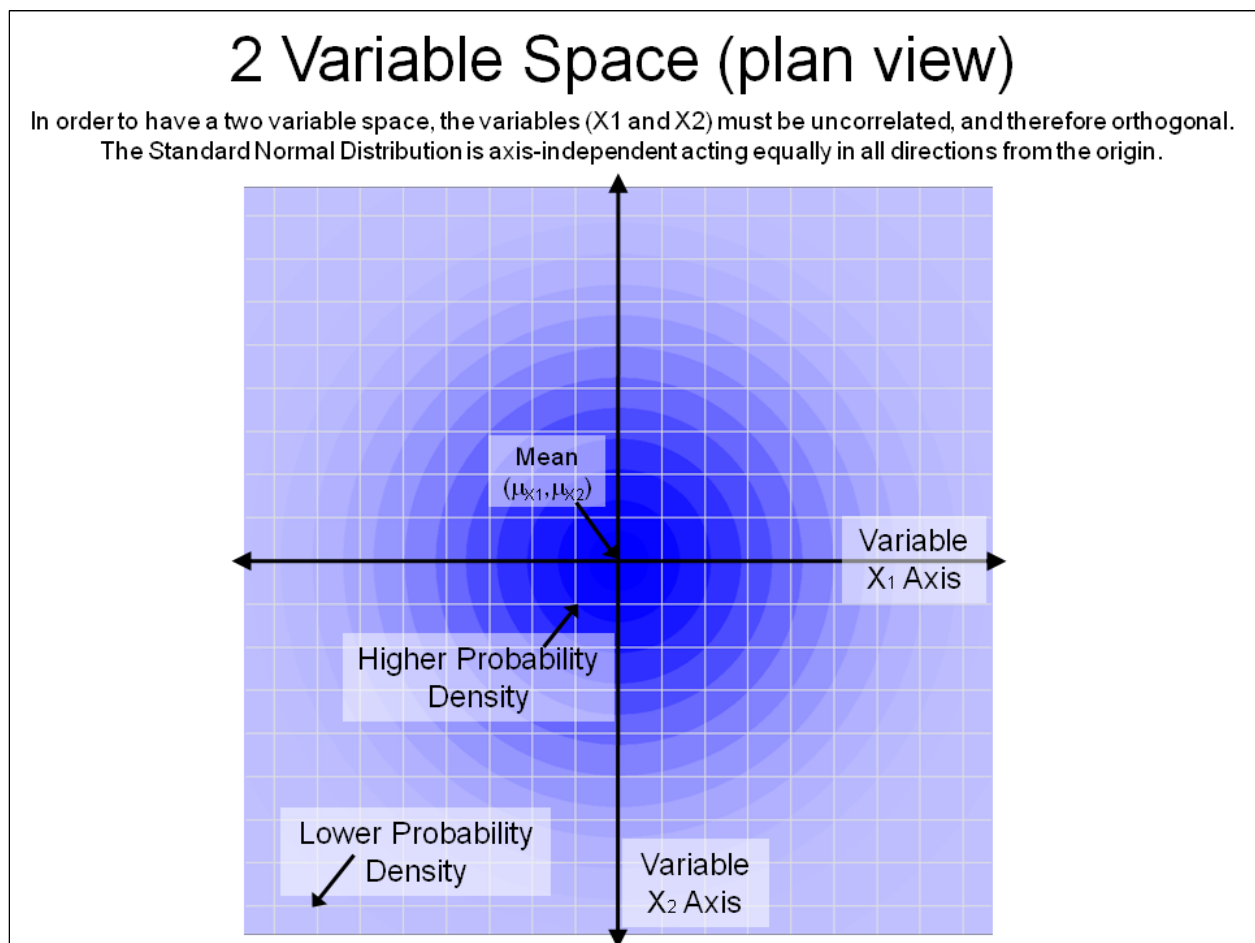
where  $f(x)$  is the performance function and  $p(x)$  is the probability of  $x$  being chosen. This leads to a discrete probability of unsatisfactory performance of:

$$P_u = \frac{1}{N} \sum_{i=1}^N I(G(\vec{V}_i)), \text{ where } \begin{cases} I = 1 & | G(\vec{V}_i) < 0 \\ I = 0 & | \text{otherwise} \end{cases} \quad (2.8)$$

The issue inherent with the Monte Carlo method for estimating the probability of unsatisfactory performance is that an inordinately large number of samples occurs where the probability density function has its

highest value. For a normal (Gaussian) distribution, this value occurs at the mean. To fully explore the region of interest also is known as the  $\vec{v}$  space (Figure 2.6), a large number of samples must be chosen (Figure 2.7).<sup>1</sup> In fact, the estimate of the probability of unsatisfactory performance can become entirely accurate with an infinite number of samples.

The Latin Hypercube simulation method partitions the  $\vec{v}$  vector space into a discrete set of regions based on equivalent cumulative distribution function (CDF) steps (Figure 2.8). This means the space is divided by areas of equal probability (Swiler and Wyss 2004). Each dimension has the same



<sup>1</sup> In these figures, each blue, circular line is concentric about the center of mean values and possesses a unique value of probability such as Figure 2.1. These blue, circular lines are included for reference when interpreting the resulting simulation data. The value of probability for each circular line is according to the normal distribution function.

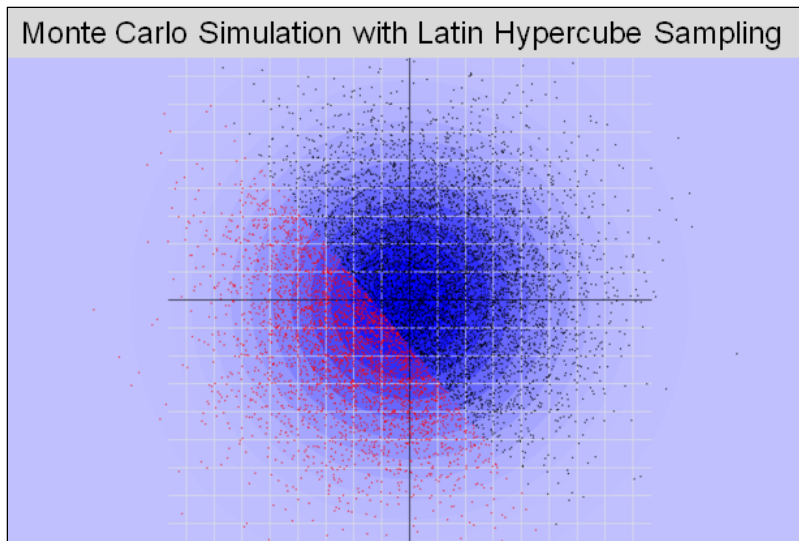


Figure 2.7. Monte Carlo simulation samples for the previous 2D variable space evaluated with the performance function (black samples have  $G(X) > 0.0$ , and red samples have  $G(X) < 0.0$ ).

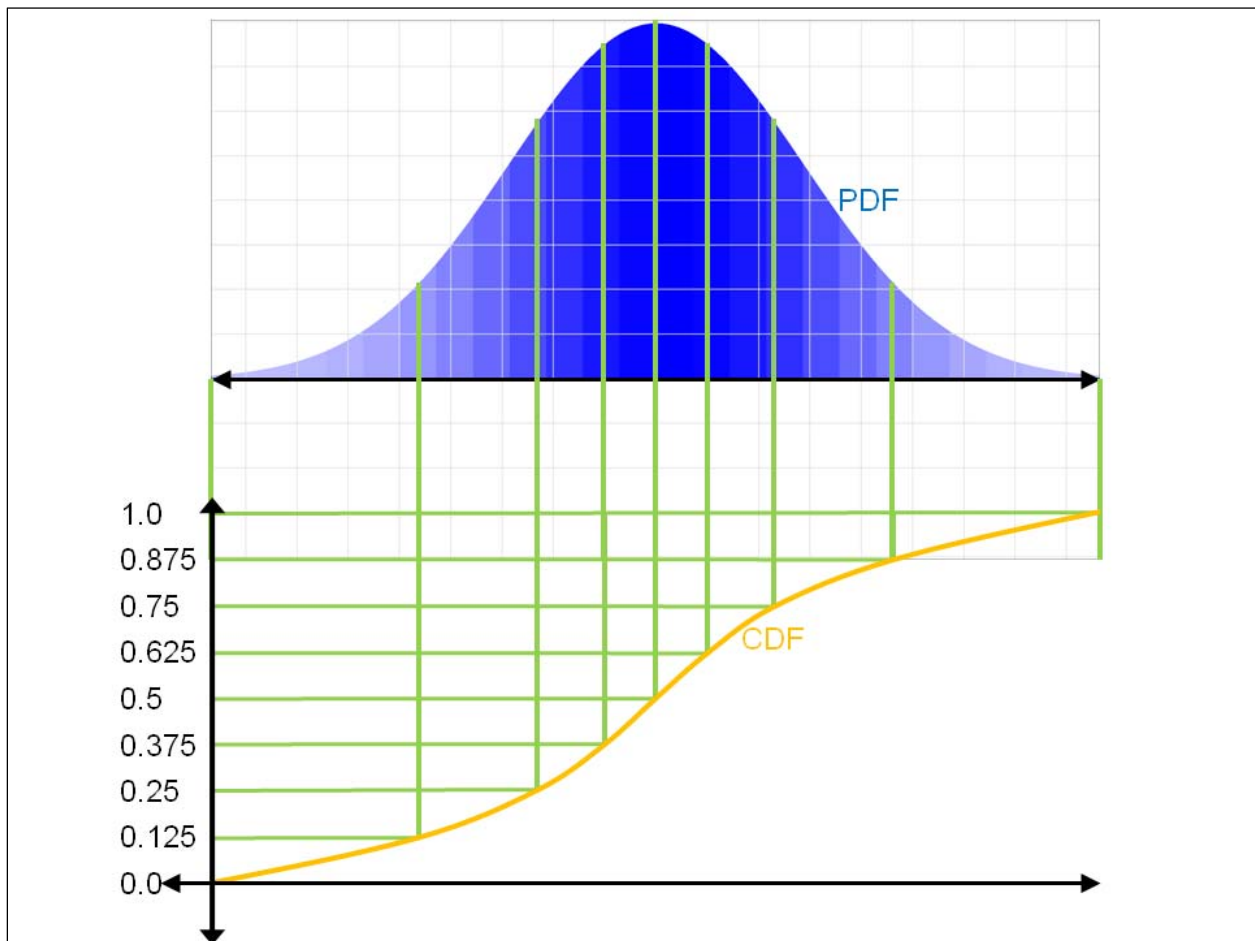


Figure 2.8. Creating a set of equal area bins in standard normal space.

number of divisions, which is equivalent to the number of samples (Figure 2.9).<sup>1</sup> For each sample,  $\vec{S}$ , each dimension has a division chosen at random. These divisions are constrained, not to be chosen again for any of the following samples. When a division for each dimension has been chosen for the sample, a value for that sample is chosen from a uniform distribution for the range of each division, generating a random value in that bin. When the final sample has been assigned, all the divisions for all the dimensions will be assigned, one to each sample (Figure 2.10). In this way, the set of samples can be smaller, but still explore a greater portion of the  $\vec{v}$  space. The advantage of this simulation technique is, typically, the number of samples can be reduced by a factor for each dimension.

The Latin Hypercube method can directly accommodate inter-variable correlation. The set of samples can be viewed as an  $N \times M$  matrix, where  $N$  is the number of samples and  $M$  is the number of variables. If variables  $p$

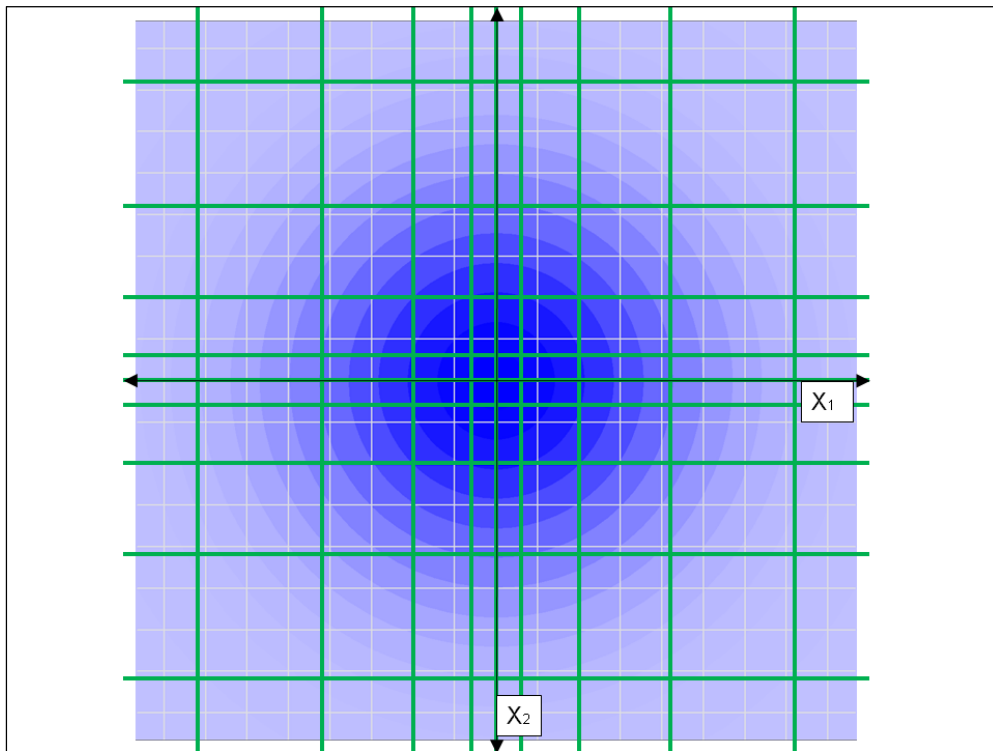


Figure 2.9. Partitioning a 2D variable space for a Latin Hypercube selection of samples for two variables with normal distributions.

<sup>1</sup> In this figure, each blue, circular line is concentric about the center of mean values and possesses a unique value of probability such as Figure 2.1. These blue, circular lines are included for reference when interpreting the resulting simulation data. The value of probability for each circular line is according to the normal distribution function.



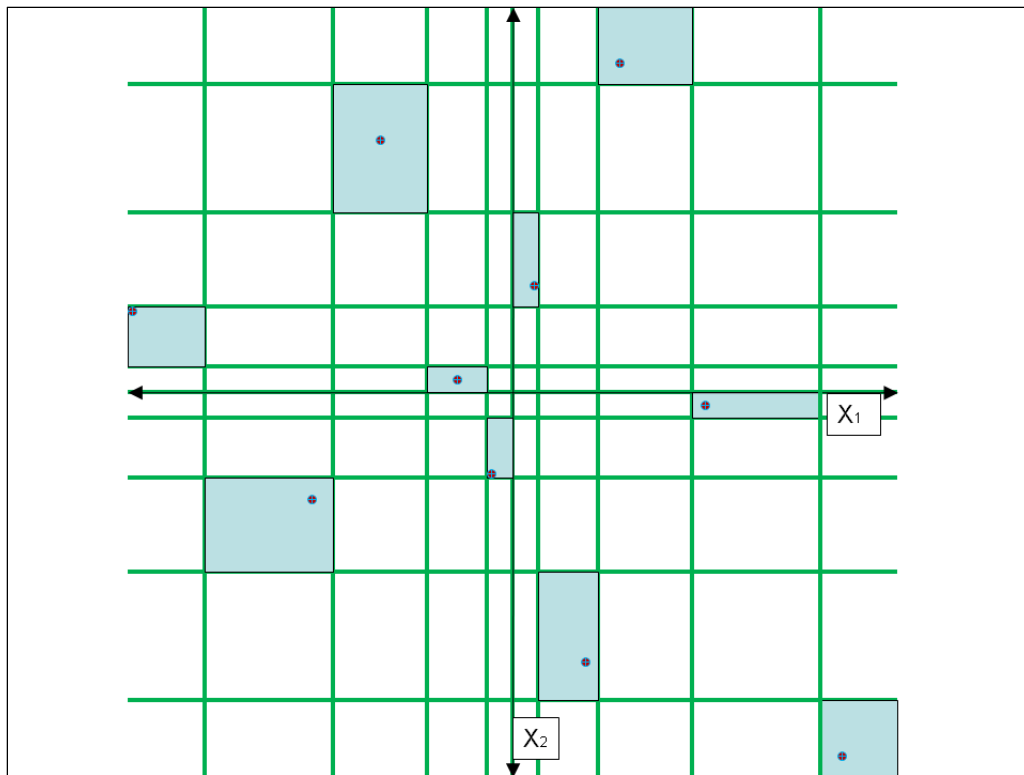


Figure 2.10. Using the normally distributed regions to assign samples according to the Latin Hypercube method for generating samples.

and  $q$  are correlated, the variables in the  $q$  column of the samples may be redistributed based on the variables in the  $p$  column to maintain the correlation coefficient value ( $\rho$ ).

## 2.5 Advanced Second Moment (ASM)

### 2.5.1 ASM for uncorrelated, normal distributions

The ASM technique, also called Advanced First Order Second Moment (AFOSM), is a method for finding the minimum distance that a capacity-vs.-demand surface, based on the function  $G()$ , is from the origin of a defined vector space. This differs from the First Order Second Moment (FOSM) technique, which approximates a nonlinear capacity-vs.-demand surface with a hyperplanar surface in multidimensional space (Melchers 2001), which forms a linear surface in 2D space (i.e., considering two independent variables). The FOSM technique uses the linear definition of the capacity-vs.-demand surface to quickly estimate the closest surface point to the origin, without having to perform multiple iterations to find the actual nonlinear capacity-vs.-demand surface's closest point.

For a reliability analysis, the surface function is the limit state boundary function. Recall that this vector space,  $\bar{v}$ , can be transformed into the vector space  $\bar{x}$ , where the probability of occurrence is based on the Euclidean distance from the origin. In this case, the distance is the reliability index of the design with respect to that point (Ditlevsen 1981). The point (in the normalized vector space,  $\bar{x}$ , Figure 2.11) on the surface  $G(\vec{V})=0$  (where the design point has been transformed from  $\bar{x}$ -space to  $\bar{v}$ -space) that is closest to the origin is called the design point. The distance from the origin to this design point in the  $\bar{x}$  space is referred to as the reliability index,  $\beta$  (Table 2.1 and Figure 2.12), and this value can be used to determine the probability that this point will be chosen from the variable distributions.<sup>1</sup> In terms of reliability analysis, the probability of unsatisfactory performance can be given by  $P_U = 1 - \Phi(\beta)$  for an arbitrary axis with a linear limit state, where  $\Phi()$  is the cumulative distribution function. Table 2.1 lists values of  $\beta$  and its corresponding  $P_U$  values.

The ASM technique works because any hyperplanar surface can be fully described by a directional cosine vector ( $\alpha$ ) and the distance from the origin ( $\beta$ ) for the closest point on the hyperplanar surface (Figure 2.12). The vector describing the resultant of all directional cosine vectors,  $\alpha$ , also is identified in Figure 2.12. This resultant directional cosine vector ( $\alpha$ ) is perpendicular to the hyperplanar surface labeled as the ASM Response Surface (i.e., where  $G(\vec{V}) = 0$ ). This resultant directional cosine vector  $\alpha$  is a unit vector, with the magnitude of each component vector along a variable  $X_i$  axis,  $|\alpha_i|$ , being a cosine value for that direction with respect to the unit vector  $\alpha$ . The components of the directional cosine vector  $\alpha_i$  multiplied by the distance,  $\beta$ , are shown for variables  $X_1$  and  $X_2$  in Figure 2.13 and lay along each respective axis. For the  $\bar{v}$  space, the vector  $\vec{V}$ 's components that define the plane are given by:

$$V_i = \mu_{v_i} - \alpha_i \beta \sigma_{v_i} \quad (2.9)$$

At the start of the reliability analysis, the directional cosine  $\alpha$  is unknown. However, it can be estimated by determining the vector on the surface,  $G(\vec{V})$ , that is approaching a 0.0 value from the mean value at the fastest rate. The rate at which each component approaches the 0.0 value can be determined by computing the partial derivative of  $G$  with respect to each variable ( $V_1, V_2, \dots$ ) at the mean value.

<sup>1</sup>  $\beta$  is the distance of the variable value from the expected value ( $\mu$ ) (i.e., its mean, in units of standard deviation ( $\sigma$ )).

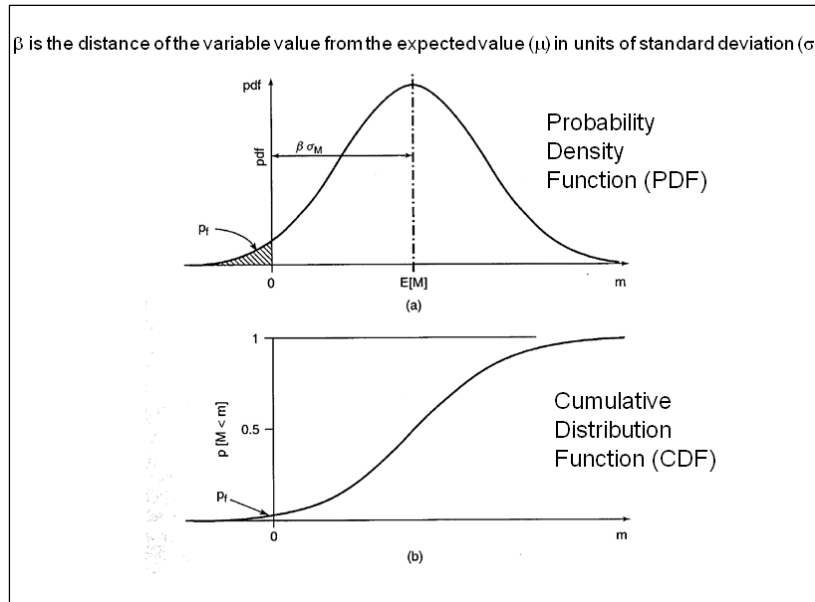


Figure 2.11. Using the reliability index ( $\beta$ ) to determine the probability and cumulative probability for an event.

Table 2.1. Reliability index ( $\beta$ ) and probability of unsatisfactory performance ( $P_U$ ).

$\beta$	$P_U = 1 - \Phi(\beta)$
0	5.000000000000E-01
1	1.586552539315E-01
2	2.275013194818E-02
3	1.349898031630E-03
4	3.167124183678E-05
5	2.866515719235E-07
6	9.865877004245E-10
6.36	1.008768624189E-10
6.71	9.731215833142E-12
7	1.279865102788E-12
8	6.661338147751E-16
9	Out of range for a double-precision variable

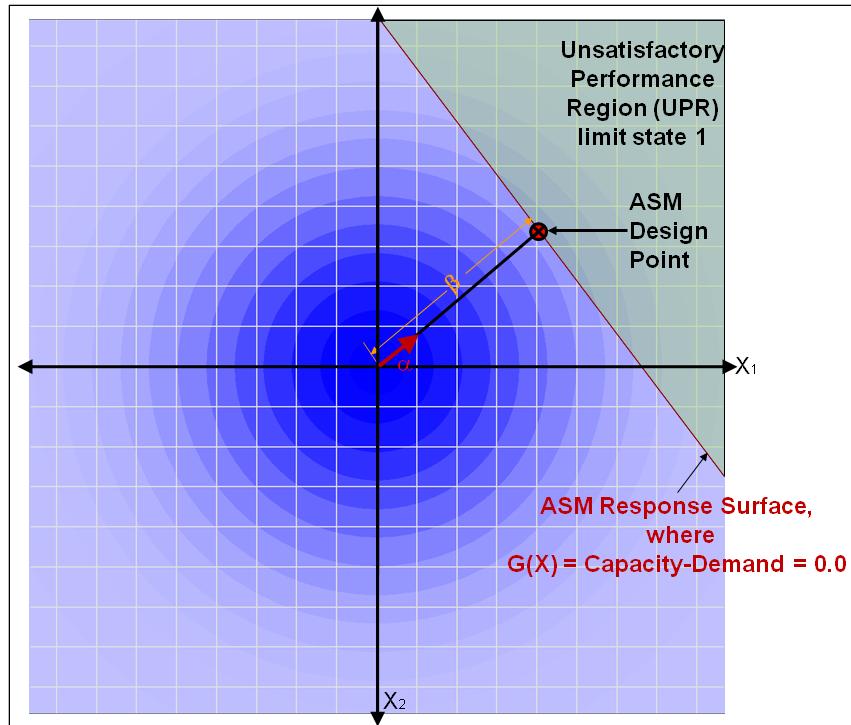


Figure 2.12. In a two-variable space with a linear response surface,  $\beta$  is the distance from the origin to a design point on the surface.

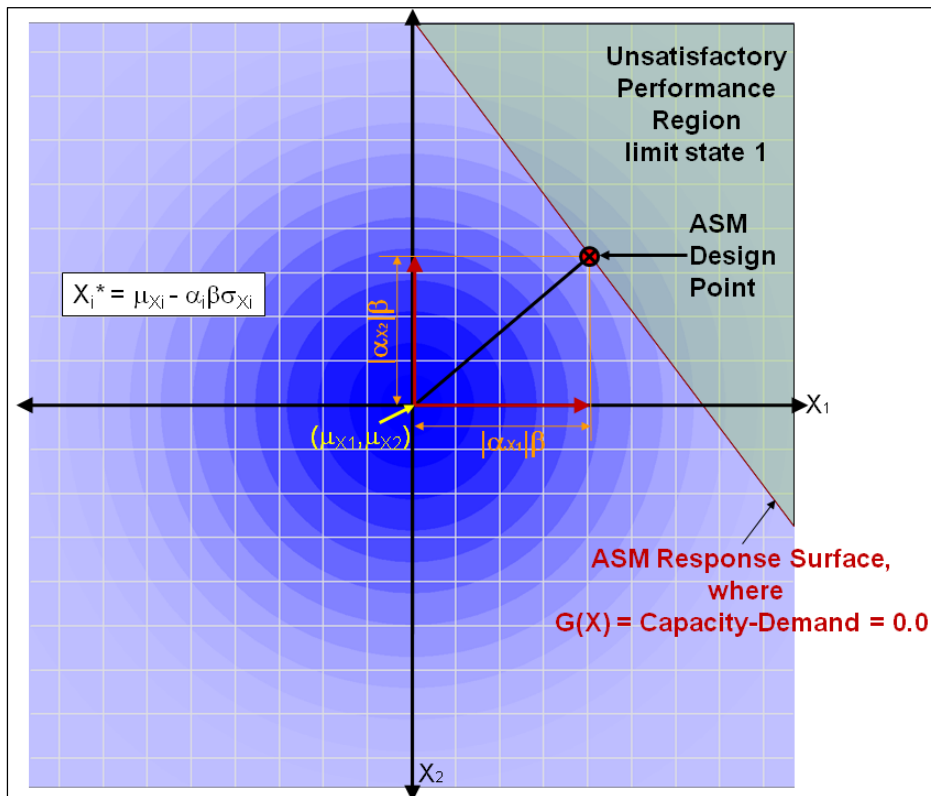


Figure 2.13. The directional cosines  $\alpha$  combine to form the unit vector directed from the origin to the design point.

Referring to Figure 2.5, which shows a nonlinear  $G(\vec{V})$  surface, with particular attention paid to the region above the origin at the means of this 2D normal space, a pair of partial derivatives are made numerically in the positive and negative direction of an individual axis resulting in a total of four partial derivatives for a two-variable problem. The direction along each variable axis with the steepest slope approaching  $G(\vec{V})=0.0$  is selected for each variable as the direction of the vector. The magnitudes of each axis,  $|\alpha_i|$ , are computed according to Equation 2.11.

Recall that the response surface for vector  $\vec{V}$  is defined by:

$$G(\vec{V}) = 0.0 \quad (2.10)$$

This can be performed by setting:

$$\alpha_i = \frac{\left( \frac{\partial G}{\partial V_i} \right) \sigma_{v_i}}{\sqrt{\sum_{i=1}^n \left( \frac{\partial G}{\partial V_i} \right)^2 \sigma_{v_i}^2}} \quad (2.11)$$

with the initial trial value for  $\beta$  set to 0.0, so that the initial vector  $\vec{V}$  is composed of only the mean values. A numerical procedure, along with Equations 2.9, 2.10, and 2.11, is to calculate the  $\alpha_i$  values for each of the  $i$  variables.

When the directional cosine ( $\alpha$ ) has been determined, it is possible to determine  $\beta$  using numerical methods (e.g., the Regula-Falsi method) so that the current design point (vector  $\vec{V}$ ) is on the response surface, where Equation 2.9 is satisfied (Figure 2.13).

For nonlinear performance functions, the current design point might not be the point with the minimum distance from the mean values. For this case, partial derivatives for each axis at the current design point (vector  $\vec{V}$ ) are computed (Equation 2.11) to determine the direction and magnitudes for a new directional cosine from the origin at the means. The  $\beta$  value is determined from Equation 2.9. This process is performed until the new  $\beta$  and the old  $\beta$  converge within a certain tolerance.

This solution might not reach the absolute minimum distance point to the response surface for particularly complex nonlinear surfaces, rather a local minima. Most engineering problems do not have particularly complex nonlinear response surfaces, so this ASM method will see widespread usage.

### 2.5.2 Dealing with non-normal distributions

For the ASM reliability method to return a value of probability based on  $\beta$ , all the random variables must be independent and distributed according to a normal distribution, says the Hasofer-Lind approach (Baecher and Christian 2003; Hasofer and Lind 1974). To handle non-normal distributions, the non-normal distribution variable must be changed to an equivalent normally distributed random variable. This is called the Rosenblatt transformation (Rosenblatt 1952). Rackwitz and Fiessler (1976 and 1978) impose two conditions on the equivalent normally distributed random variable that enable the determination of the two parameters of that distribution,  $\mu_{V_i}^N$  and  $\sigma_{V_i}^N$ . The cumulative distribution functions and probability density functions of the non-normal and normal distributions should be equivalent at the current design point for the performance function.

These conditions (CDF and PDF) can be expressed, respectively, in:

$$\Phi\left(\frac{V_i - \mu_{V_i}^N}{\sigma_{V_i}^N}\right) = F_i(V_i) \quad (2.12)$$

$$\phi\left(\frac{V_i - \mu_{V_i}^N}{\sigma_{V_i}^N}\right) = f_i(V_i) \quad (2.13)$$

where  $F_i$  is the non-normal CDF,  $f_i$  is the non-normal PDF,  $\Phi$  is the standard normal CDF, and  $\phi$  is the standard normal PDF. From these conditions, it can be shown that the standard deviation and mean, respectively, are:

$$\sigma_{V_i}^N = \frac{\phi\left(\Phi^{-1}\left[F_i(V_i)\right]\right)}{f_i(V_i)} \quad (2.14)$$

$$\mu_{V_i}^N = V_i - \Phi^{-1}\left[F_i(V_i)\right]\sigma_{V_i}^N \quad (2.15)$$

The PDF of a standard normal distribution is a continuously positive function. Bounded distributions including triangular PDFs are not. While it is possible to get equivalent CDF values between the standard normal distribution and a bounded non-normal distribution (Figure 2.14), it might be impossible to find an equivalent PDF between distributions. In this case, the standard deviation can be calculated and the mean of the standard deviation varied to find the appropriate CDF value. The PDF in this case will be a close estimate at convergence.

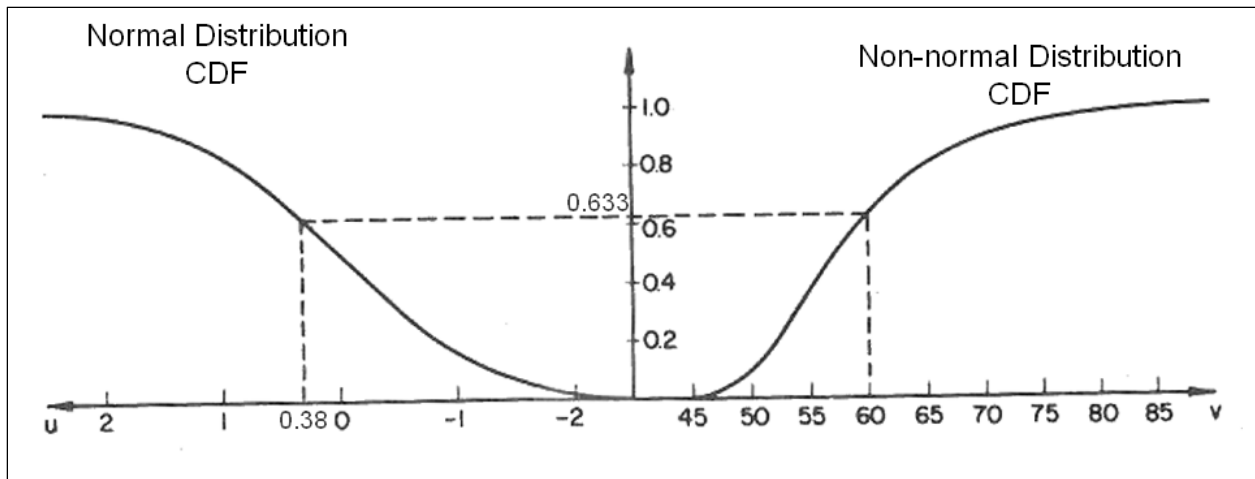


Figure 2.14. Finding the position of equivalent cumulative probability for a normal distribution as from a non-normal distribution (after Ang and Tang 1984).

### 2.5.3 Correlated random variables

In certain situations, it is unrealistic to believe that variables chosen for a reliability analysis will be independent of one another. In these other instances, such as the case in which the variables are the soil material properties of the angle of internal friction and cohesion for soil layers, variables might be related to some degree. For our discussion, a pair of variables ( $V_1$  and  $V_2$ ) is correlated with a correlation coefficient ( $\rho$ ). If the two variables have a standard normal distribution, they can be changed to a pair of non-correlated variables by solving for two eigenvalues and the corresponding eigenvectors:

$$V_1' = \frac{1}{2t} \left( \frac{V_1 - \mu_{V_1}}{\sigma_{V_1}} + \frac{V_2 - \mu_{V_2}}{\sigma_{V_2}} \right) \quad (2.16a)$$

$$V_2' = \frac{1}{2t} \left( \frac{V_1 - \mu_{V_1}}{\sigma_{V_1}} - \frac{V_2 - \mu_{V_2}}{\sigma_{V_2}} \right) \quad (2.16b)$$

where  $t=\sqrt{0.5}$ . The variances for these two variables are equal to the eigenvalues ( $\lambda$ ):

$$\sigma_{V_1}^2 = \lambda_1 = 1 + \rho \quad (2.17a)$$

$$\sigma_{V_2}^2 = \lambda_2 = 1 - \rho \quad (2.17b)$$

The directional cosines for these newly uncorrelated values must be determined from the original correlated values using:

$$\alpha_{V_1} = \frac{\left[ \left( \frac{\partial G_0}{\partial V_1} \right) t \sigma_{V_1} + \left( \frac{\partial G_0}{\partial V_2} \right) t \sigma_{V_2} \sqrt{1 + \rho} \right]}{\left[ \left( \frac{\partial G_0}{\partial V_1} \right)^2 \sigma_{V_1}^2 + \left( \frac{\partial G_0}{\partial V_2} \right)^2 \sigma_{V_2}^2 + 2\rho \left( \frac{\partial G_0}{\partial V_1} \right) \left( \frac{\partial G_0}{\partial V_2} \right) \sigma_{V_1} \sigma_{V_2} \right]^{1/2}} \quad (2.18a)$$

$$\alpha_{V_2} = \frac{\left[ \left( \frac{\partial G_0}{\partial V_1} \right) t \sigma_{V_1} - \left( \frac{\partial G_0}{\partial V_2} \right) t \sigma_{V_2} \sqrt{1 - \rho} \right]}{\left[ \left( \frac{\partial G_0}{\partial V_1} \right)^2 \sigma_{V_1}^2 + \left( \frac{\partial G_0}{\partial V_2} \right)^2 \sigma_{V_2}^2 + 2\rho \left( \frac{\partial G_0}{\partial V_1} \right) \left( \frac{\partial G_0}{\partial V_2} \right) \sigma_{V_1} \sigma_{V_2} \right]^{1/2}} \quad (2.18b)$$

and

$$V_1 = \mu_{V_1} - \sigma_{V_1} t \beta \left( \alpha_{V_1} \sqrt{\lambda_1} + \alpha_{V_2} \sqrt{\lambda_2} \right) \quad (2.19a)$$

$$V_2 = \mu_{V_2} - \sigma_{V_2} t \beta \left( \alpha_{V_1} \sqrt{\lambda_1} - \alpha_{V_2} \sqrt{\lambda_2} \right) \quad (2.19b)$$

Ditlevsen (1981) presents a detailed derivation of these equations for transforming correlated random variables into corresponding non-correlated random values.

#### 2.5.4 ASM algorithm

The ASM algorithm presented in this subsection has been modified from the AFOSM method to include ones for working with non-normal distributions and correlated random variables.

The ASM algorithm:



1. Assign the mean value for each random variable as a starting design point value (i.e.,  $(V_1, V_2, \dots, V_N) = (\mu_1, \mu_2, \dots, \mu_N)$ ).
2. Compute the standard deviation and mean of the equivalent normal distribution for each non-normal random variable by using Equations 2.14 and 2.15 or by adjusting the mean so that an equivalent CDF is determined for the standard deviation of the original data.
3. Compute the partial derivative,  $\partial G(\mathbf{V})/\partial V_i$ , of the performance function with respect to each non-correlated random variable evaluated at the design point as needed to satisfy Equation 2.11.
4. Compute the directional cosine,  $\alpha_i$ , for each non-correlated random variable as given in Equation 2.11 at the design point. For correlated pairs of random variables, Equations 2.18a and b should be used.
5. Compute the reliability index,  $\beta$ , by substituting Equation 2.11 for non-correlated random variables and Equations 2.18a and b for correlated random variables into the  $G(\mathbf{V})$  performance function of the vector  $\vec{V}$  (Equation 2.9) and satisfying the limit state  $G(\mathbf{V}) = 0$  (Equation 2.10) by using a numerical root-finding method.
6. Compute a new estimate of the design point by substituting the resulting reliability index,  $\beta$ , obtained in Step 5 into Equation 2.9 for non-correlated random variables and Equations 2.19a and b for correlated random variables.
7. Repeat Steps 2 through 6 until the reliability index,  $\beta$ , converges within an acceptable tolerance,  $\delta$ .

### 2.5.5 ASM caveats

The ASM method is merely an estimate of the actual probability of unsatisfactory performance. It is accurate only if the limit state (response) surface, where  $G(\mathbf{V})=0$ , is linear. The response surface might be nonlinear if the  $G(\mathbf{V})$  function is nonlinear or if multiple limit states are included in the  $G(\mathbf{V})$  function (Figure 2.15).

For these nonlinear response surfaces, sampling (simulation) methods provide better results because they represent a weighted area sampling of the entire variable space, rather than partitioning the space with a hyperplane. This is shown by combining two limit states and their response surfaces to create a new response surface (Figures 2.16a through c).

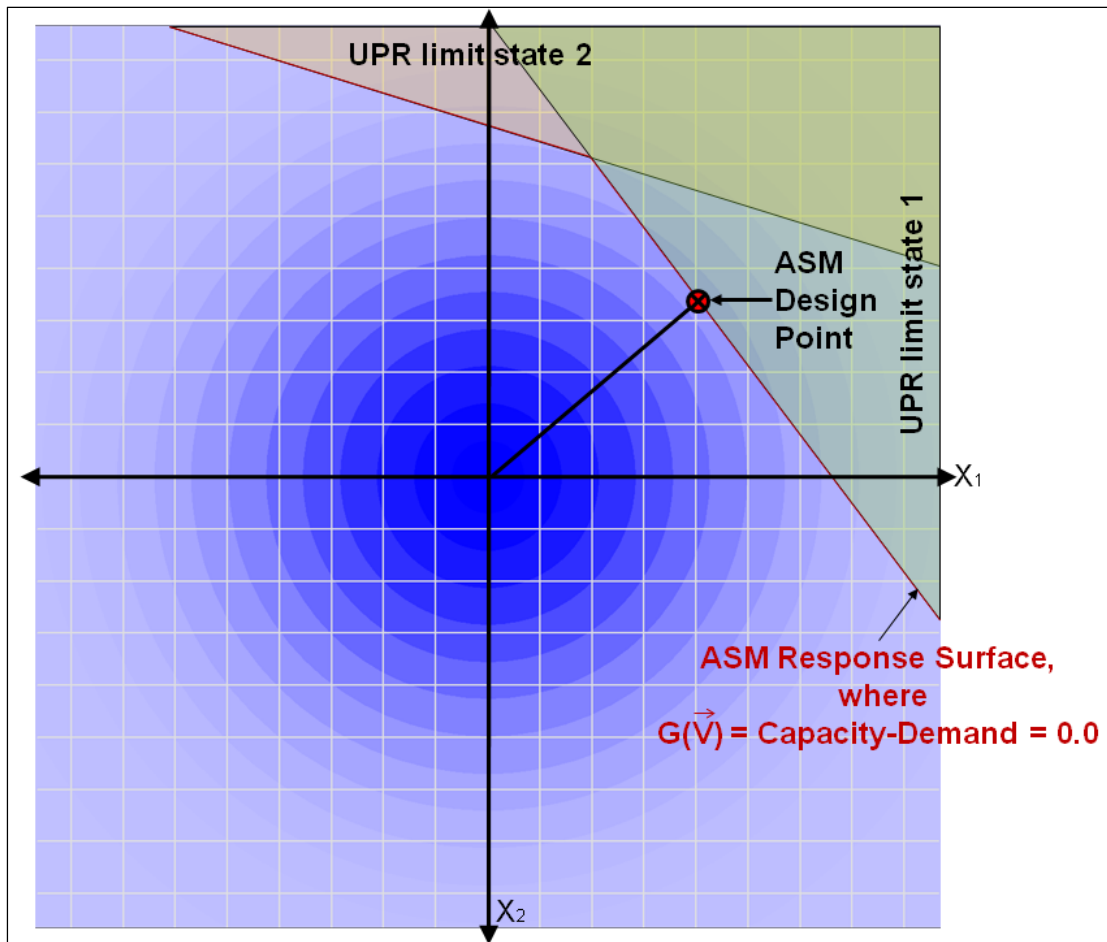
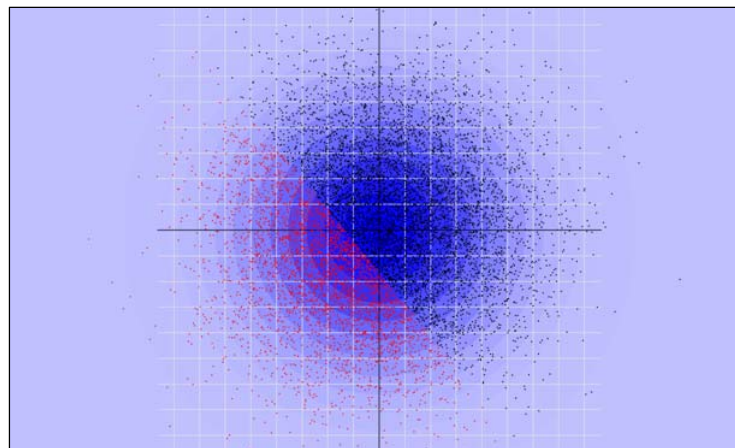


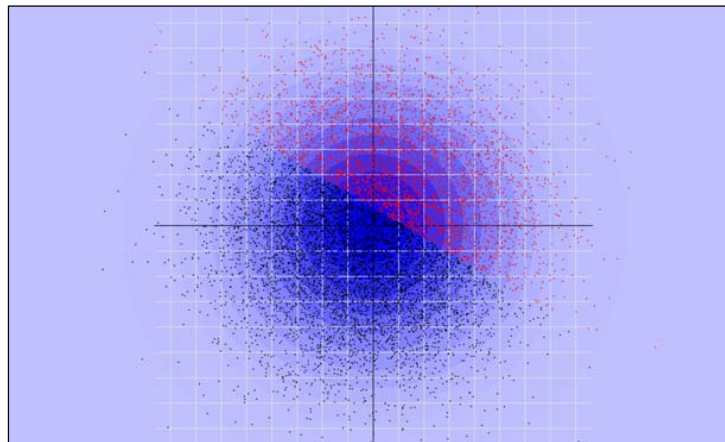
Figure 2.15. Combining limit states creates a nonlinear ASM response surface.

Despite its nonlinear limitations, the ASM serves two important purposes. It provides a vector in variable space to the most likely failure mechanism. This vector can be analyzed to investigate possible designs or remediation strategies for the structural system being investigated and for the combination of factors defined in terms of multiple variables that decrease the probability of unsatisfactory performance.

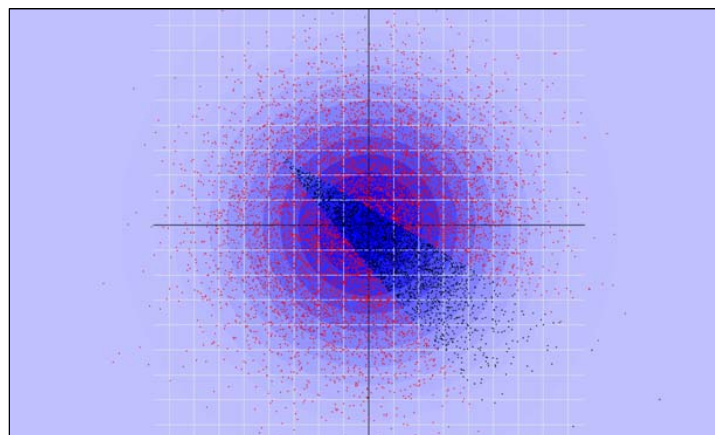
Second, the ASM-generated vector provides a point in the weighted space at which sampling can be enhanced for better precision. If more sample points are collected in the region of highest probability for changing from satisfactory to unsatisfactory performance, on either side of the response surface  $G(\vec{V})=0$ , the precision can be enhanced. This is discussed in the next section.



(a)



(b)



(c)

Figure 2.16. (a and b) Two response surfaces, with Latin Hypercube samples; each have a  $P_U < 0.5$ , but (c) combining the two creates  $P_U > 0.5$ .

## 2.6 Importance Sampling

This method attempts to improve the accuracy of a simulation by using a different distribution to sample from ( $Q$ ) than the actual variable distribution ( $P$ ). Figure 2.17 shows these two distributions. The objective is to minimize the required number of simulation runs. This method relies on choosing an appropriate distribution to sample from, typically one that is closer to the area of interest, where the data is changing (Lemaire 2009). For reliability, that distribution would have to be close to the point where the  $G()$  approaches 0.0.

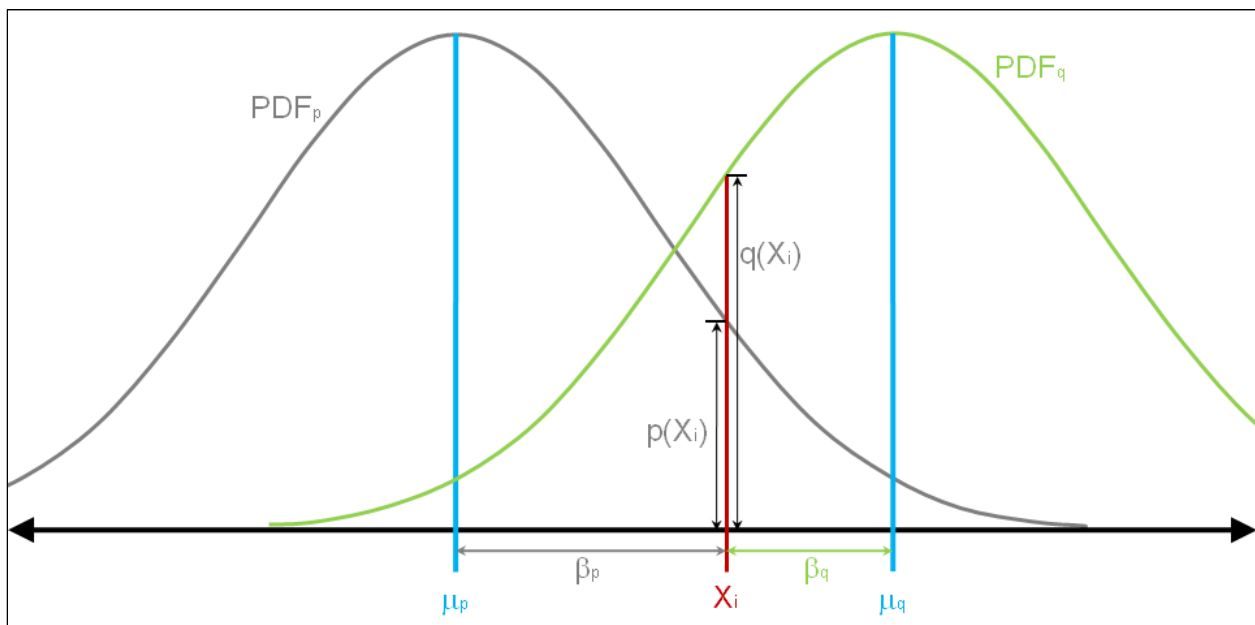


Figure 2.17. For sample  $X_i$ , the distance to the original mean and the distribution mean can be determined and the probabilities computed.

Because the design point from the ASM method lies on this response surface, it is more efficient and accurate to sample around this point, substituting it as the mean for the distributed points ( $Q$ ). The standard deviation of each variable is maintained. If the distribution is a non-normal or truncated distribution, a semi-equivalent standard normal distribution is computed and substituted for the non-normal distribution, with a mean moved to the design point.

However, these sample points must be weighted to correspond to the original distribution. Equation 2.7 shows how to compute the estimation of the probability of unsatisfactory performance for samples taken according

to the original distribution. If we multiply the equation by the probability of the second distribution divided by itself, then (Melchers 2001):

$$P_u = \int f(x) \frac{p(x)}{q(x)} q(x) dx \quad (2.20)$$

with  $f(x)$  being the performance function,  $p(x)$  being the probability according to the original distribution space, and  $q(x)$  being the probability of occurrence for the sample distribution space. One prerequisite must be met: the  $p(x)$  probability needs to be 0.0 when the  $q(x)$  probability is 0.0. This ensures absolute continuity between  $q(x)$  and  $p(x)$ . Otherwise, the equation suffers from a division by 0. Stated mathematically:

$$\forall q(x), \{q(x) = 0\} \Rightarrow \{p(x) = 0\} \quad (2.21)$$

This condition can be guaranteed by making both  $p(x)$  and  $q(x)$  probabilities from a standard normal distribution, which is defined always to have a non-zero probability.

The probability of unsatisfactory performance can be approximated for a discrete number of samples by:

$$P_u = \frac{1}{N} \sum_{i=1}^N I(G(\vec{V}_i)) \frac{p(\vec{V}_i)}{q(\vec{V}_i)} \text{ where } \begin{cases} I = 1 & | G(\vec{V}_i) < 0 \\ I = 0 & | \text{ otherwise} \end{cases} \quad (2.22)$$

It is possible to determine the distance in standard normal space for the original distribution and the sampling distribution, respectively:

$$\vec{\beta}_p = \frac{\vec{X}_i - \vec{\mu}_p}{\sigma_p} \quad (2.23a)$$

$$\vec{\beta}_q = \frac{\vec{X}_i - \vec{\mu}_q}{\sigma_q} \quad (2.23b)$$

The weighting function based on these  $\beta$  vectors is then:

$$W(\vec{V}_1) = \frac{P(\beta_p)}{Q(\beta_q)} \quad (2.24)$$

where  $P(\beta)$  is the probability in the original vector space and  $Q(\beta)$  is the probability in the sampling vector space. This simplifies Equation 2.22 to:

$$P_u = \frac{1}{N} \sum_{i=1}^N I(G(\vec{V}_i)) W(\vec{V}_1) \text{ where } \begin{cases} I = 1 & | G(\vec{V}_i) < 0 \\ I = 0 & | \text{otherwise} \end{cases} \quad (2.25)$$

Figure 2.18 shows the accuracy improvements derived from using a sample space at an ASM design point for a CPGA-R reliability analysis of a pile group-founded structure. When samples are drawn in the original distribution space (via the Latin Hypercube simulation technique), no samples are drawn in the unsatisfactory region. By sampling from the distribution centered at the ASM design point, using Importance Sampling, the shape of the performance surface can be ascertained and very small but non-zero probability of unsatisfactory performance can be returned (Figure 2.19).

## 2.7 Specific CPGA information for running a reliability analysis

### 2.7.1 Introduction

The  $G(\vec{V})$  function is the method by which unsatisfactory performance can be measured for a reliability analysis. Unsatisfactory performance of individual piles can be caused by combined loads that exceed pile strength, and/or excessive deformations. To make such an assessment, two types of performance measures are needed: pile strength and pile cap displacement.

The limit states for CPGA include the axial loads and bending factors introduced at each pile because a load is applied to a pile cap, as well as pile cap displacement. The axial loads consider soil failures due to plunging and pull-out of the pile. The combined bending and axial compression on the pile can lead to failure of the connection of a pile to the pile cap or hinging of the pile at or near to the mudline.

USACE (1991) constrains the combined bending and axial compression in the upper pile region to:

$$\left| \frac{f_a}{F_a} \mp \frac{f_{bx}}{F_b} \mp \frac{f_{by}}{F_b} \right| \leq 1.0 \quad (2.26)$$

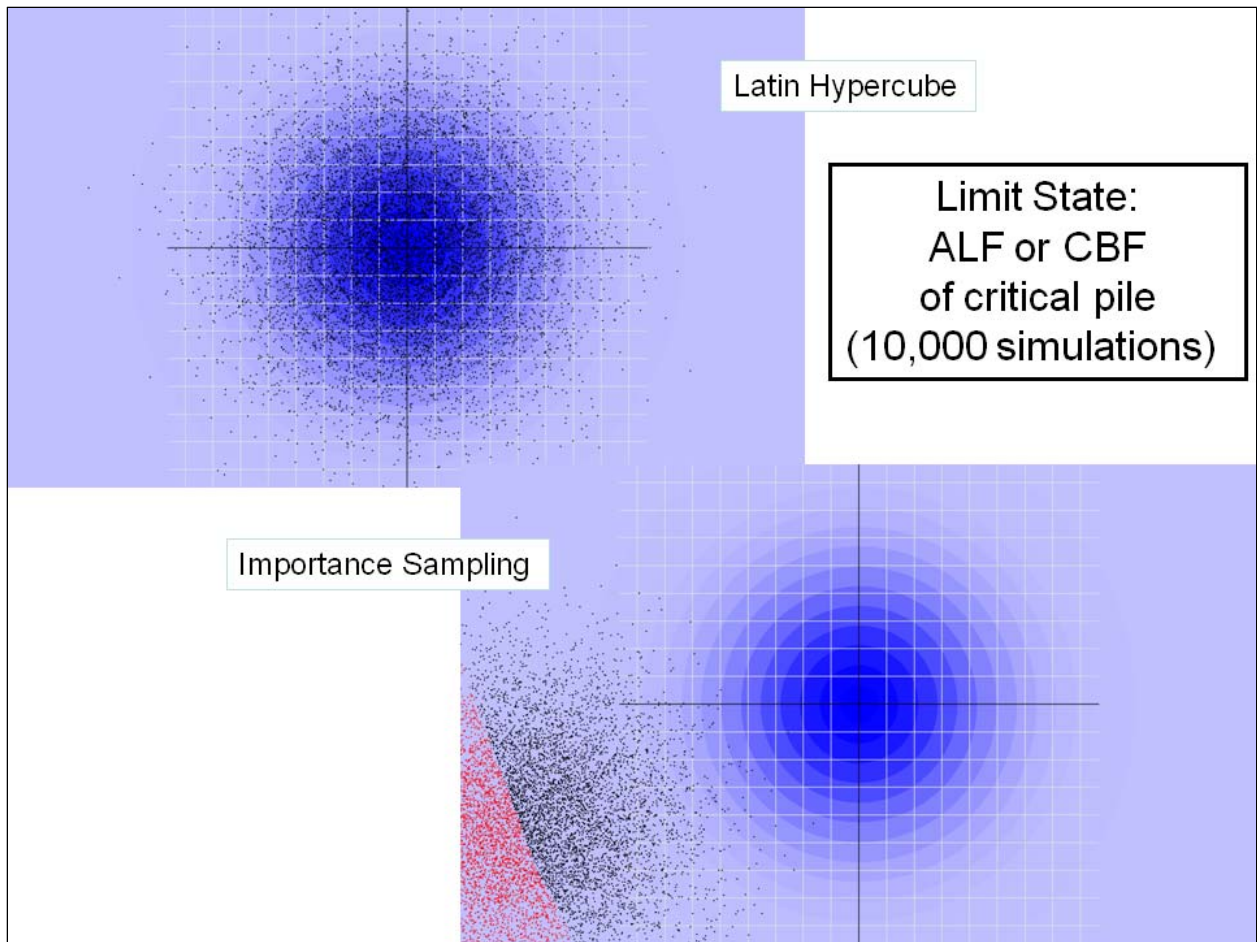


Figure 2.18. An example of Importance Sampling giving better results than sampling about the original distribution.

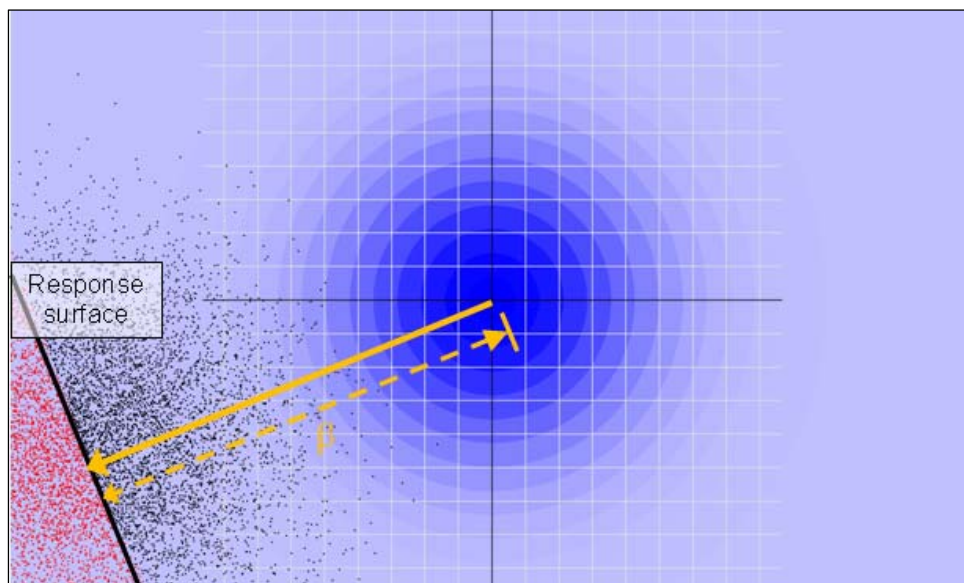


Figure 2.19. The sampling distribution is centered at the ASM design point on the response surface.

where:

- $f_a$  = computed axial unit stress;
- $F_a$  = allowable axial stress;
- $F_a = 5/6 \times 3/5 F_y = 1/2 F_y = 18$  ksi (for A-36 materials);
- $f_{bx}$  and  $f_{by}$  = computed unit bending stress;
- $F_b$  = allowable bending stress;
- $F_b = 5/6 \times 3/5 F_y = 1/2 F_y = 18$  ksi (for A-36 noncompact sections);

or

$$F_b = 5/6 \times 2/3 F_y = 5/9 F_y = 20 \text{ ksi (for A-36 compact sections).}$$

A 1991 Corps EM discusses displacement limitations at the pile cap for proper operations at locks and dams. It says the horizontal and vertical displacements resulting from applied loads should be limited to maintain the proper operation and integrity of the structure (USACE 1991). For locks and dams, experience has shown that vertical deflections of 1/4 in. and lateral deflections of 1/4 to 1/2 in. represent long-term movements, although operational requirements might dictate tighter restrictions on deformations. These limitations should be maintained in the calculated pile head movements. The EM displacement guidance needs to be adapted for use with next-generation, flexible approach walls. Specifically, loadings of the impact beam or deck can occur tens of feet above the pile-to-soil foundation interface that is below the mudline (i.e., at the top of the foundation). The additional deflections that occur in cases where the pile extends above the ground surface will need to be accounted for in the displacement criteria for flexible approach walls.

### 2.7.2 Pile stiffness

Lateral, axial, and torsional stiffness must be determined for a wide range of pile-soil conditions (Ayyub et al. 1997). The stiffness of a pile is a function of pile properties such as length, pile head boundary conditions, cross-sectional area, and moment of inertia; soil properties such as soil strength, unit weight, and stiffness; environmental factors such as ground-water table, deposit characteristics, and driving methods; and loading conditions such as cyclic, group, and time effects (Hartman et al 1989). A pile stiffness matrix can be represented by a 6-by-6 matrix of stiffness coefficient relating pile head forces to pile head displacements. Consult



Hartman et al. (1989) for general information about the methods used in CPGA to determine the lateral, axial, and torsional stiffness for a single pile.

The applied shearing forces and applied moments to a specified pile head engage the lateral stiffness of the pile and the soil foundation (that provides reactions for the piles). Several methods are available to determine stiffness. CPGA uses the classic beam-on-elastic foundation theory to model the behavior of a single pile, and represents the actual nonlinear modules of subgrade reaction by equivalent elastic secant modules. Such a model considers variation of pile displacement, skin friction resistance, and axial force along the pile length (Hartman et al. 1989). The axial stiffness of a pile is the axial force required to displace the pile cap a unit distance in an axial direction.

The CPGA analysis approach accounts for the pile-soil effect by applying an empirical factor to the axial stiffness coefficient for axially loaded structures. For compression piles, this coefficient ranges from 0.5 to 2.0. The accuracy of this approach depends on the accuracy in selecting this coefficient, which is correlated with available geotechnical data. Axial load in compression piles is transferred to the soil by a combination of tip bearing and skin friction (Hartman et al. 1989). The axial stiffness of tension piles usually is taken as 0.5 in sand and 0.75 to 0.8 in clay of the axially compression stiffness for that pile (Hartman et al. 1989). The torsional pile stiffness does not have a big effect on the pile group stiffness. Neglecting the torsional stiffness can be adequate for piles that are not fixed into the pile cap. The torsional pile stiffness can be considered in design, as described by O'Neill (1964), Stoll (1972), and Scott (1981). The 1989 CPGA manual notes that, for complex pile-soil conditions, pile head lateral, axial, and torsional stiffness should be calculated numerically using methods described by Dawkins (1978).

### **2.7.3 Pile strength performance limits**

#### **Pure axial load**

The interaction value ( $IV$ ) for a pile subjected to a pure axial load is given by:

$$IV = \left( \frac{F3}{AC} \right) \left( \frac{1}{OSF} \right) \leq 1.0 \text{ for piles in compression} \quad (2.27a)$$

or

$$IV = \left( -\frac{F3}{AT} \right) \left( \frac{1}{OSF} \right) \leq 1.0 \text{ for piles in tension} \quad (2.27b)$$

where  $AC$  and  $AT$  = allowable axial compressive and tensile loads;  $F3$  = actual axial load (positive equals compression); and  $OSF$  = overstress factor modifier where, for usual loads,  $OSF = 1.0$  and, for unusual or short duration cases,  $OSF = 1.33$ . As the interaction value ( $IV$ ) becomes 1 or larger, the potential of unsatisfactory performance in terms of strength failure of a pile becomes more imminent.

### Combined loads

The interaction method is used to deal with combined loads. The actual bending moments first are multiplied by a moment magnification factor to account for the second-order effect of load deformation for unsupported piles. The magnified moment and the actual axial loads then are compared to pile strength in bending and axial load using interaction equations (Hartman et al. 1989). The actual moments used in the interaction equations are the maximum moments in each pile for the load condition under consideration. For pinned piles, the maximum moments occur some distance below the pile cap level, which acts as a support to the piles. For a fixed pile, the maximum moments occur at the pile cap level or some distance below the ground level. In this section, interaction equations used to assess the adequacy of piles subjected to combined axial and bending loads are summarized for steel and timber piles. These equations are based on service-loads conditions and the working strength method (Hartman et al. 1989).

For steel H-piles subjected to axial compression and bending, the interaction value ( $IV$ ) is given by:

$$IV = \left( \frac{F3}{AC} + MF1 \left( \frac{|M1|}{AM1} \right) + MF2 \left( \frac{|M2|}{AM2} \right) \right) \left( \frac{1}{OSF} \right) \leq 1.0 \quad (2.27c)$$

where  $F3$  = actual axial load;  $AC$  = allowable axial load in compression;  $M1$  = actual bending moment about the 1 axis, where the 1 and 2 axes are the local axis for the each pile, (Hartman et al. 1989);  $M2$  = actual bending moment about the 2 axis;  $AM1$  = allowable bending moment about the 1

axis;  $AM2$  = allowable bending moment about the 2 axis;  $MF1$  = moment magnification factor about the 1 axis;  $MF2$  = moment magnification factor about the 2 axis; and  $OFS$  = overstress factor. For steel H-piles subjected to axial tension and bending, the interaction value ( $IV$ ) is given by:

$$IV = \left[ \frac{-F3}{AT} + \frac{|M1|}{AM1} + \frac{|M2|}{AM2} \right] \left( \frac{1}{OSF} \right) \leq 1.0 \quad (2.27d)$$

where  $AT$  = allowable axial load in tension. For rounded timber and steel piles, the corresponding equations are:

$$IV = \left( \frac{F3}{AC} + \left( \frac{MF1}{AM1} \right) \sqrt{M1^2 + M2^2} \right) \left( \frac{1}{OSF} \right) \leq 1.0 \quad (2.27e)$$

and

$$IV = \left( \frac{-F3}{AT} + \left( \frac{1}{AM1} \right) \sqrt{M1^2 + M2^2} \right) \left( \frac{1}{OSF} \right) \leq 1.0 \quad (2.27f)$$

As the interaction value ( $IV$ ) becomes 1 or larger, the potential of unsatisfactory performance in terms of strength failure of a pile becomes more imminent.

### **Pile cap displacement performance**

The pile cap displacement matrix of size 6 is determined by CPGA (Hartman et al. 1989) as:

$$\{Q\} = [K]\{DS\} \quad (2.28)$$

where  $Q$  = applied loads;  $K$  = stiffness matrix; and  $DS$  = displacements. The  $Q$  and  $DS$  vectors (i.e., 6-by-1 matrices) are given by:

$$\{Q\} = \begin{Bmatrix} Px \\ Py \\ Pz \\ Mx \\ My \\ Mz \end{Bmatrix} \quad (2.29)$$

and

$$\{DS\} = \begin{Bmatrix} Dx \\ Dy \\ Dz \\ Rx \\ Ry \\ Rz \end{Bmatrix} \quad (2.30)$$

where  $P$  and  $M$  are applied loads and moments in the  $x$ ,  $y$ , and  $z$  directions; and  $D$  and  $R$  are displacements and rotation in the  $x$ ,  $y$ , and  $z$  directions. The  $K$  matrix is for the pile group. Equation 2.21 can be used to solve for the six  $DS$ . The performance function for displacements is:

$$DS < DL \quad (2.31)$$

where  $DL$  = the displacement limit that need to be set for the six displacement types. The user specifies this value in a CPGA-R reliability analysis. As the displacement ( $DS$ ) reaches the displacement limit ( $DL$ ) or larger, the potential of unsatisfactory performance in terms of displacement failure of a pile cap becomes more imminent.

Recall, for locks and dams, experience has shown that vertical deflections of 1/4 in. and lateral deflections of 1/4 to 1/2 in. represent long-term movements, although operational requirements might dictate tighter restrictions on deformations (USACE 1991).

## 3 CPGA-R Graphical User Interface (GUI)

### 3.1 Revisiting the CPGA GUI

The original CPGA GUI allows for the definition of and solution to pile group problems. It permits input of as many as 2,000 piles and databases of pile and soil properties, as well as a database of loads to be applied to the pile group. The piles are specified individually by the location of the top of the pile, the batter and angle, and whether the top is fixed, pinned, or free of the pile cap. Pile properties and limits are assigned to a pile as indexes into a property database.

The databases of properties can hold 20 entries each that might hold multiple properties. For instance, a pile properties database entry contains the Young's modulus for the pile ( $E$ ), moments of inertia along the two lateral axes of the pile ( $I1$  and  $I2$ ), the area of the pile ( $Area$ ), and matrix terms for pile interactions with the soil ( $C33$  and  $B66$ ).

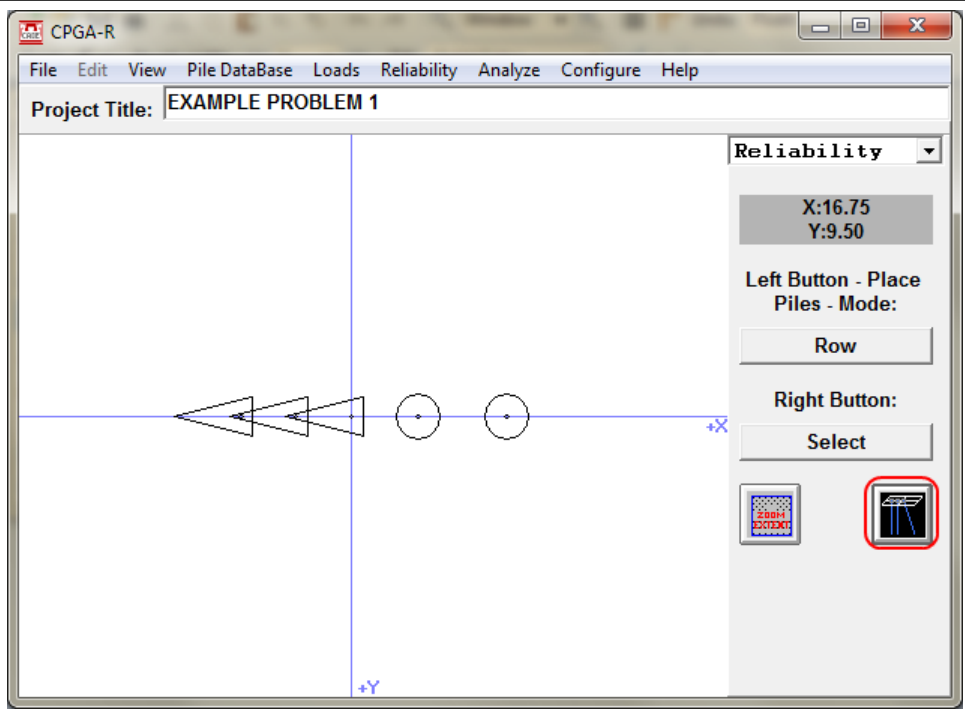
Load cases are entered into their own database. These entries include the forces and moments acting at the origin of the system. As many as 40 load case database entries can be created. These loads are applied to the whole system and not associated with individual piles.

These pile and database details will be important in the following discussion of GUI additions for reliability analysis.

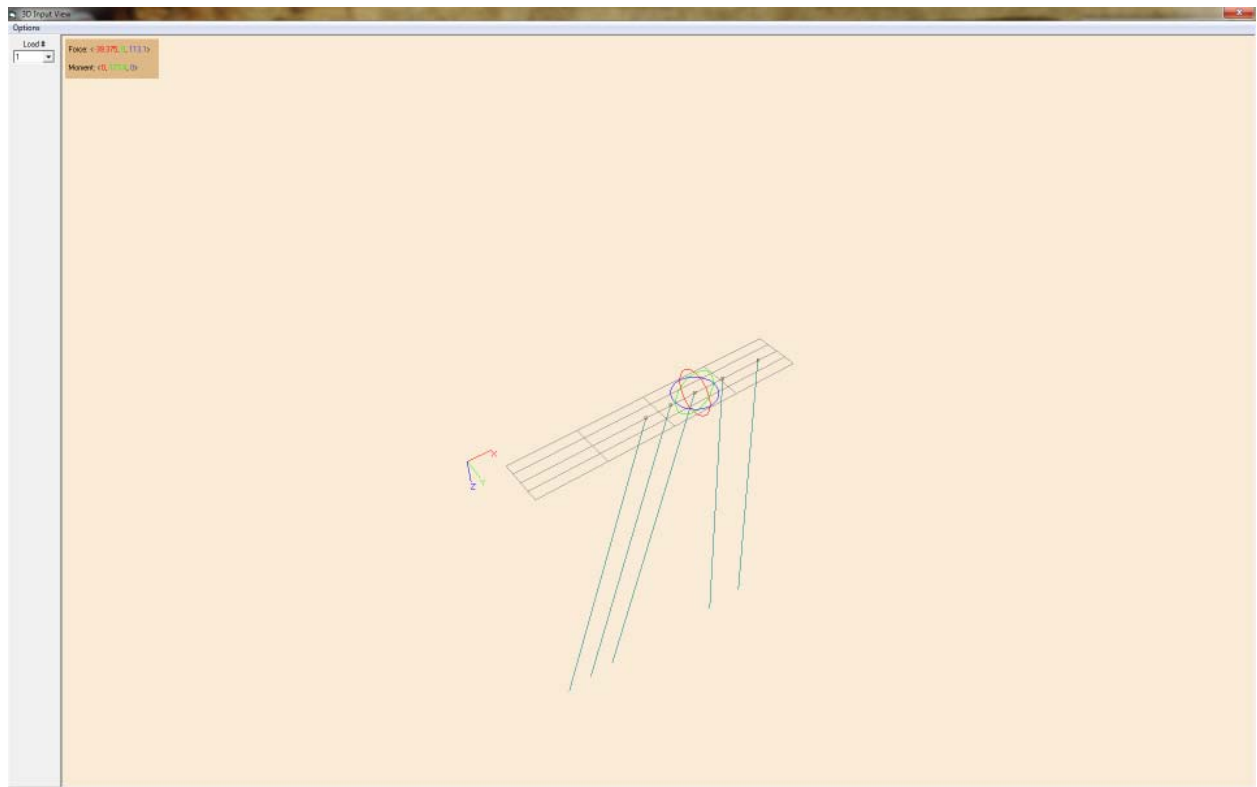
As with any revisitation of a software product, new features were added to make the original interface better and to preposition the additions. Most of the upgrades were cosmetic, but two features should be mentioned.

#### *Preview function*

A new method for previsualizing the data input as a 3D plot of piles has been added so the user can verify the pile layout and load conditions applied to the system. This new feature is accessed by using a button to the right of the pile entry area (Figure 3.1a). A new window then opens, showing the pile layout and the origin of the coordinate system, where load cases are applied. A drop-down list allows the user to select a specific load case to visualize. The user can right-click-drag on the view area to look at the system



(a) The CPGA-R GUI with added 3D input viewing feature.



(b) The input piles, displayed with loads and load directions in 3D.

Figure 3.1. Illustration of the new 3D input viewing features of CPGA-R.

from another angle (Figure 3.1b). The magnitudes of the currently selected loads are displayed in the upper-left corner of the display area. A menu option allows the user to close this window.

### *Pile Information function*

When the user moves the mouse cursor over a pile in the pile entry area, that pile is colored dark green and an information box appears to the right of the pile entry area. This box contains the pile number, position, batter, angle, and database assignments for properties of the pile (Figure 3.2).

## **3.2 GUI additions to support CPGA reliability analysis**

To apply reliability techniques to CPGA, the GUI needed to be changed to allow for variable creation, definition of limit states, and for elements to perform the reliability analysis (i.e., Latin Hypercube simulation, ASM, or Importance Sampling based on an ASM analysis). Input files and the methods to access them also have been added to the interface for the original CPGA program. The resulting program is called CPGA-R, with the R reflecting the reliability analysis capability of the software.

The CPGA-R program has been modified to allow for a standard CPGA deterministic analysis, plus a reliability analysis. To differentiate between data that allows for only a standard run and data that includes reliability information, a drop-down list selector was added at the upper-right corner of the main window with options for either standard or reliability input (Figure 3.3). A circle in this window designates a vertical pile, while a triangle designates a batter pile. Figure 3.3 shows there are two vertical piles and three batter piles being used in this model. When the standard mode for data input is selected, the menu items related to input of reliability information and the menu items associated with running a reliability analysis are disabled. Choosing the reliability option enables these menu items.

Data for a complete CPGA analysis should be entered before reliability input is created. The CPGA model, of course, defines which data may be varied. This does not mean that the CPGA data may not be altered, but deletion of previously existing data could mean reliability data might not match the newly executed model. It is highly recommended that reliability data not be entered until a complete CPGA pile group input model is created.

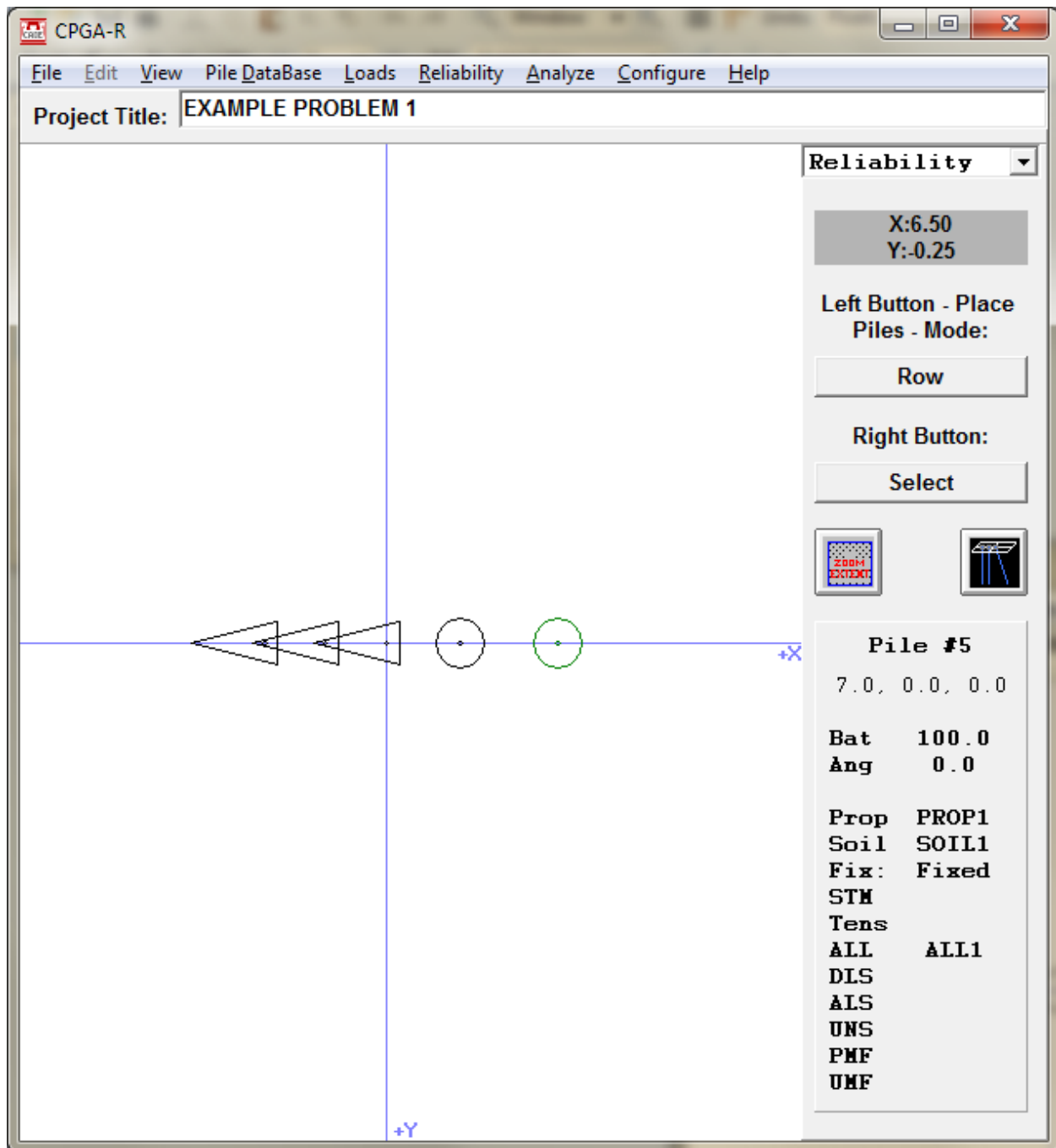


Figure 3.2. The Pile Information addition to the CPGA-R GUI.

To create reliability input, select the Reliability->Set Parameters option from the main menu (Figure 3.4). This opens the Reliability Input window (Figure 3.5).



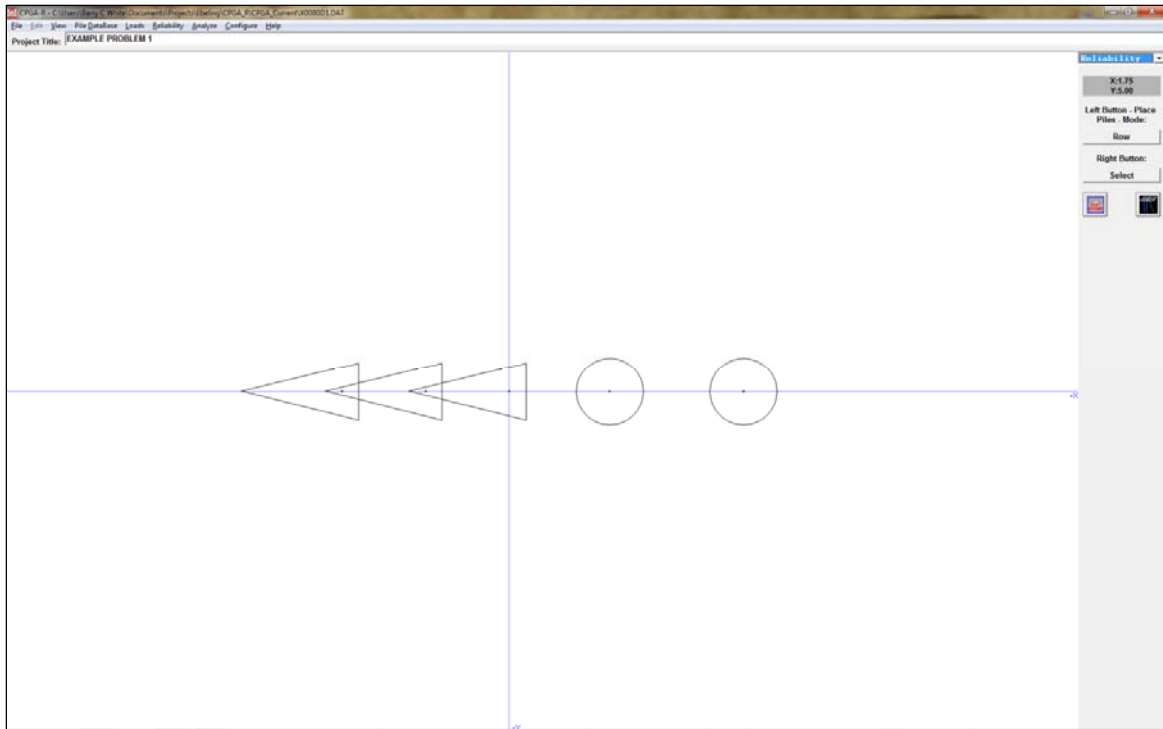


Figure 3.3. The CPGA-R window (with reliability input).

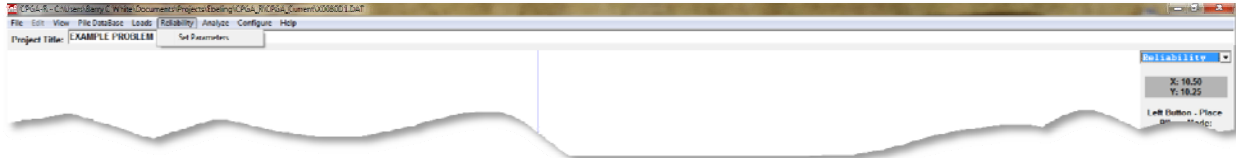


Figure 3.4. The Set Parameters menu.

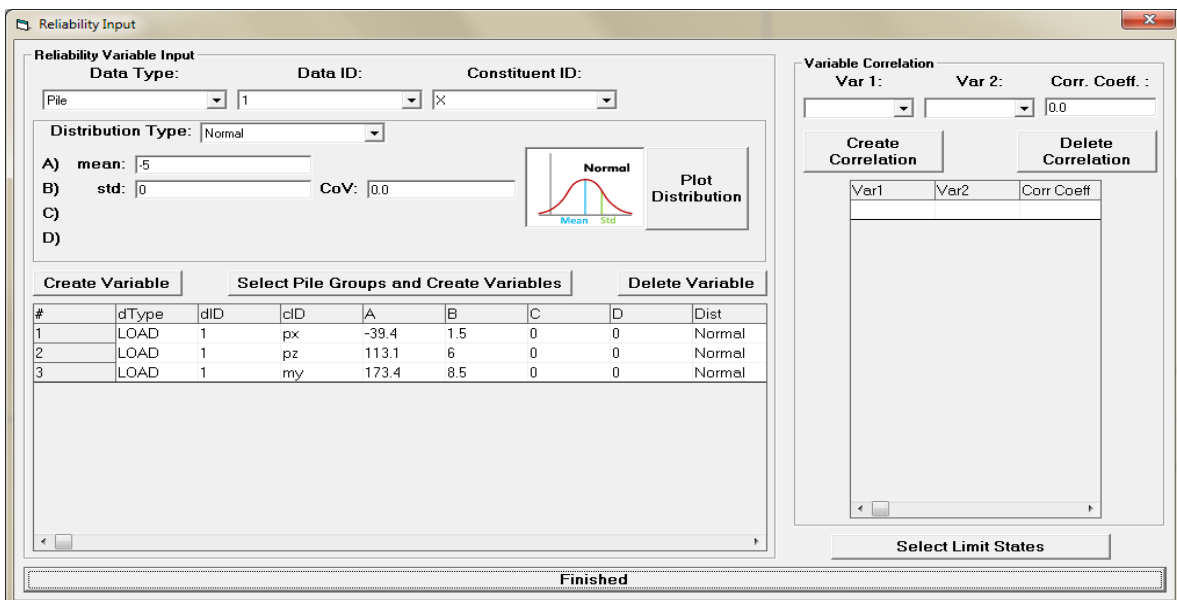


Figure 3.5. The Reliability Input window.

The Reliability Input window has three parts: the Reliability Variable Input and Variable Correlation sections, and the Select Limit States button, which opens the Select Limit States window.

### 3.2.1 Reliability Variable Input

This section is where the variables for a reliability analysis are defined. Variables are defined based on existing data items in the pile group model. Specifying which input data will vary is the job of the top three drop-down input lists. These drop-down lists allow the user to select a Data Type, Data ID, and Constituent ID. The Data Type can be a pile (for individual piles), a property database, or the load database. The Data ID is either a pile number or an index for an entry in a database. The Constituent ID is the selector for a specific entry for a pile or database. For instance, the user might select a Data Type of Pile, a Data ID of 5, and a Constituent ID of X to make a variable of the fifth pile's  $X$  coordinate. Similarly, selecting a Data Type of Soil, a Data ID of Soil2, and a Constituent ID of the soil modulus of elasticity  $e_{soil}$  allows the engineer to make a variable of the 2<sup>nd</sup> soil database entry of  $e_{soil}$ .

How the data varies is specified below the variable selectors. The first entry is the Distribution Type. The types available in the drop-down list are Normal, Bounded Normal, Log-Normal, Bounded Log-Normal, Uniform, and Triangle. Each distribution has a different subset of input data. A diagram to the right of the Distribution Type selector shows a graphical plot of the different inputs and how they are applied.

Normal Distribution extends to plus and minus infinity, but has the greatest probability at the mean, a spread determined by the standard deviation or the coefficient of variation ( $COV$ ), which is the standard deviation divided by the mean.

Bounded Normal Distribution has boundaries for how far the variable will vary. The mean and standard deviation/coefficient of variation are specified as before, but the limits for how the variable varies are entered in absolute model coordinates. The area of the PDF must still equal 1.0; therefore, the area of the PDF distribution beyond the boundaries is calculated and that area is redistributed under the bounded region as a uniform region and summed to the original PDF values at that location. The upper and lower bounds are enforced in the input.

Log-Normal Distribution is the logarithm of the Normal Distribution. This PDF distribution extends from a 0.0 to plus infinity or from 0.0 to minus infinity, depending if the mean is positive or negative, respectively. The inputs for this distribution are the mean and the standard deviation.

Bounded Log-Normal Distribution has boundaries for how far the variable will vary. The mean and standard deviation/coefficient of variation are specified as before, but the limits for how the variable varies are entered in absolute model coordinates. Specifying a limit that is of the opposite sign of the mean implies that boundary is not needed, because the PDF is 0.0 at that location. The area of the PDF must still equal 1.0; therefore, the area of the PDF curve beyond the boundaries is calculated and that area is distributed under the bounded region as a uniform region and summed to the original PDF values at that location.

Uniform (Bounded Uniform) Distribution is defined only by the absolute boundary conditions. Because the area of the PDF is guaranteed to be 1.0, the Bounded Uniform Distribution is a rectangle with fixed probability between the bounds.

Triangular Distribution is defined by three absolute coordinates: the lower boundary, upper boundary, and point of peak probability. The data input is limited so the lower bound is less than or equal to the peak coordinate which, in turn, is less than or equal to the upper boundary. The lower boundary for this PDF is less than the upper boundary. In this manner, triangular regions can be created that are right rectangular in either direction, and any distribution may lay between bounds.

Left of the Distribution Type plot is a Plot Distribution button. Clicking this button brings up a plot of the currently input distribution, enabling the user to view the PDF and verify the data will be dispersed in a fashion consistent with the user's intention. The window that displays the data will show the distribution in terms of a PDF or a CDF.

When the data entered is correctly tailored for the selected Data Type, Data ID, and Constituent ID, the user can create the variable for a reliability analysis by clicking the Create Variable button beneath the distribution creation box. The variable is created in the list beneath the Create Variable button.

CPGA-R allows for the creation of as many as 2,000 piles with their own locations, angles, and batters. Because there might be a large number of

piles needing variable geometric properties, the Select Pile Groups and Create Variables button was added to the Reliability Input window. This button is centered above the defined variable grid.

Pressing the Select Pile Groups and Create Variables button activates the Select Piles for Assigning Variable Properties window (Figure 3.6), which allows the user to select a set of piles that will have variable properties.

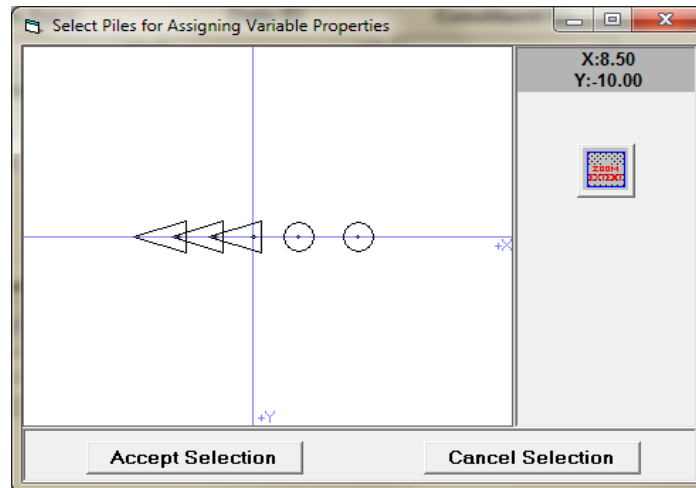
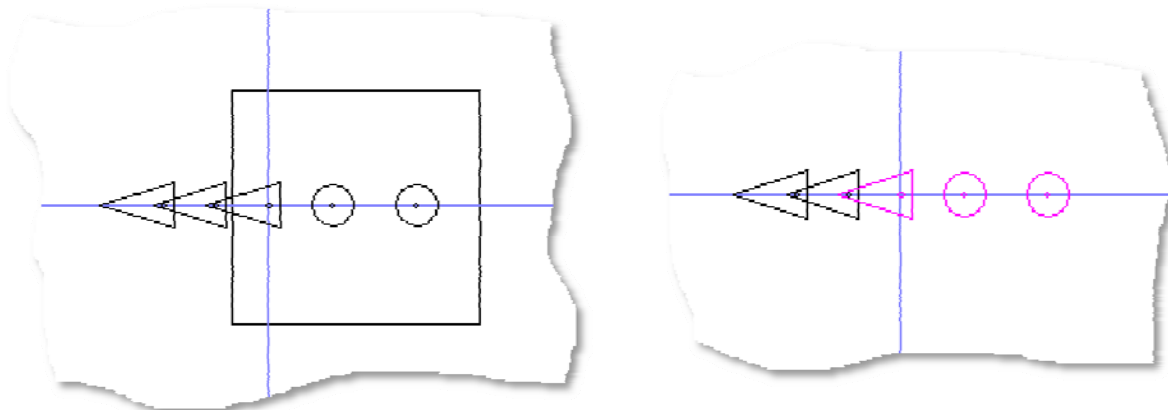


Figure 3.6. The Select Piles for Assigning Variable Properties window for creating groups of pile variables.

Piles are selected by using a left mouse click-drag operation (Figure 3.7a). Piles that have their pile centers in the selection box are selected. Selected piles are shown in pink (Figure 3.7b). Using the Ctrl key during the selection process allows for more piles to be added to the set. To deselect all piles, use the left mouse click-drag operation, without pressing the Ctrl key, to choose an area containing no pile centers.

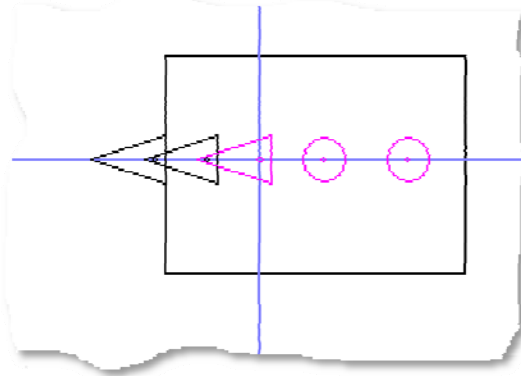


(a) Left mouse click-drag selection box.

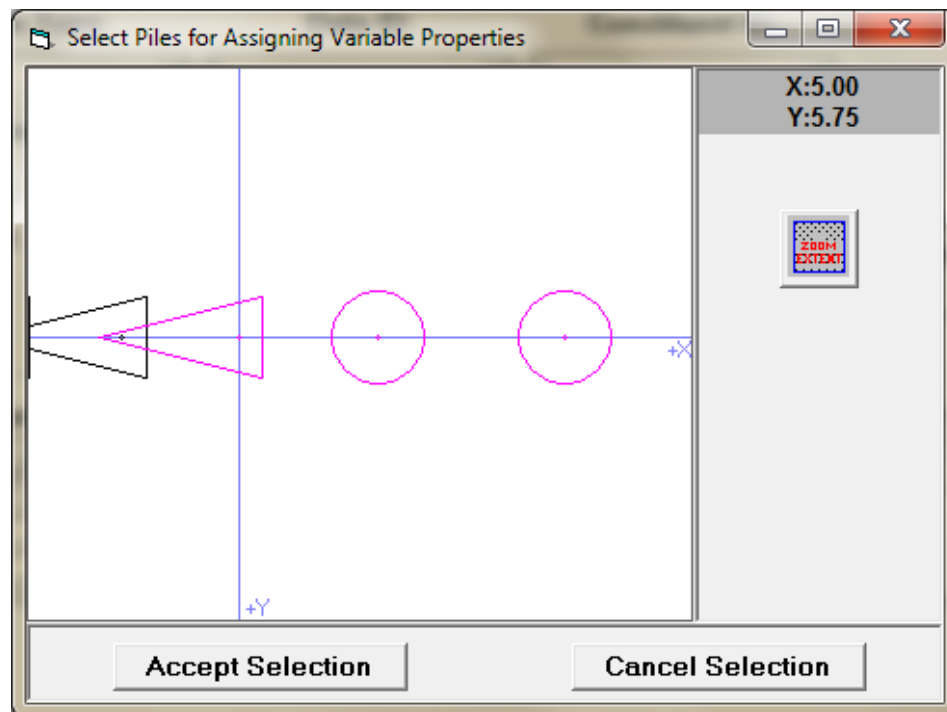
(b) Selected piles.

Figure 3.7. Using the left mouse click-drag operation to select multiple piles.

Because a large number of piles can occupy a large area, the pile selection area has a zoom feature that is accessed using the right mouse. The area defined by the right mouse click-drag operation is zoomed to fill the screen and make pile selection easier (Figure 3.8). To show the full extent of the piles, press the Zoom Extents button to the right of the pile selection area.



(a) Right mouse click-drag operation to create a zoom area.



(b) Magnified window when the area is selected.

Figure 3.8. Zooming to aid in the selection process.

When the proper piles have been selected, press the Accept Selection button. Pressing the Cancel Selection button ends the process, with no variables created. Pressing the Accept Selection button opens the Selected

Pile Variable Definition window (Figure 3.9), allowing multiple variables to be created for each pile in the selection list.

For the selected piles, check the variables desired then input the distribution information for that variable (distances are given relative to the pile location or mean):

	Distribution	Std. Dev.	Start	Mid	End	
<input type="checkbox"/> Position X:	Normal	1.0	-1.0	0.0	1.0	
<input type="checkbox"/> Position Y:	Normal	1.0	-1.0	0.0	1.0	
<input type="checkbox"/> Position Z:	Normal	1.0	-1.0	0.0	1.0	
<input type="checkbox"/> Batter:	Normal	1.0	-1.0	0.0	1.0	
<input type="checkbox"/> Angle:	Normal	1.0	-1.0	0.0	1.0	

Buttons: Add Variables, Cancel

Figure 3.9. The Selected Pile Variable Definition window.

The check-boxes to the left of the window permit the user to choose which geometry properties will vary for the selected piles. If the Position X check-box was checked, the user could input data for how each selected pile's X-position would vary. Once a box is checked, properties distribution can be determined using the drop-down combo box. The choice of distributions is the same as the options available in the Reliability Input window (Normal, Bounded Normal, Log-Normal, Bounded Log-Normal, Uniform, and Triangle). An iconic representation of the chosen distribution is at the far right of the window.

Different inputs are required for different distributions. For instance, Normal Distribution requires only the standard deviation to be input, whereas Triangular Distribution requires the start point, end point, and point at the peak of the distribution (mid). The input windows for these variables are enabled based on the chosen distribution (Figure 3.10). Keep in mind, the distribution variables are supposed to be input relative to the current location, angle, and batter of each selected pile.

Figure 3.11 shows the result of pressing the Add Variables button in the Selected Pile Variable Definition window, with the selected piles and variables defined in Figure 3.10. For piles 3, 4, and 5, new variables were defined for the X and Z locations and added to the list. Pile numbers can be recovered in the input window's pile input area by moving the mouse over individual piles, as discussed in Subsection 3.1 of this chapter. The X location variables use a Normal Distribution and the Z location variables use a Triangular Distribution.

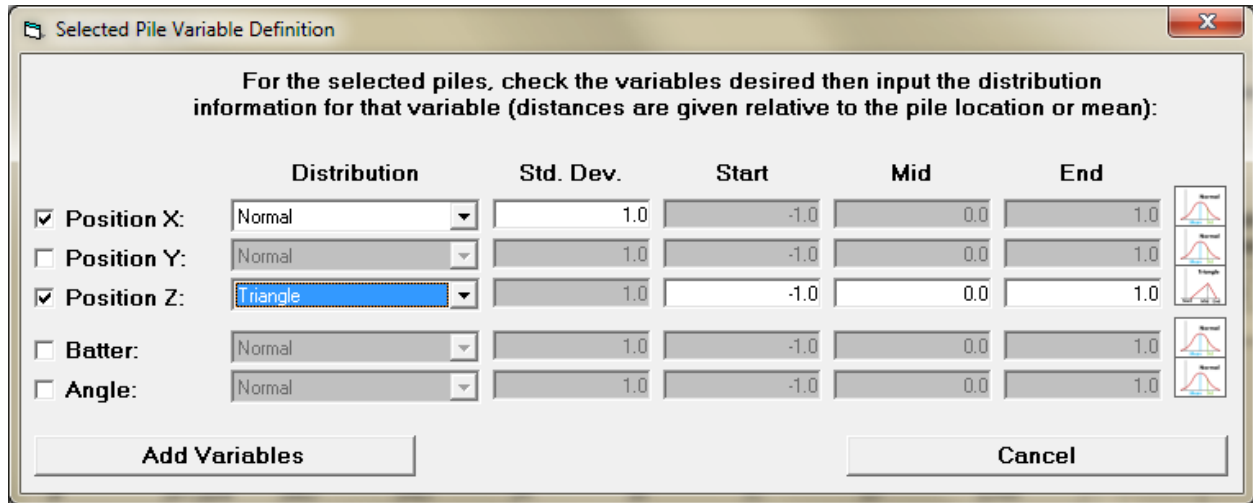


Figure 3.10. Chosen properties and their distribution inputs.

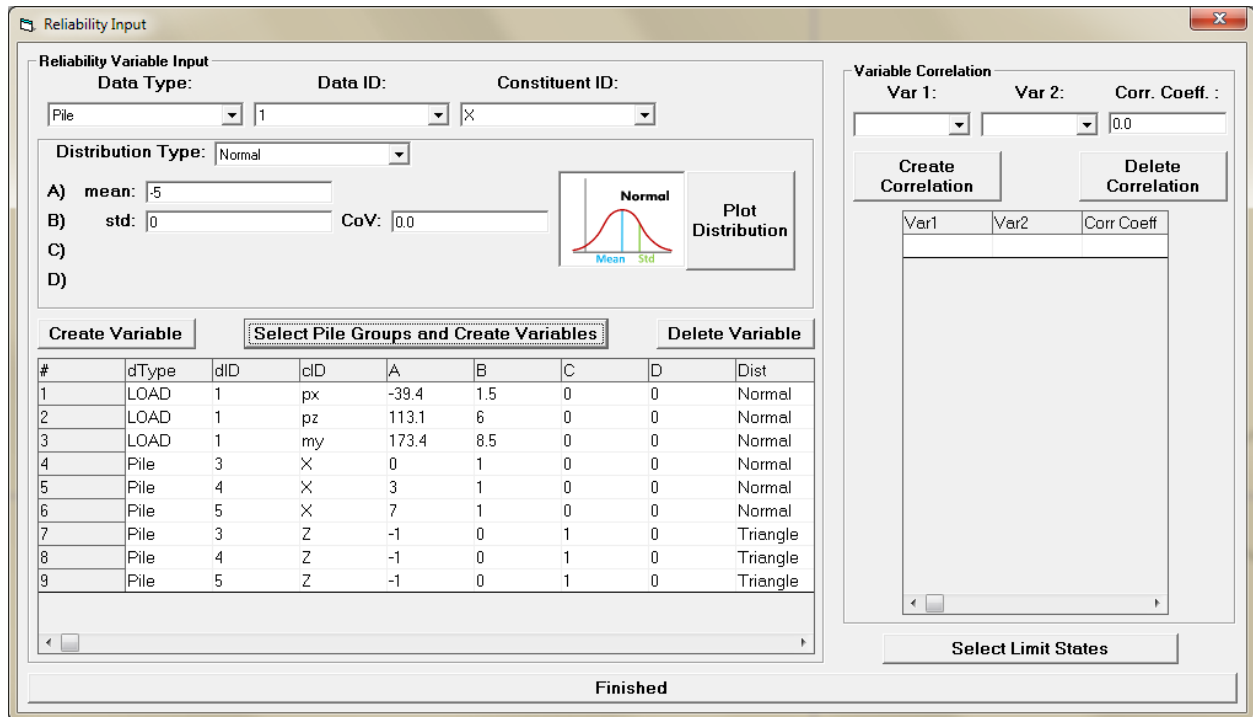


Figure 3.11. Variables created with the selected piles.

To delete a variable, select it in the list below the Create Variable button and click the Delete Variable button. The currently selected reliability variable will be removed from the list.

### 3.2.2 Variable Correlation

This section is in the upper-left part of the Reliability Input window. A list of correlations among the variables can be created by specifying any two

variables and the value for their correlation coefficient ( $\rho$ ). Two drop-down lists allow the user to select variables, according to their indexes in the variable list in the Reliability Variable Input section. The correlation coefficient text box allows for the input of a correlation coefficient ( $\rho$ ) between -1.0 to 1.0. When the correlation has been specified, clicking Create Correlation checks the input for correctness, then, if the data is correct, adds this correlation to the list. If a correlation has been created between the two selected variables, the correlation coefficient for the existing correlation is changed to the new value for  $\rho$ . Selecting a correlation on the list and clicking the Delete Correlation button removes the selected correlation from the list.

### 3.2.3 Assign Limit States

Pressing this button in the Reliability Input window opens the Assign Limit States window (Figure 3.12), which contains methods for assigning specific limit states that will be checked in ASM and simulation runs. This window is divided among three areas: Displacement and Rotations, Individual Pile Limit State Grid, and Group Pile Selection.

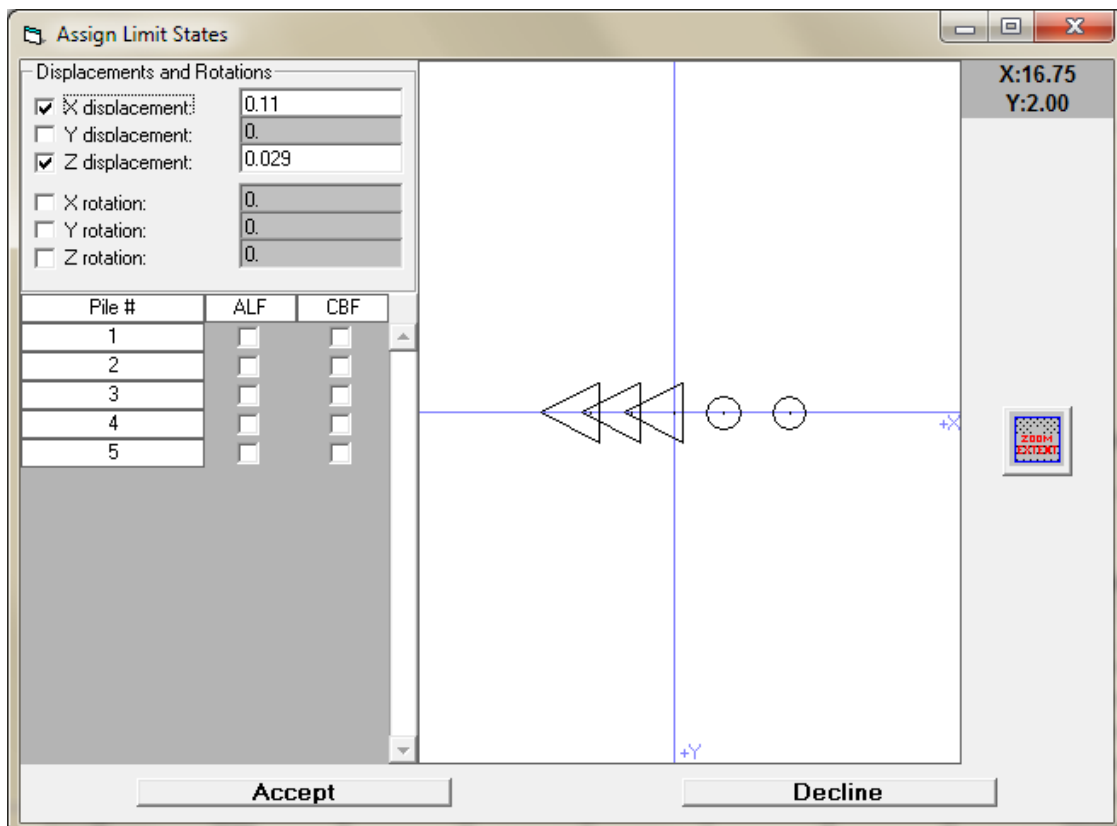


Figure 3.12. The Assign Limit States window, with two limit states selected.



The Displacements and Rotations area has a series of check-boxes for  $X$ ,  $Y$ , and  $Z$  displacements and rotations about the  $X$ ,  $Y$ , and  $Z$  axes. Each checked item has an input text box to enter the pile cap motion allowed before a limit state is exceeded. For instance, in the input above, if the pile cap is displaced by more than 0.25 in. (0.11 ft) in either direction of the  $X$  axis, a limit state is exceeded.

The Individual Pile Limit State Grid area has a check-box for the Axial Load Factor (ALF) and Combined Bending Factor (CBF) for each individual pile. Checking a box means the limit state for that individual pile will be tested for a simulation or ASM run.

Because there can be as many as 2,000 piles in a CPGA-R input file, it can become difficult to check the check-boxes for a large number of individual piles. In these circumstances, the group pile selection area becomes important. Selection and zooming can be performed with the left and right click-drag operations, respectively. This occurs in much the same manner as pile selection occurs in the Pile Selection window. However, when piles are selected with the left click-drag operation (Figure 3.13), they are not highlighted. Instead, when a selection is finished, a window appears that lets the user choose which limit state(s) will be assigned to each individual pile in the selection (Figure 3.14).

When this window is accepted, the Individual Pile Limit State Grid area is updated to reflect the changes to the selected piles (Figure 3.15).

When the correct limit states have been changed, the user can accept the changes. Declining the changes will keep the limit states the same as before the Assign Limit States window was opened.

### **3.3 GUI additions for saving and restoring reliability information**

Once reliability information has been entered for a CPGA-R analysis, the user probably will want to save that information. Also, the user might want to re-create the output, to solve with minor model changes, or to make edits to the reliability input. For these circumstances, a pile group reliability (.PGR) file was created. The .PGR file contains all the information typed in the Reliability Input window. This information is kept in a separate file from the CPGA data file because it is not required by the CPGA processor. However, the CPGA data file path is stored in the .PGR file, so the files can be retrieved together. The format for the .PGR file is in Appendix C.

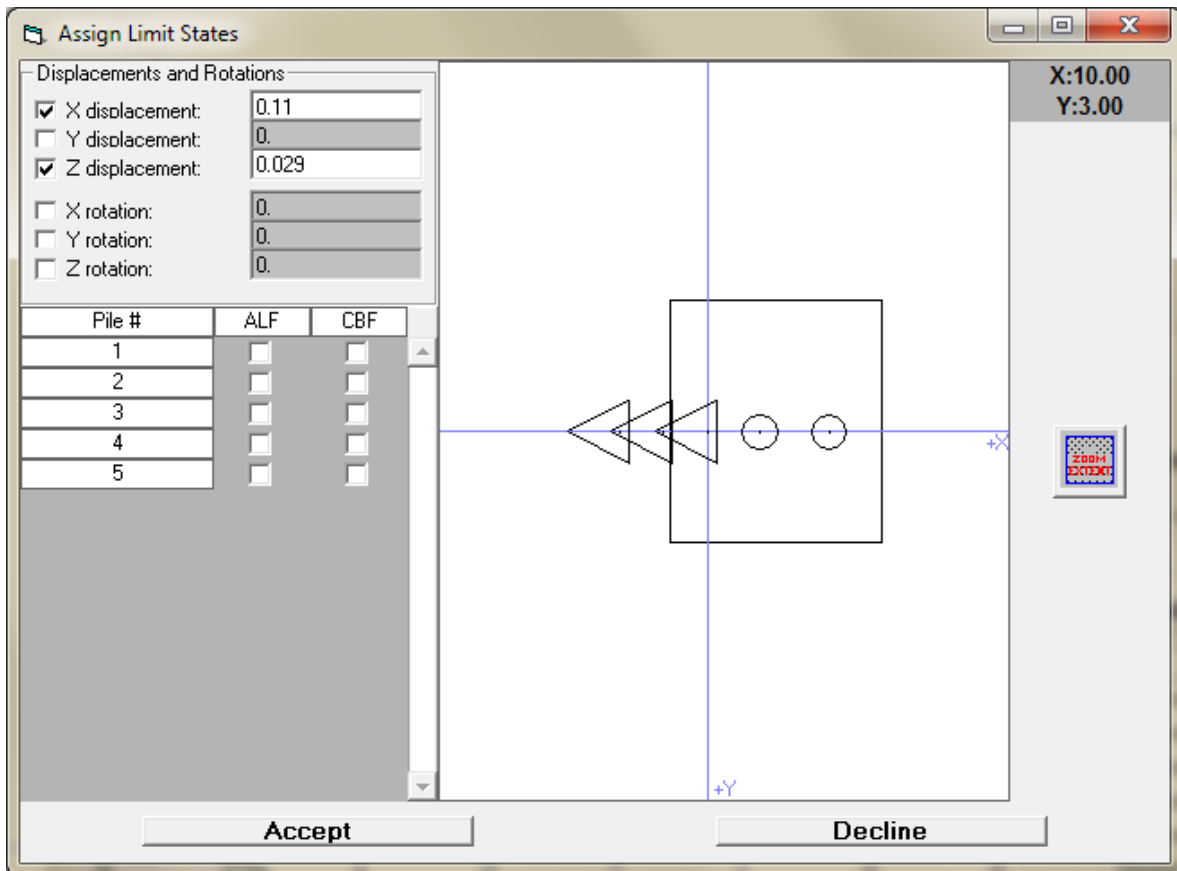


Figure 3.13. Selecting multiple piles for limit state assignment.

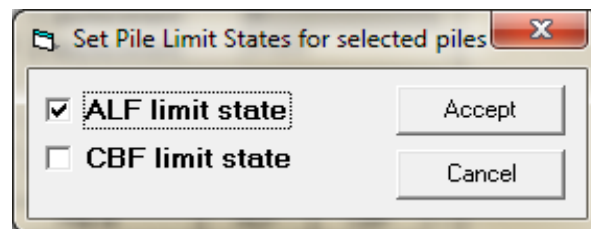


Figure 3.14. Setting the limit state for selected piles.

To save the file, the user must choose from the main menu on the CPGA-R window File->Save Reliability or File->Save Reliability As (Figure 3.16). If a new .PGR is being created, a file dialog is opened so the user can name the file.

To load a .PGR file, the user must choose the File->Open Reliability option from the main menu on the CPGA-R window. This will bring up a file dialog to open an existing .PGR file. The sister CPGA data file is loaded with the .PGR file so the variables defined match the CPGA input. When the .PGR data has been loaded, the drop-down menu in the upper left of the CPGA-R main window will be changed to show reliability data has been input.

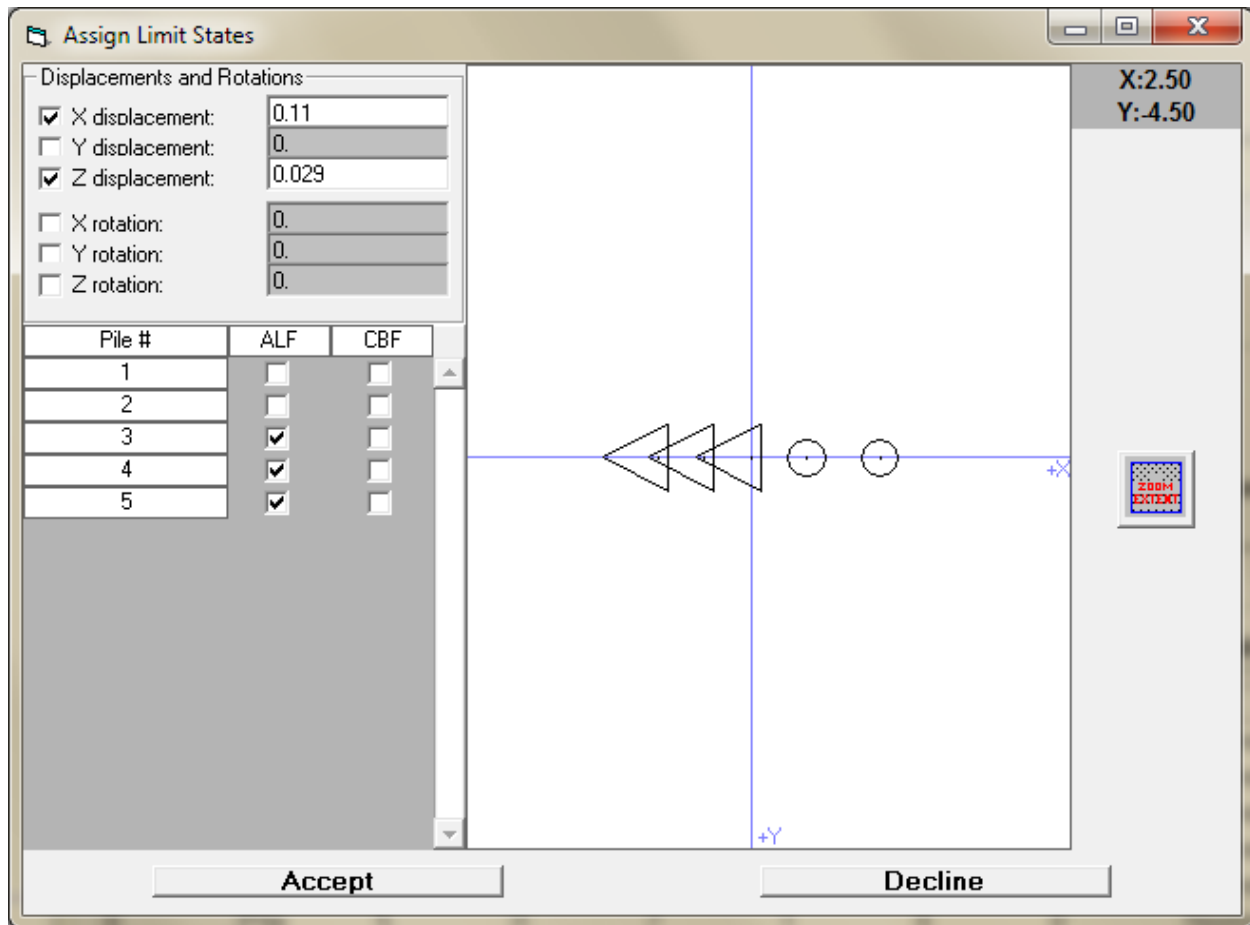


Figure 3.15. Updating the individual piles.



Figure 3.16. The reliability file options from the CPGA-R main menu.

### 3.4 Performing a reliability run

There are a couple of ways to perform a CPGA reliability analysis. These options are available from the CPGA-R Analyze main menu option, when the reliability mode has been set for the program (Figure 3.17).

They are the ASM option, and the Latin Hypercube and Importance Sampling combined with Latin Hypercube simulation options.



Figure 3.17. CPGA-R Analyze options (with reliability options).

The difference between the ASM and simulation options is explained in Chapter 2. To perform an ASM analysis, the user can click the menu option and the program will perform the necessary runs, and converge to a solution for all possible limit states. Also, the most likely limit state to occur is revealed at the end of the analysis output data.

When the user selects the Latin Hypercube or Importance Sampling simulation method, he will be asked to enter a number of simulation runs to make. The runs will be started, checking for any limit state to be reached.

When the reliability run is finished, the results will be shown in the Reliability Output window (Figure 3.18) and can be saved to another location. The results give the probability of unsatisfactory performance for the limit states involved and the overall or greatest probability of unsatisfactory performance. Detailed information about intermediate and final values for the reliability parameters discussed in Chapter 2 is presented in this ASCII output file. This output provides the information for use in a risk and reliability engineering for major rehabilitation studies (USACE 2011).

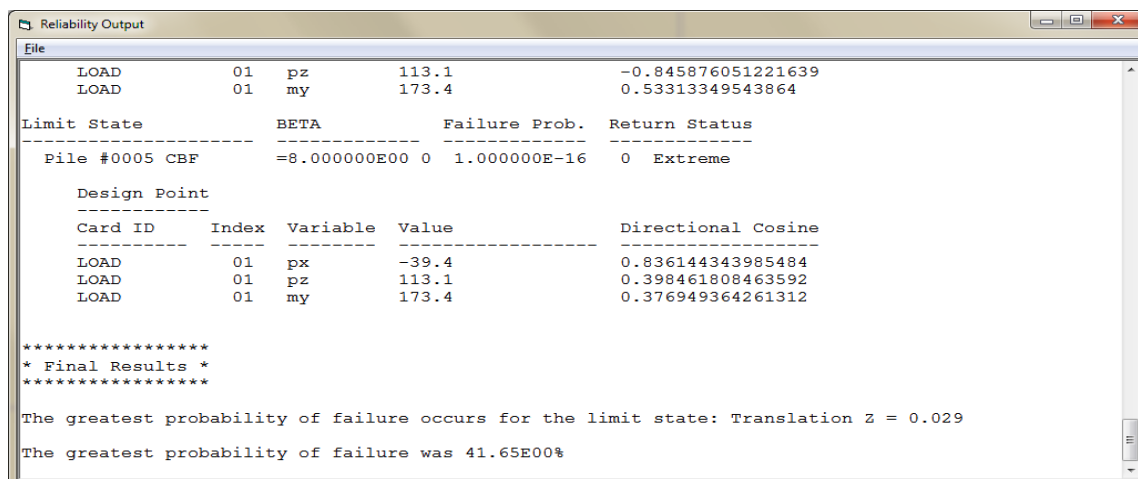


Figure 3.18. CPGA-R Reliability Output window.

## 4 Testing CPGA-R

CPGA-R testing is the focus of this chapter. Comparisons are made to results computed using RCPGA in the initial test problems (Ayyub et al. 1997). Additional problems aim to highlight fundamental differences among the reliability methods of ASM, Latin Hypercube simulation, and Importance Sampling with Latin Hypercube simulation.

### 4.1 CPGA-R

To perform an execution, CPGA-R requires two files: a fully qualified CPGA input file and the reliability data, either input through the reliability main menu item or from a .PGR file. To test CPGA-R, an example CPGA base file was used with varying reliability data. Described next are the input data and the resulting output for different reliability analyses.

#### 4.1.1 CPGA base input file

Ayyub et al. (1997) used one of the example problems provided with the original distribution of CPGA for his own. This problem was chosen because it represents a typical batter pile system for supporting the base reinforced concrete slab of the retaining wall section, and that first had been analyzed by Hrennikoff (1950). This example features a low number of piles, and the system vertical and batter piles supporting the cap.

Hrennikoff (1950) presented a retaining wall supported by transverse rows of piles centered at 3-ft intervals along the wall (Figure 4.1). There are five piles in a row, with the first two back piles being vertical and the three front piles inclined with a 3-to-1 batter. The unit weight of the concrete is 150 lb/ft<sup>3</sup>, and the unit weight of the soil is 100 lb/ft<sup>3</sup>. The angle of friction for the soil is 30°. The earth pressure is found using Rankine's theory. The pressure, along the imaginary section cut B-B in Figure 4.2, at the back is given by:

$$P_A = \frac{1}{2} \gamma_{moist} H_{B-B}^2 k_A \quad (4.1)$$

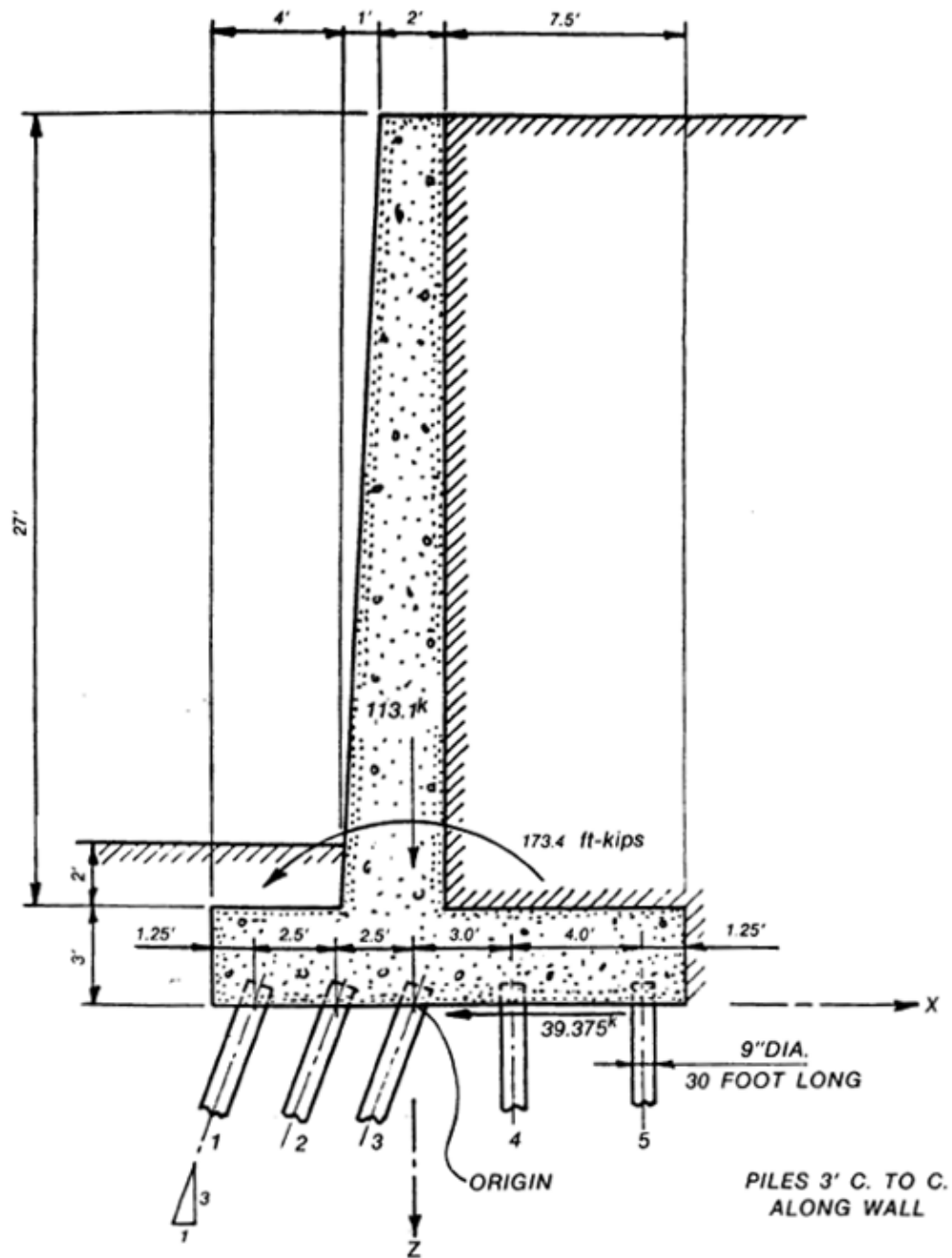


Figure 4.1. Example problem of retaining wall on piles (after Hrennikoff 1950).

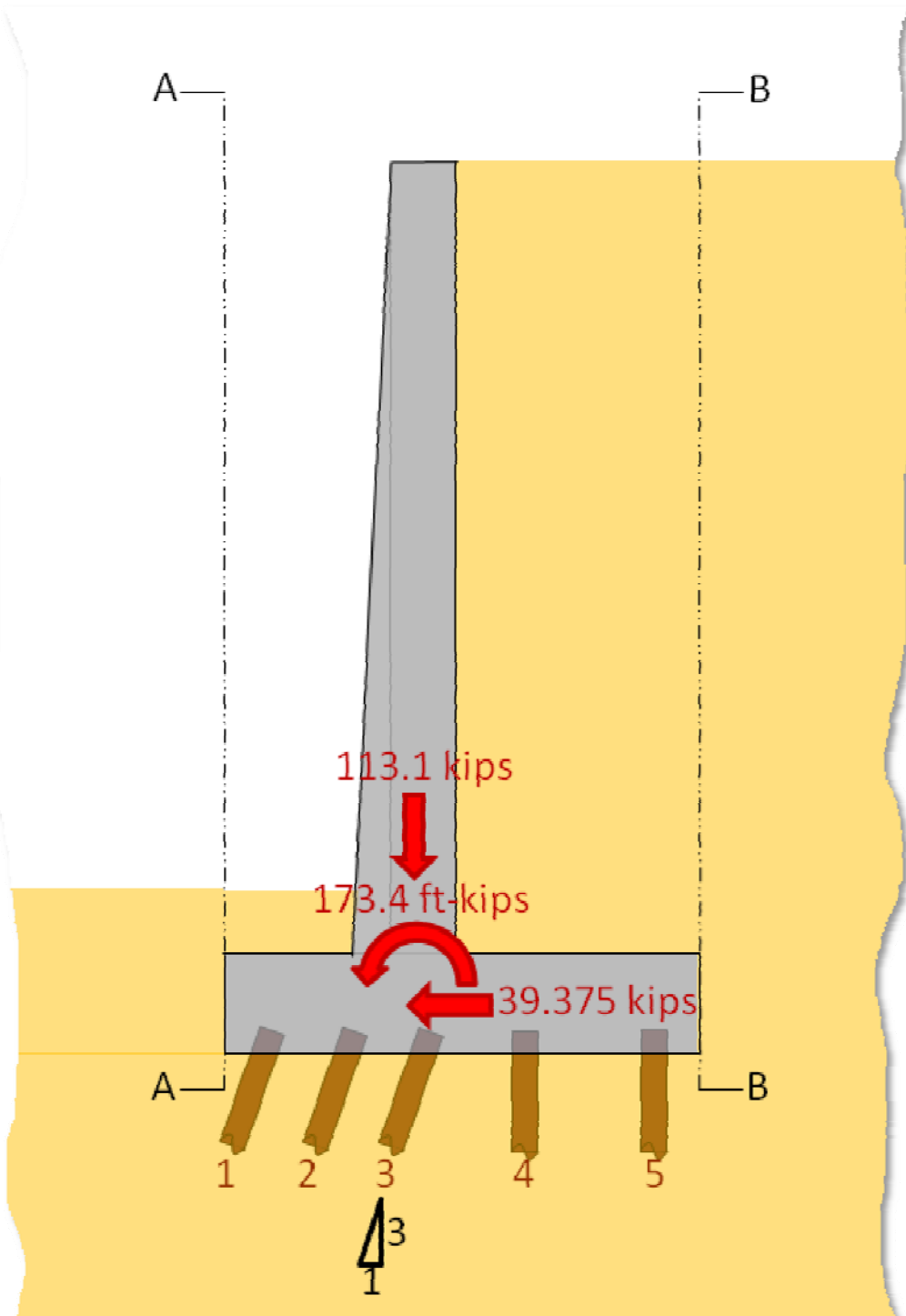


Figure 4.2. A simplified model of the Hrennikoff example.

By Rankine's equation:

$$k_A = \frac{1 - \sin\phi}{1 + \sin\phi} \quad (4.2)$$

where  $H_{B-B}$  is 27'+3', or 30'. The earth pressure, along the imaginary section cut A-A in Figure 4.2, at the front is given by Hrennikoff as equal to half the passive earth pressure resultant force:

$$\frac{1}{2} P_P = \frac{1}{2} \left( \frac{1}{2} \gamma_{moist} H_{A-A}^2 k_P \right) \quad (4.3)$$

By Rankine's equation:

$$k_P = \frac{1 + \sin\phi}{1 - \sin\phi} \quad (4.4)$$

where  $H_{A-A}$  is 2'+3', or 5'. The downward acting force at the base of the structure, shown in the figure to be acting above the third pile, is the weight of the entire structure and soil contained between imaginary sections A-A and B-B, or 113.1 kips. The horizontal force acting on the structure is  $P_A - \frac{1}{2} P_P$ , or 39.375 kips. The moment acting at the base of the structure and shown in the figure to be acting the third pile is:

$$M_C = \frac{1}{2} H_{B-B} P_A - \frac{1}{2} \left( H_{A-A} \frac{1}{2} P_A \right) - D_{CG} W \quad (4.5)$$

where  $D_{CG}$  is the horizontal distance from the center of gravity of the section between imaginary sections A-A and B-B and located in the figure that is near to the third pile. The weight of the structure ( $W$ ) is 113.1 kips. The computed moment is 173.4 kips.

One of the first intentions of this software development and testing effort was to replicate Ayyub's results. Therefore, this same input file, which is shown graphically in Figure 4.3 for the Figure 4.4 pile-founded retaining wall model and using the Table 4.1 text file input data, was used to test CPGA-R.

Ayyub et al. (1997) considered five variables in the Hrennikoff test problem: shear force, axial force, moment applied to the pile cap, and the  $X$  coordinates for Piles 1 and 2. They are listed in Table 5.1 in Figure 4.3. The mean values and standard deviations for each distribution (chosen as Normal) are listed in this table. Six limit states were specified in this problem: the axial failures of Piles 1 and 2; the bending failures of Piles 1 and 2; a pile-cap  $X$ -displacement limit state,  $DX$ , with a displacement limit of  $DL=0.110$  ft; and a pile-cap  $Z$ -displacement limit state,  $DZ$ , with a displacement limit of  $DL=0.0.029$  ft.



Table 5-1. Characteristics of Input Random Variables in Example 1

X	Name	Meaning	Mean	COV(Srddy)	Type
1	oad11	Load	-39.4	(1.50)	Normal
2	oad13	Load	113.1	(6.00)	Normal
3	oad15	Load	173.4	(8.50)	Normal
4	X1	x coordinate for pile 1	-5.0	(0.50)	Normal
5	X2	x coordinate for pile 2	2.5	(0.25)	Normal

Table 5-2a. Reliability Results for Piles Using Advanced Second Moment Method in Example 1

Pile	Limit State	Beta	$P_f$
1	1	7.47992	0.371925D-13
2	1	13.7780	0.000000D+00
1	2	4.53881	0.282858D-05
2	2	4.54760	0.271312D-05

Table 5-2b. Reliability Results for Pile Cap Displacements Using Advanced Second Moment Method in Example 1

Displacement	Displacement Limit (DL)	Beta	$P_f$
1	0.110	0.3640	0.35790
3	0.029	0.2109	0.41647

Figure 4.3. Input and output details from the RCPGA Example1 analysis made by Ayyub et al. (1997).

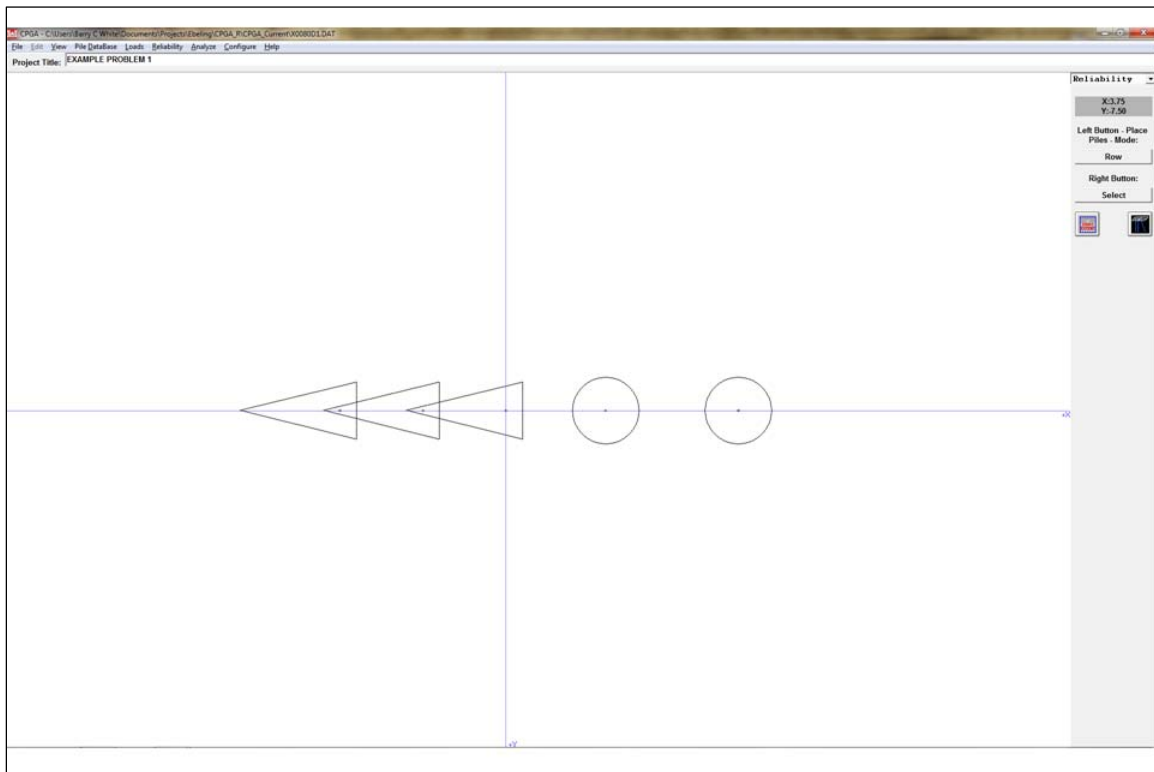


Figure 4.4. Example 1 CPGA problem (after Ayyub et al. 1997).

Table 4.1. Example input file.

```

10 EXAMPLE PROBLEM 1
15 title line 2
20 PROP 1500 322.06 322.06 63.6 2.0 0 ALL
30 SOIL ES 0.312 L 30.0 0 ALL
40 FIX ALL
50 ALLOW R 50.0 25.0 63.6 127.2 143.2 143.2 ALL
60 BATTER 3.0 1 2 3
70 ANGLE 180 ALL
80 PILE 1 -5.0 0 0
90 ROW X 5 1 2.5 2.5 3.0 4.0
100 LOAD 1 -39.375 0 113.1 0 173.4 0
115 FOUT 1 3 4 5 6 7
120 PSO
130 PFO ALL

```

These six limit states are prescribed for the selected piles and pile cap in the reliability analysis input as:

- the Axial Load Factor, ALF, for Piles 1 and 2 (labeled Limit State #1 in Table 5-2a in Figure 4.3);
- the Combined Bending Factor, CBF, for Piles 1 and 2 (labeled Limit State #2 in Table 5-2a in Figure 4.3);
- the pile cap displacement limit, DL, for a DX displacement (labeled Displacement 1, set equal to 0.110 ft, in Table 5-2b in Figure 4.3); and
- the pile cap displacement limit, DL, for a DZ displacement (labeled Displacement 3, set equal to 0.029 ft, in Table 5-2b in Figure 4.3).

The 1997 RCPGA computed values for the six limit states using the ASM reliability analysis method are summarized for each variable in Tables 5-2a and 5-2b in Figure 4.3. These values are given in terms of beta and probability of unsatisfactory performance,  $P_U$ . The  $P_U$  values for the two displacement limit values at the pile cap have much higher probabilities than the  $P_U$  values for the ALF and CBF at Piles 1 and 2. For this pile group system, the  $P_u$  value is computed by ASM as equal to 0.41647.

This batter pile example has two vertical piles and three batter piles. The loads in this system are applied directly above the central batter pile (#3) and point along the negative  $X$  axis. All the piles are fixed to the pile cap, meaning rotation at the pile cap is not allowed. The piles are in a row along the  $X$  axis, which means there is less resistance to loads in the  $Y$  direction.

### 4.1.2 Reliability Test Run 1

For Test Run 1, the input for Ayyub's first ASM test was re-created for the five variables in Figure 4.5. The ALF and CBF limit states were specified for all five piles, as well as the X- and Z-displacement limit states for the pile cap (Figure 4.6). This example problem made variables of the load forces in the  $X$  and  $Y$  directions and the moment about the  $Y$  axis at the origin (above the center batter pile) of the CPGA input of Subsection 4.1.1. Also varied were the  $X$  positions for batter Piles 1 and 2. The amount of limit state displacement allowed for the pile cap was set to 0.11 ft in the  $X$  direction and 0.029 ft in the  $Z$  direction. All these variables were set as Normal Distributions, with a set mean and standard deviation. These values are shown in the Figure 4.6 input screen.

This input set was created to be run in an ASM analysis for comparison with Ayyub's 1997 results. It was hoped these results would validate the CPGA-R implementation, but the CPGA-R computed results were different than expected. This disparity is discussed in Subsection 4.2 of this chapter. It turns out that the original RCPGA<sup>1</sup> implementation by Ayyub did not make changes to all the variables defined for the reliability run. The  $X$  positions of the pile locations were not varied.

The screenshot shows the 'Reliability Input' window. The 'Reliability Variable Input' section includes fields for Data Type (set to 'Pile'), Data ID (set to '1'), and Constituent ID (set to 'X'). The 'Distribution Type' is set to 'Normal'. Input fields for mean (5), standard deviation (0), and CoV (0.0) are present. A 'Plot Distribution' button and a normal distribution curve are also visible. Below this is a table with columns for #, dType, dID, cID, A, B, C, D, and Dist. The table contains five rows of data. To the right, the 'Variable Correlation' section has fields for Var 1, Var 2, and Corr. Coeff. (set to 0.0), along with 'Create Correlation' and 'Delete Correlation' buttons. A 'Select Limit States' button is at the bottom right. The window title bar says 'Reliability Input' and the status bar says 'Finished'.

#	dType	dID	cID	A	B	C	D	Dist
1	LOAD	1	px	-39.4	1.5	0	0	Normal
2	LOAD	1	pz	113.1	6	0	0	Normal
3	LOAD	1	my	173.4	8.5	0	0	Normal
4	Pile	1	X	-5	0.5	0	0	Normal
5	Pile	2	X	-2.5	0.25	0	0	Normal

Figure 4.5. Run 1 probabilistic variable input.

<sup>1</sup> The software RCPGA was never finalized nor placed in the Corps Computer-Aided Structural Engineering (CASE) library of software. The authors of this report were not able to locate the RCPGA software.

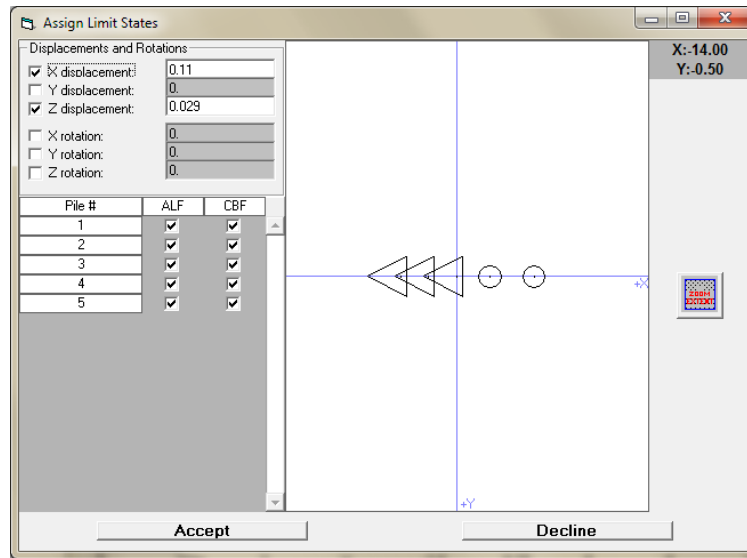


Figure 4.6. Run 1 limit state input.

For this test case, runs were performed with the CPGA-R ASM implementation technique, the Latin Hypercube simulation method with 10,000 samples, and the Importance Sampling with Latin Hypercube simulation with 10,000 samples. These results, along with those reported in Ayyub et al. (1997) for the RCPGA ASM implementation technique, are summarized in the first row of Table 4.2.

Table 4.2. Results for example problem test runs.

Probability of Unsatisfactory Performance, %						
	# of Variables	Limit States*	Ayyub	ASM	LHC	IS
Run 1	5	Dx, Dz	ASM 41.65	42.01	78.54	78.62
Run 2	3	Dx, Dz	ASM 41.65	41.65	77.68	76.82
Run 3	3	Dx	IS 36.02	35.79	36.25	35.74
Run 4	3	Dz	IS 41.51	41.65	41.79	41.67
Run 5	2	Dx		35.68	35.89	35.90
Run 6	2	Dz		41.6	42.1	41.41
Run 7	2	Dx, Dz		41.6	76.99	76.66
Run 8 – 10,000 Simulations	2			27.94E-5	0.0	31.0E-5
Run 9 - 1,000 Simulations	2			27.94E-5	0.0	34.34E-5

\* These are the user input limit states. The ALF and dCBF are being computed for each pile. The ALF and CBF values are extremely small.

The computed values for the 1997 RCPGA and CPGA-R ASM methods have similar, but not exact, values. These values are different from the Latin Hypercube and Importance Sampling with Latin Hypercube simulation results. Further tests would reveal why the simulation methods were different than the ASM results.

#### 4.1.3 Reliability Test Run 2

Figures 4.7 and 4.8 show the input for CPGA-R, altered to match the actual execution of the RCPGA implementation of the ASM method, considering three variables of the shear force, the axial force, and the moment applied to the pile cap. After careful evaluation and making additional CPGA-R executions, it was concluded that the RCPGA results reported in Ayyub et al. (1997) indicated that the 1997 software likely had a deficiency. CPGA-R results proved to the authors of this report that the 1997 RCPGA program did not vary the  $X$  locations of the first two piles. Therefore, in a subsequent problem execution, the CPGA-R variables for those two conditions were removed. The reliability analyses then were re-run to determine if the ASM implementation would return the same design point and, thus, the same probability of unsatisfactory performance between the two ASM software implementations. As expected, the CPGA-R three-variable input run results matched exactly the 1997 Ayyub implementation in RCPGA for both the design point and the probability of unsatisfactory performance (Run 2 results in Table 4.2).

The screenshot shows the 'Reliability Input' software window. The 'Reliability Variable Input' section has the following settings:

- Data Type:
- Data ID:
- Constituent ID:
- Distribution Type:
- A) mean:
- B) std:  CoV:

Below these settings is a 'Normal' distribution plot and a 'Plot Distribution' button. At the bottom of this section are buttons for 'Create Variable', 'Select Pile Groups and Create Variables', and 'Delete Variable'.

#	dType	dID	cID	A	B	C	D	Dist
1	LOAD	1	px	-39.4	1.5	0	0	Normal
2	LOAD	1	pz	113.1	6	0	0	Normal
3	LOAD	1	my	173.4	8.5	0	0	Normal

The 'Variable Correlation' section on the right has:

- Var 1:
- Var 2:
- Corr. Coeff.:
- Buttons: 'Create Correlation', 'Delete Correlation'
- Table with columns: Var1, Var2, Corr Coeff.
- Buttons: 'Select Limit States'

The status bar at the bottom of the window displays 'Finished'.

Figure 4.7. Run 2 probabilistic variable input.

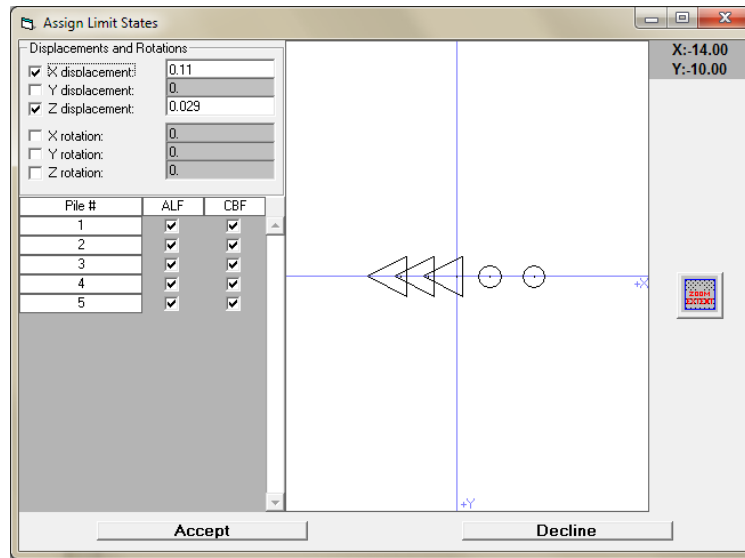


Figure 4.8. Run 2 limit state input.

Again, this input data set was run in simulation mode using both Latin Hypercube simulation and Importance Sampling with Latin Hypercube simulation. The results were different from the previous ones for those methods and still varied greatly from the two ASM results. The reason will be discussed next.

#### 4.1.4 Reliability Test Run 3

So far, the input values of Figures 4.7 and 4.8 show the altered input for CPGA-R to match the execution of the 1997 RCPGA implementation of the ASM method. There was a disparity between the results of the simulation methods (Latin Hypercube and Importance Sampling with Latin Hypercube) and the ASM results. As described in Chapter 2, the ASM technique creates an estimate of the probability of unsatisfactory performance,  $P_U$ , by finding the most likely failure condition in which the design point is closest to the mean values for the variables using a weighted Euclidean distance, where each axis is scaled by the inverse of the standard deviation (Figure 2.2b), and assuming that the area of failure exists on one side of the hyperplane that is tangent to the vector from the mean origin to the design point. A design point is determined for each limit state, and the closest design point is chosen for the estimate.

However, for multiple design points, this estimate might be inaccurate because the design point sets must be combined and the design surface might no longer be linear (planar, hyperplanar) in nature. To test this, the input in Figures 4.9 and 4.10 was developed. The variables are exactly the

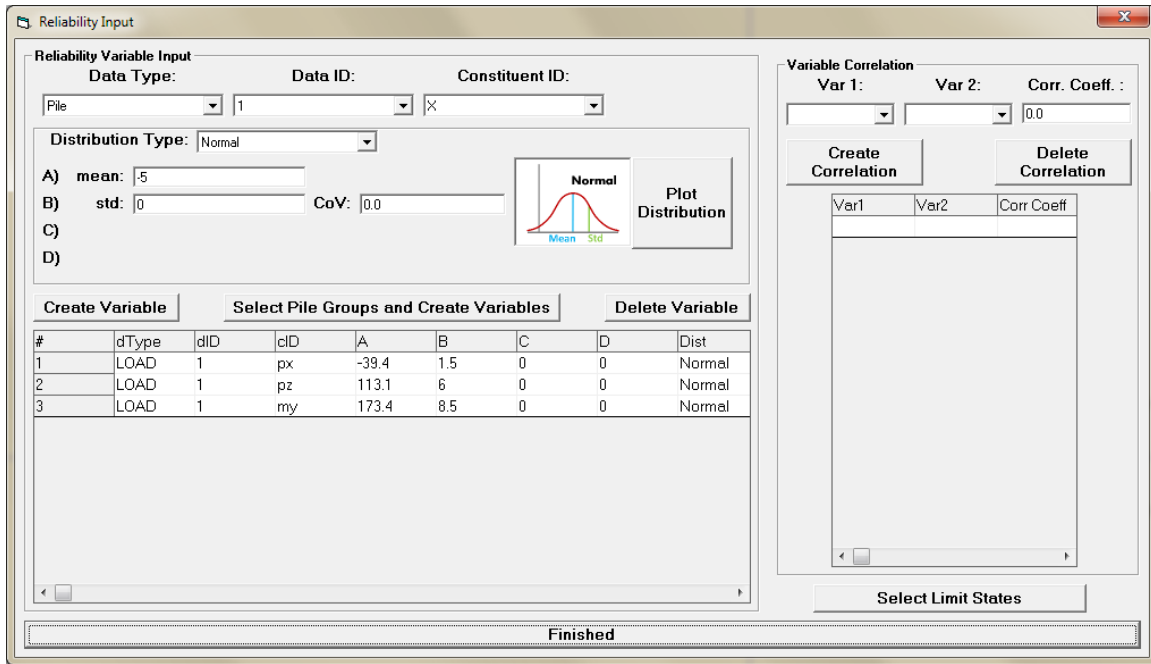


Figure 4.9. Run 3 probabilistic variable input.

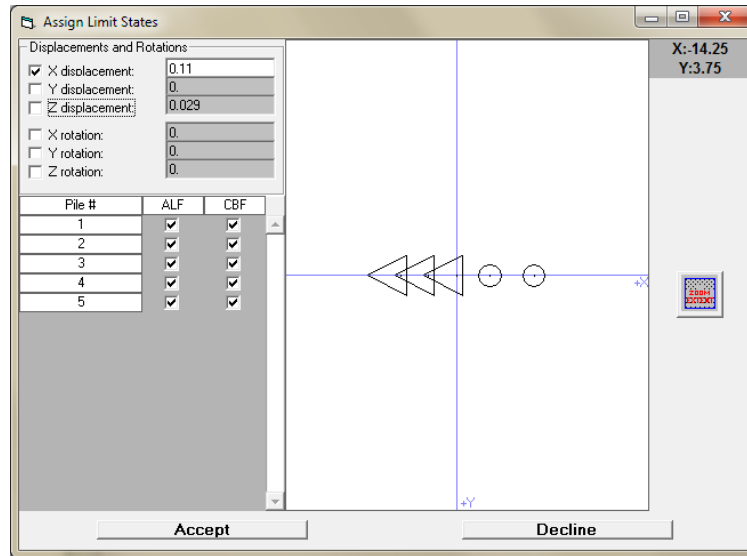


Figure 4.10. Run 3 limit state input.

same as the variables in Test Run 2; but, instead of creating pile cap displacement limits for both the X and Z directions, the only displacement limit state was the X-displacement limit state. It was recognized from the output that the limit states for the ALF and CBF of the piles had little bearing on this problem, as the design point was distant and the probability of unsatisfactory performance was low.

The results of Test Run 3 revealed this assumption was indeed correct and that removing one of the driving limit states would cause the probability of unsatisfactory performance for ASM, Latin Hypercube simulation, and Importance Sampling with Latin Hypercube simulation to give remarkably similar results. The Run 3 computed results in Table 4.2 show the percentage probability of unsatisfactory performance among the three methods was in a range of less than 0.5%.

#### 4.1.5 Reliability Test Run 4

For the input data of Test Run 4 (Figures 4.11 and 4.12), verification was needed that the results of Test Run 3 were not a coincidence, but an actual result of minimizing the number of limit states. To that end, the variable input was kept the same as in Test Run 3, but the pile cap displacement limit was changed from the original X-displacement limit to the original Z-displacement limit only. If the theory that a single limit state would yield the most accurate ASM correlation to the simulation methods (Latin Hypercube and Importance Sampling with Latin Hypercube simulation), the probability of unsatisfactory performance should be nearly the same for all of them.

Reliability Variable Input

Data Type: File Data ID: 1 Constituent ID: X

Distribution Type: Normal

A) mean: -5  
 B) std: 0 CoV: 0.0  
 C)  
 D)

Normal Plot Distribution

Create Variable Select Pile Groups and Create Variables Delete Variable

#	dType	dID	cID	A	B	C	D	Dist
1	LOAD	1	px	-39.4	1.5	0	0	Normal
2	LOAD	1	pz	113.1	6	0	0	Normal
3	LOAD	1	my	173.4	8.5	0	0	Normal

Variable Correlation

Var 1: Var 2: Corr. Coeff. : 0.0

Create Correlation Delete Correlation

Var1	Var2	Corr Coeff

Select Limit States

Finished

Figure 4.11 Run 4 probabilistic variable input.



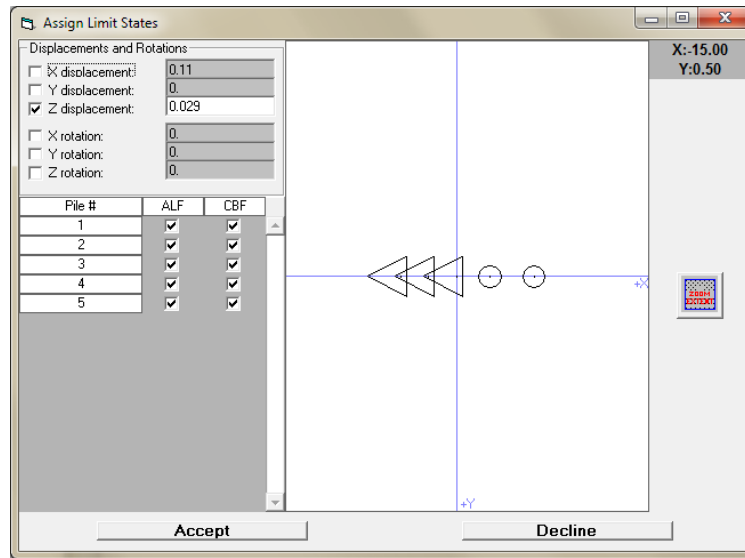


Figure 4.12. Run 4 limit state input

The results of Test Run 4 revealed that this assumption was indeed correct and that removing one of the driving limit states would cause the probability of unsatisfactory performance for ASM, Latin Hypercube simulation, and Importance Sampling with Latin Hypercube simulation to give remarkably similar results. The Run 4 computed results in Table 4.2 show the percentage probability of performance among the three methods was, again, in a range of less than 0.5%.

#### 4.1.6 Visualizing ASM and simulation method results (Test Runs 5, 6, and 7)

To visualize the computed results of simulation runs (Latin Hypercube and Importance Sampling with Latin Hypercube simulation), test cases with only two variables were constructed so the variable axes could be displayed in a 2D plot. The test run inputs above were modified to reduce the number of variables by one, from three variables to two (Figure 4.13). A single limit state of X displacement was specified so the results could be shown and compared to the planar division point at the ASM design point for Test Run 5 (Figure 4.14).

Plots were made from the simulation runs (Figure 4.15). Each plot shows the coordinate system for the two variables (with the mean values at the origin), discrete levels of probability (the differently shaded circular blue lines of constant probability about the origin have been added for reference), and the samples given by location and state (red samples mean a limit state has been exceeded; black, no limit states exceeded).

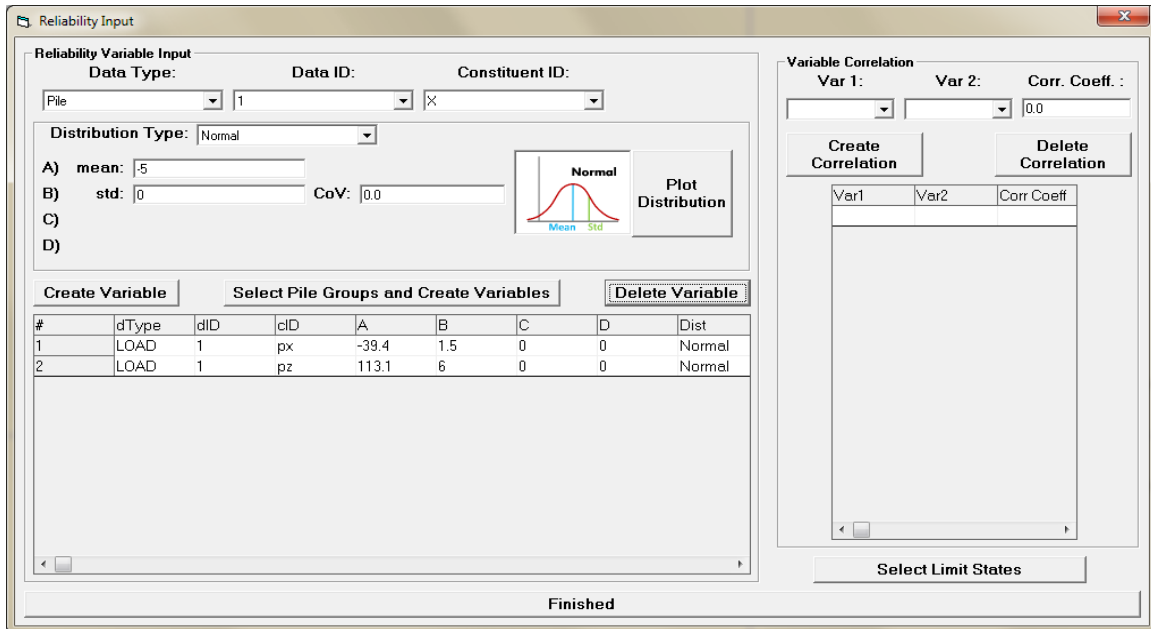


Figure 4.13. Runs 5, 6, and 7 probabilistic variable input.

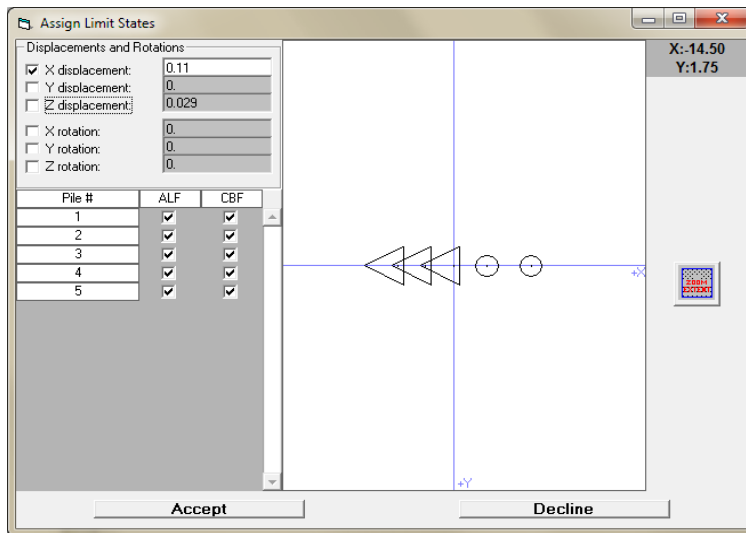


Figure 4.14. Run 5 limit state input.

Samples were taken using the Latin Hypercube method, with samples distributed about the origin for the upper left plot, and using Importance Sampling points by weighing variable locations about the design point from an ASM run. The probability of unsatisfactory performance for the simulation methods involves determining the area on either side of the curve by taking the samples and determining a ratio between the number of unsatisfactory performance samples (in red) and the total number of samples for the Latin Hypercube method, and by applying a weighted ratio for the Importance Sampling run based on the distance from the variable mean to the sampling mean, as discussed in Chapter 2.

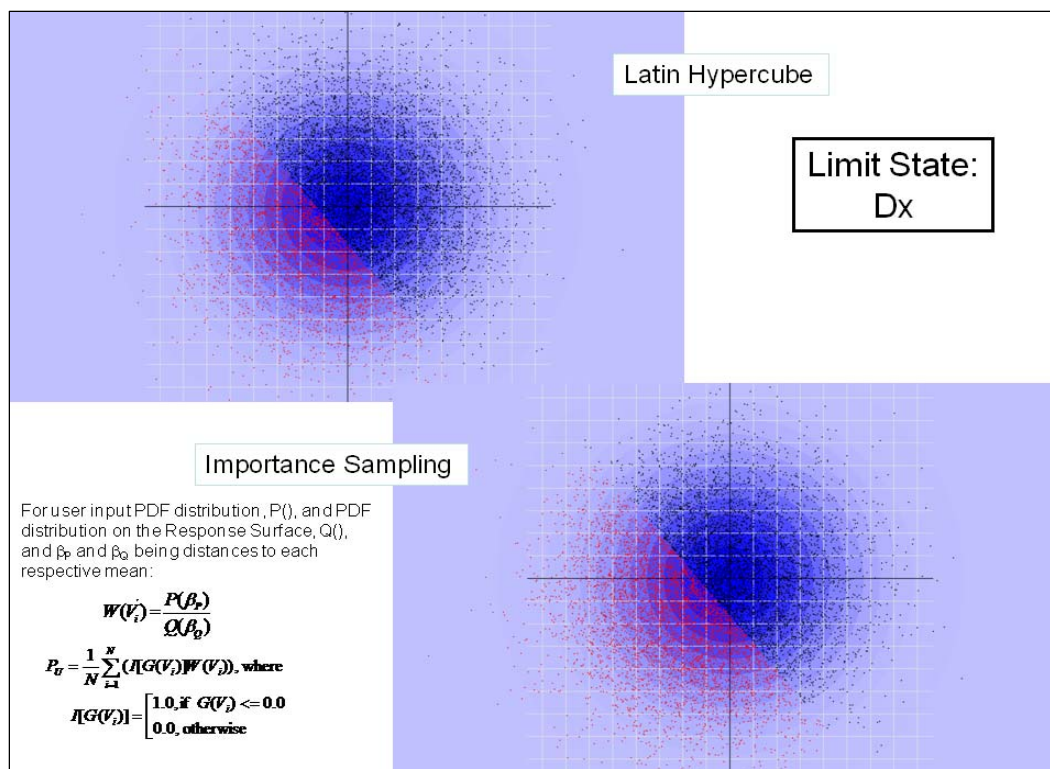


Figure 4.15. Distribution of samples and results for Run 5 (using Latin Hypercube and Importance Sampling).

The dividing surface between the unsatisfactory and satisfactory samples (in red and black, respectively) is linear. This implies the ASM method should account properly for the probability of unsatisfactory performance because, for ASM, the design point is the closest point on that line to the origin (at the means) that fully describes the line (normal to the origin to design point vector). The Run 5 computed results in Table 4.2 verify this, as the probability of unsatisfactory performance is within 0.3%.

Test Run 6 follows the same procedure, but a different limit state (Figure 4.16). In this case, the variables are the same as in Test Run 5, but the driving limit state is set to the Z displacement. The results are in Figure 4.17. Again, the resulting limit state division appears to be linear, which implies the ASM method for determining the probability of unsatisfactory performance should be accurate. The Run 6 computed results in Table 4.2 confirm this by returning a range of 1% for the probability of unsatisfactory behavior between the ASM and simulation methods.

Test Run 7 shows a situation in which the ASM method does not match the actual performance of the system. In this case, the two driving limit states from the previous two test runs are combined (Figure 4.18). Figure 4.19

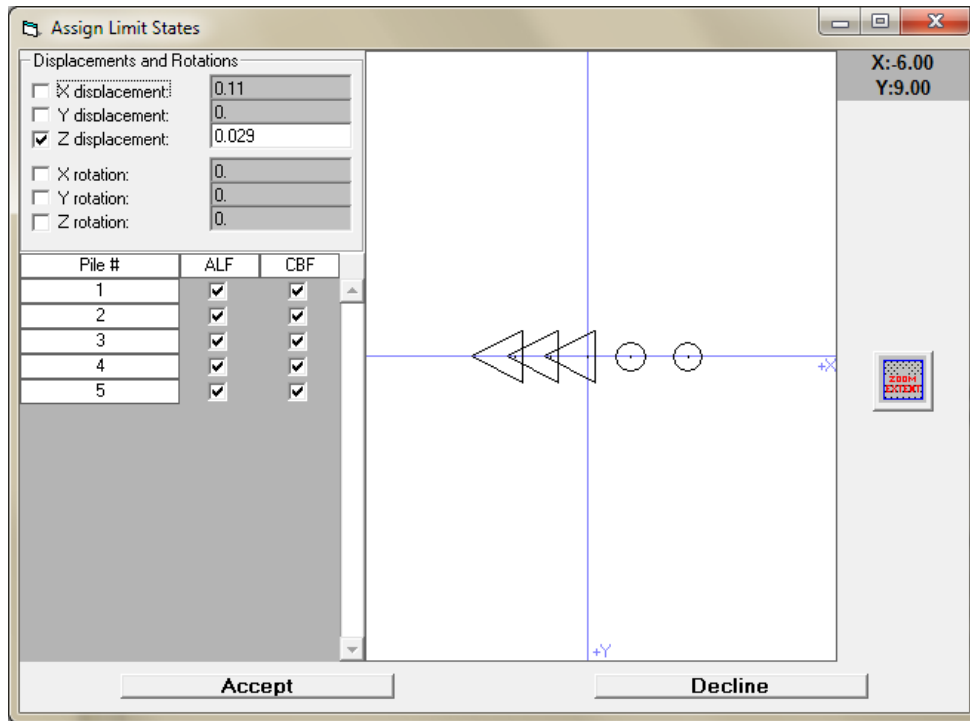


Figure 4.16. Run 6 limit state input.

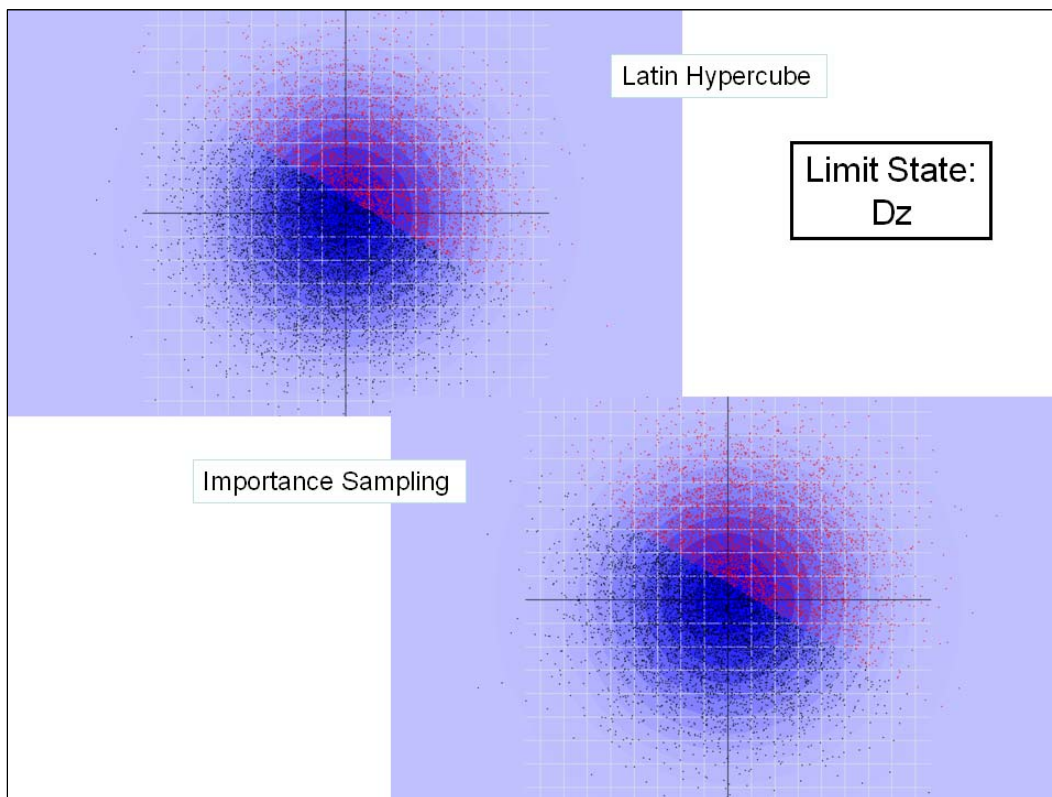


Figure 4.17. Distribution of samples and results for Run 6 (using Latin Hypercube and Importance Sampling).

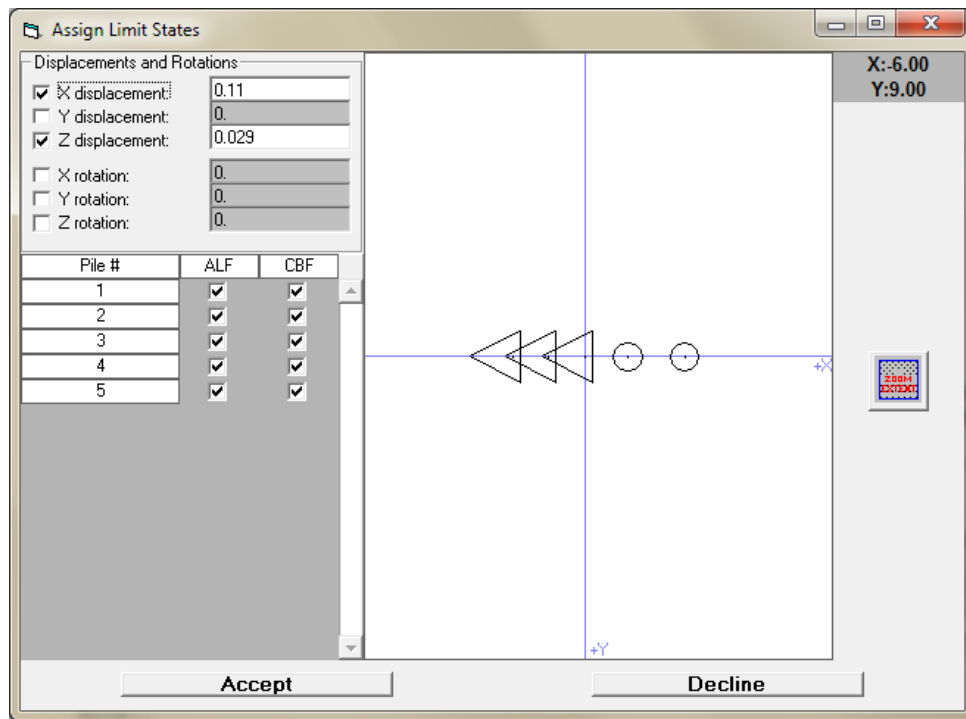


Figure 4.18. Run 7 limit state input.

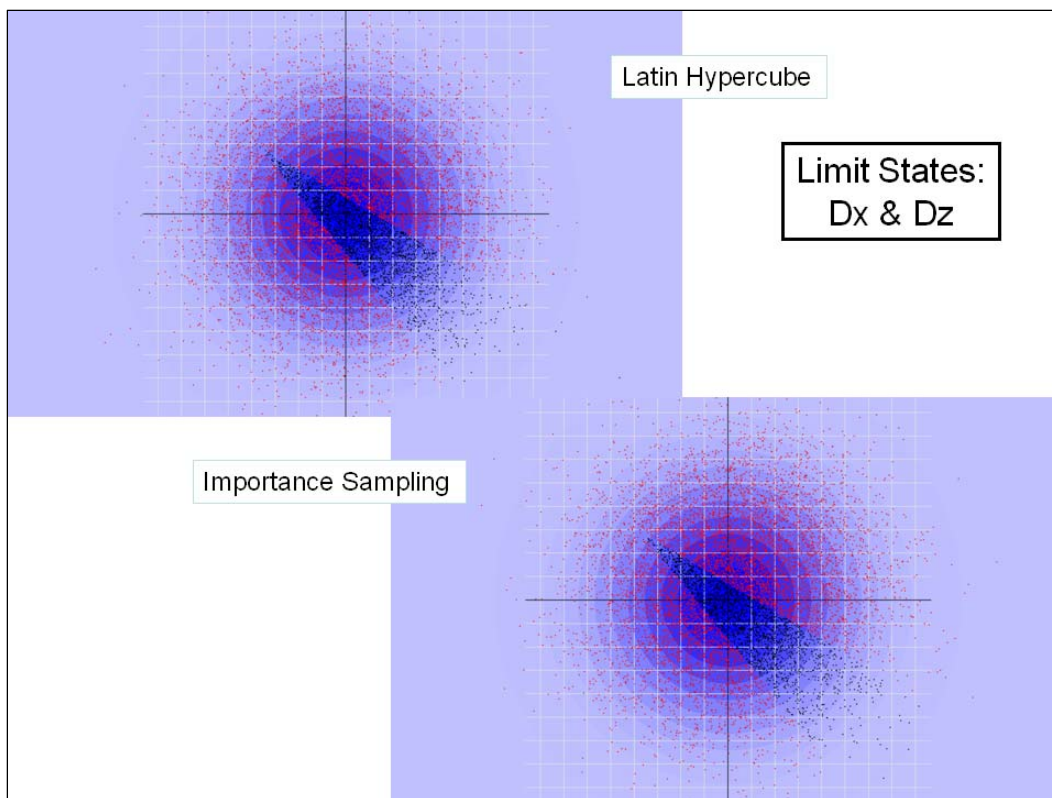


Figure 4.19. Distribution of samples and results for Run 7 (using Latin Hypercube and Importance Sampling).

shows the decidedly nonlinear, V-shaped limit state curve that results from this combination. The ASM design point method will find only the closest point to the V-shaped surface, which is on one of the legs of the curve. This will result in an inaccurate estimation of the probability of unsatisfactory performance. This is verified in Table 4.2, where for Run 7 the probability of unsatisfactory performance for the ASM method stays the same as for the previous test run (41.6%), and the Latin Hypercube and Importance Sampling with Latin Hypercube methods both agree on a higher probability of unsatisfactory performance (near 77%).

#### **4.1.7 Difference in Latin Hypercube and Importance Sampling (Test Runs 8 and 9)**

The same two variables used in the three previous test runs were used for Test Runs 8 and 9 (Figure 4.20). However, the limit state has been reduced to the limits states in the piles (i.e., ALF and CBF, Figure 4.21) with no displacement limit states specified. These limit states are much less likely to occur than the driving limit states of pile cap displacement shown in the three previous test runs. Therefore, when an ASM run is performed, the design point is at a greater distance from the mean origin. This impacts the Latin Hypercube method because simulation samples are more likely to be chosen about the origin (or mean values). Importance Sampling with Latin Hypercube takes samples about the design point from an ASM run and, therefore, catches the probabilities at the point of interest (i.e., on the design surface). If the limit states were to form a nearly linear design surface, the ASM value should be close to the Importance Sampling with Latin Hypercube simulation probability of unsatisfactory performance.

Figure 4.22 shows Latin Hypercube and Importance Sampling with Latin Hypercube simulation with 10,000 samples taken. These simulation runs show the power of the Importance Sampling technique, as there are few samples for the Latin Hypercube method that begin to approach the design surface. The Importance Sampling technique has samples drawn from a mean value on the design surface and scaled to represent their actual probabilities.

Figure 4.23 shows the same simulation with 1,000 samples chosen. In this case, the Latin Hypercube method would lose precision; but, because the Importance Sampling method takes samples close to where the design surface is, fewer samples are required for close precision.

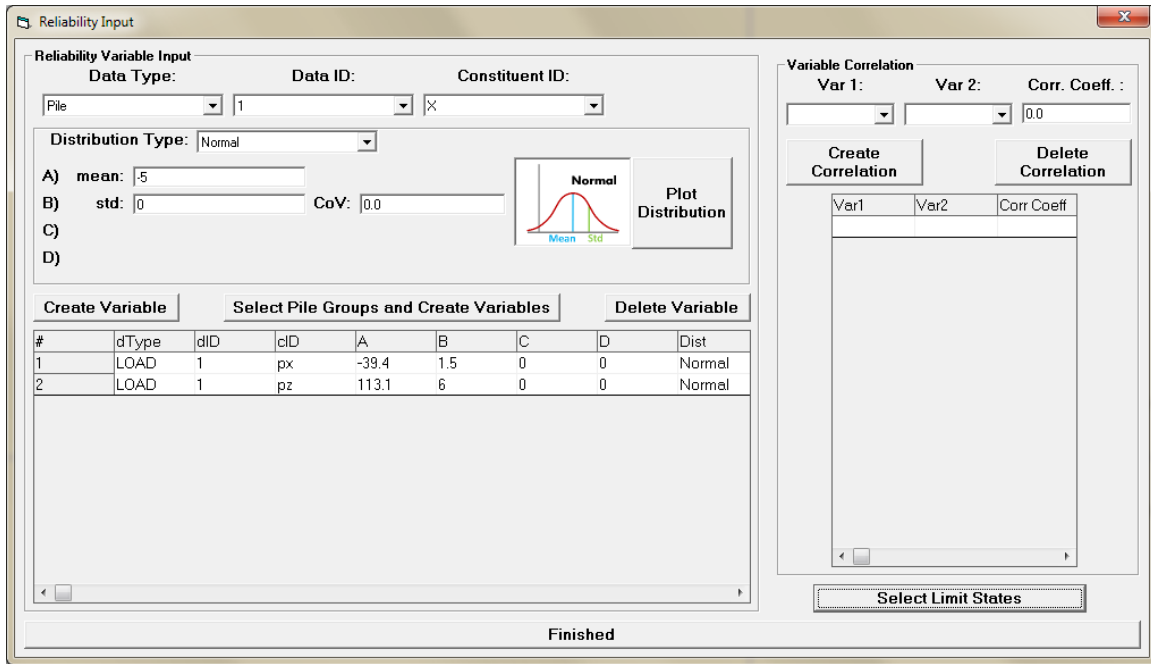


Figure 4.20. Runs 8 and 9 probabilistic variable input.

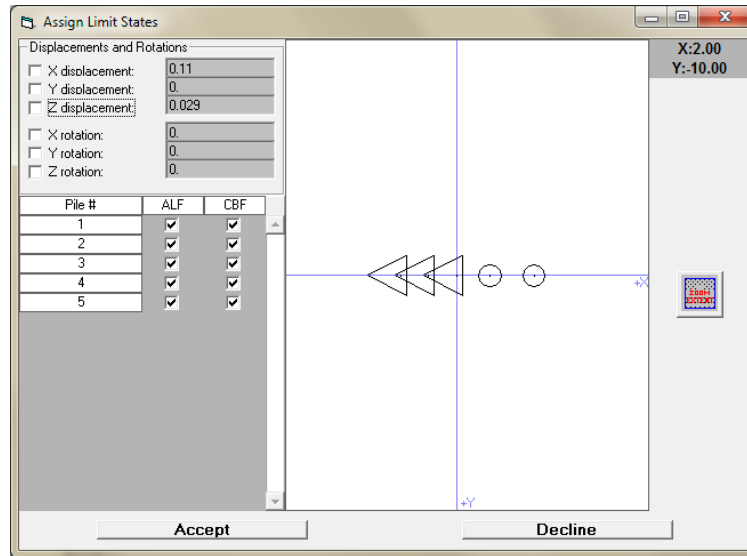


Figure 4.21. Runs 8 and 9 limit state input.

Table 4.2 shows the results of Runs 8 and 9, for which the Latin Hypercube method did not work for extremely low probabilities of unsatisfactory performance, but the ASM design point-based Importance Sampling with Latin Hypercube simulation gave consistent values of the same magnitude as the ASM runs. For the higher and lower number of samples, the values also were of consistent magnitude.

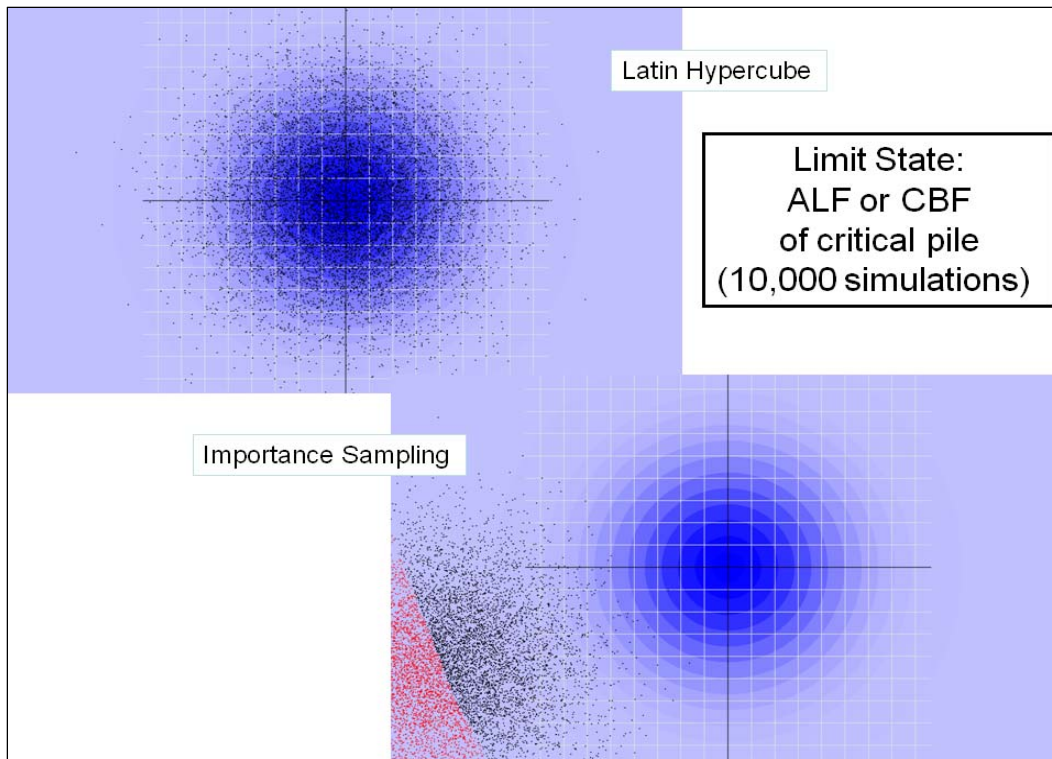


Figure 4.22. Distribution of 10,000 samples and results for Runs 8 and 9 (using Latin Hypercube and Importance Sampling).

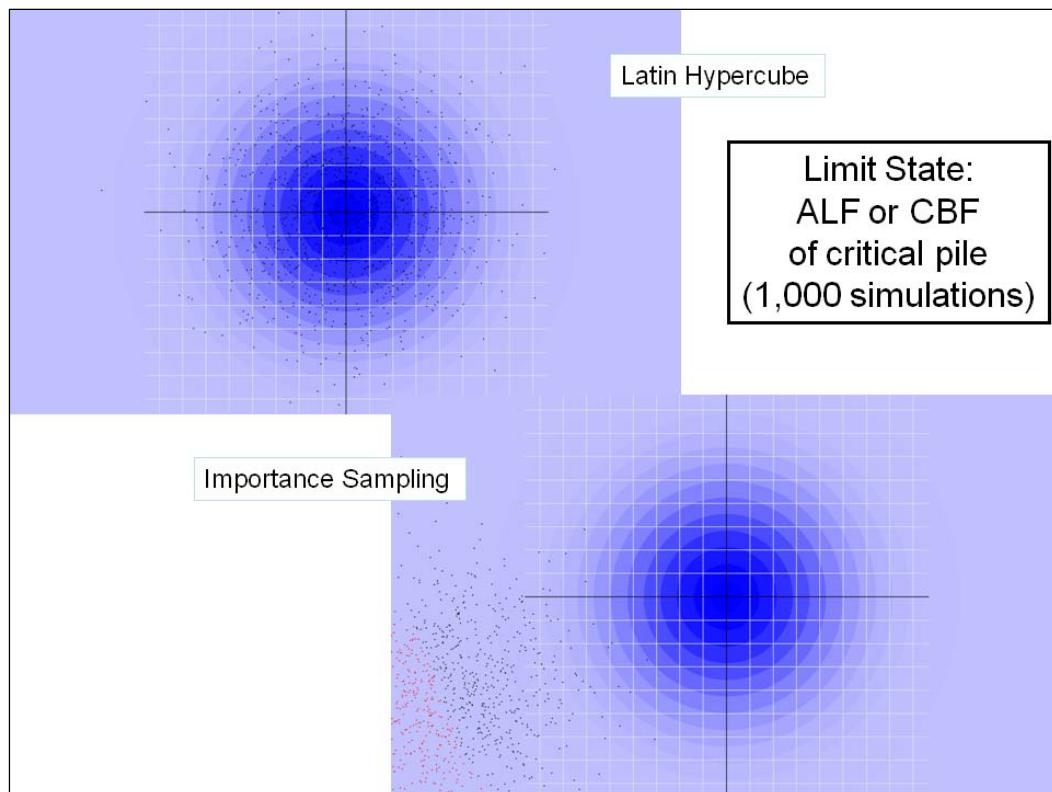


Figure 4.23. Distribution of 1,000 samples and results for Runs 8 and 9 (using Latin Hypercube and Importance Sampling).



#### 4.1.8 Influence of correlating variables in CPGA-R

Figure 4.24 shows a reliability input for a two-variable problem in which the two variables have a 0.85 correlation coefficient. A positive correlation coefficient results in a direct correlation, not an inverse correlation for which a negative correlation coefficient value is specified. These variables are defined with the same values and limit states as in Run 7, with the first variable being a load along the  $X$  direction with magnitude of -39.4 kips, and the other variable being a load along the  $Z$  axis with a magnitude of 113.1 kips. The two primary limit states are a displacement of 0.11 in. in the  $X$  direction and a displacement of 0.029 in. in the  $Z$  direction. A Latin Hypercube simulation run was performed. The text output results are shown in Figure 4.25, and the output visualization is shown in Figure 4.26.

Correlating variables always leads to a scattering of sample points along the diagonal, because of the correlated nature of the two variables. Since the triangular shape of the resulting output stays the same, the probability of unsatisfactory performance changes only by altering the correlation. The Run 7 results in Table 4.1 show the uncorrelated probability of unsatisfactory performance is 76.99%. Linking the variables with a correlation coefficient of 0.85 gives a probability of unsatisfactory performance of 82.92% (Figure 4.25).

The screenshot shows the 'Reliability Input' window. The 'Reliability Variable Input' section includes fields for Data Type (Pile), Data ID (1), and Constituent ID (X). The Distribution Type is set to Normal, with mean: -5, std: 0, and CoV: 0.0. A 'Plot Distribution' button is visible. The 'Variable Correlation' section shows Var 1 and Var 2 with a Corr. Coeff. of 0.85. A table below lists the variables:

#	dType	dlD	clD	A	B	C	D	Dist
1	LOAD	1	px	-39.4	1.5	0	0	Normal
2	LOAD	1	pz	113.1	6	0	0	Normal

The 'Variable Correlation' table shows:

Var1	Var2	Corr Coeff
1	2	0.85

The 'Select Limit States' button is at the bottom right. The status bar at the bottom indicates 'Finished'.

Figure 4.24. Correlated variable input for Run 7 variables and limit states with a correlation factor of 0.85.

```
Reliability Output
File
CPGA-R Latin Hypercube Analysis Output 12/10/2012 8:55:12 AM
Time to completion = 00:21:00      Total number of CPGA runs = 10000
Probability of unsatisfactory performance = .8292 with a coefficient of variation of :
4.53852034344488E-03
```

Figure 4.25. Results from the run with a correlation factor of 0.85.

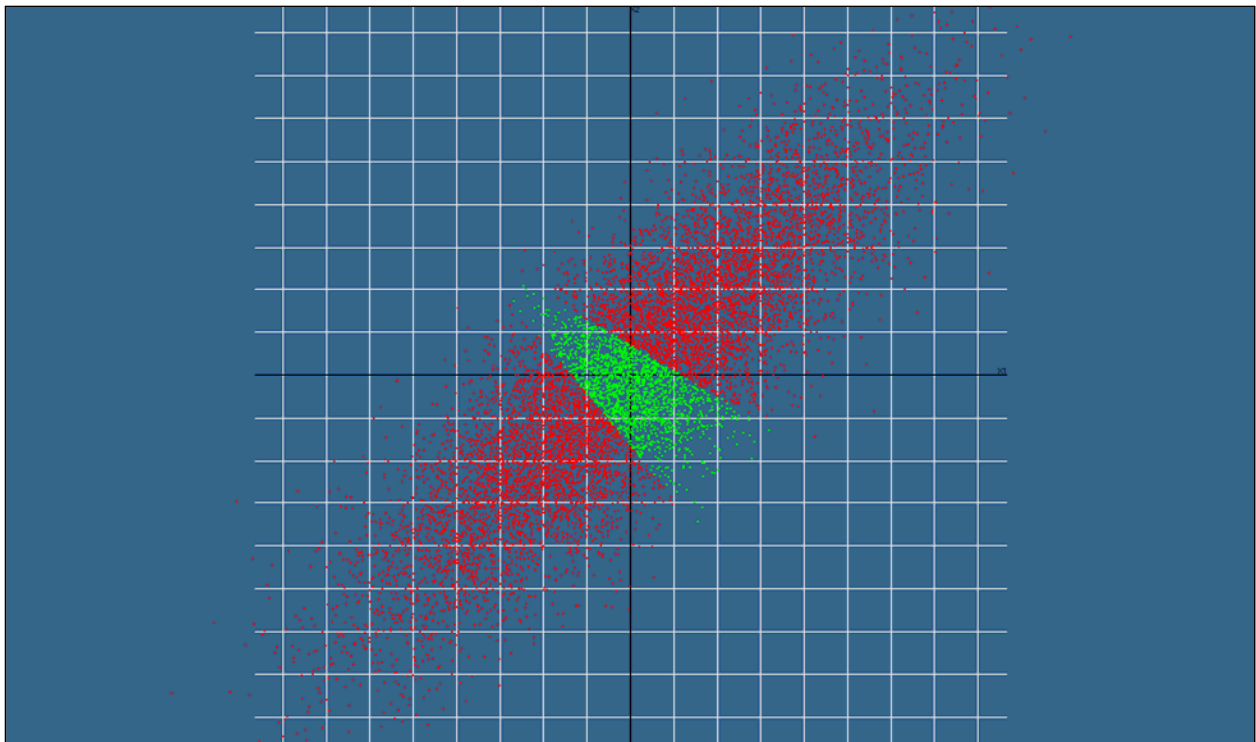


Figure 4.26. The spread and results of the simulation runs with a correlation factor of 0.85.

Figure 4.27 shows the same input variables from the previous run with a negative correlation coefficient. A negative correlation coefficient is known also as an inverse correlation. The samples from an inverse correlation are drawn against the opposite diagonal as the direct correlation. Figure 4.28 shows the results of running this inverse correlation, which results in a

much lower probability of unsatisfactory performance (50.44%) than with the direct correlation (82.92%) or uncorrelated (76.99%). Figure 4.29 explains why. The samples are taken along the diagonal that follows the triangular area where satisfactory performance occurs, which lowers the probability of finding a sample with unsatisfactory performance.

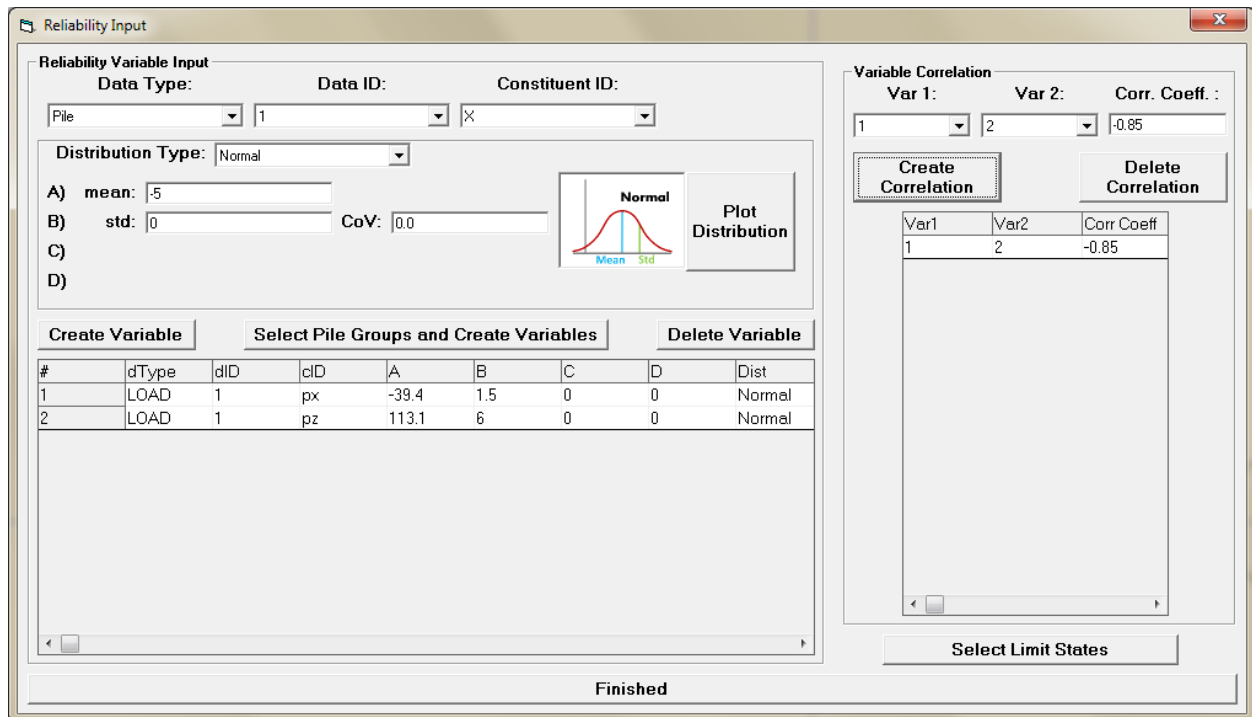


Figure 4.27. Using an inverse correlation factor (-0.85).

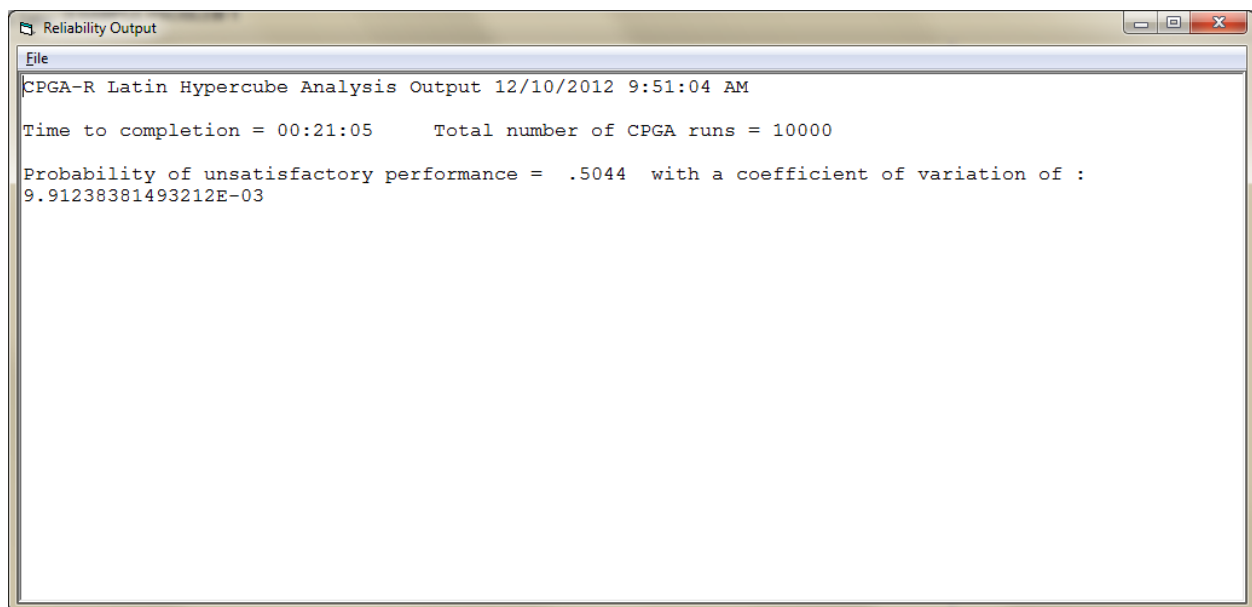


Figure 4.28. Results given an inverse correlation factor (-0.85).

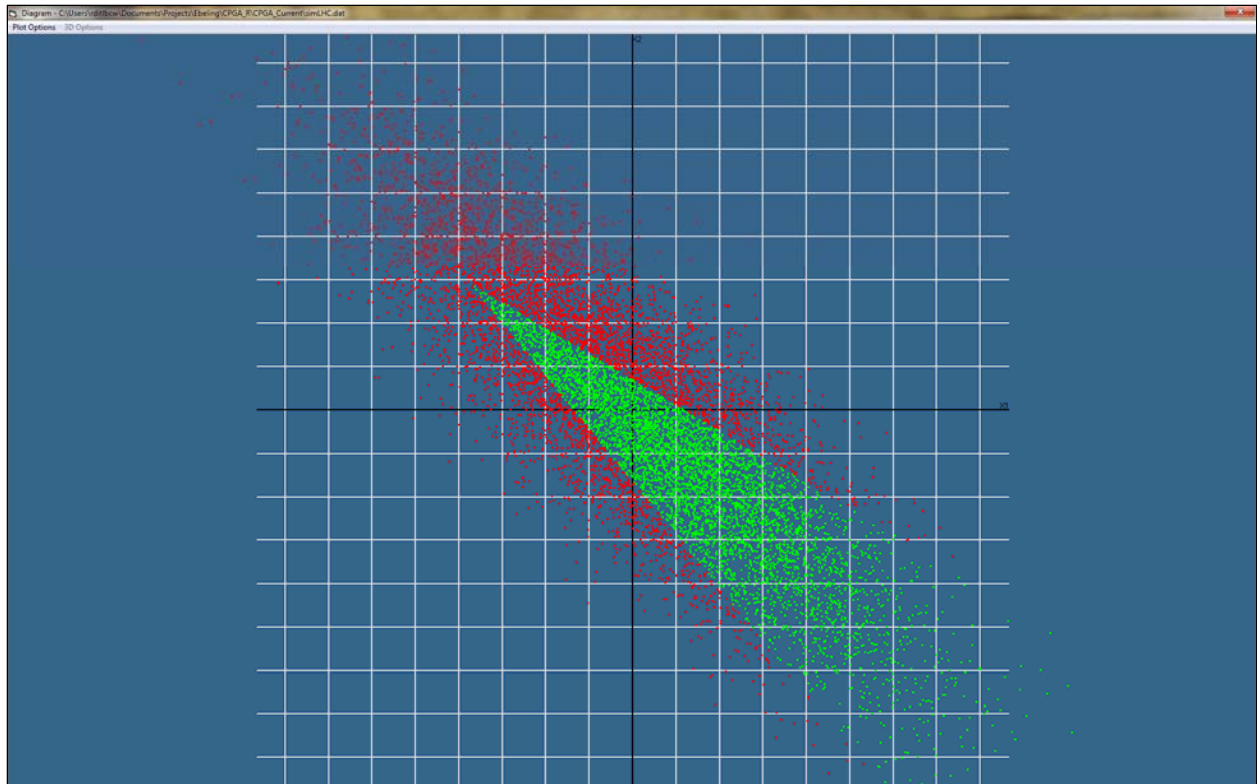


Figure 4.29. The spread and results of the simulation runs with an inverse correlation factor (-0.85).

Table 4.3 shows the results of changing the correlation coefficient using a well-established correlation code for Latin Hypercube sampling, with results from adding the correlation code for the ASM method (for a single limit state, for testing purposes), and with Importance Sampling using Latin Hypercube methods. These results agree within 3%, which validates the correlation values are accurate.

Table 4.3. Examples of correlating pairs of variables and the effects on the probability of unsatisfactory performance.

Probability of Unsatisfactory Performance, %			
Corr. Factor	LHC 10,000 samples	ASM	IS 10,000 Samples
-0.9	31.8	32.2	33.91
-0.5	39.4	38.86	42.52
0.0	42.1	41.6	41.41
0.5	42.76	42.98	40.14
0.9	43.5	43.7	39.22

## 4.2 Understanding CPGA-R output formats

### 4.2.1 Advanced Second Moment (ASM) output

Table 4.4 shows the output from the CPGA-R software when an ASM run has been performed using input data equivalent to that of the RCPGA Example 1. This data uses the same five-pile Hrennikoff example in Figures 4.1, 4.2, and 4.4. The variables defined are in Figures 4.3 and 4.5, and the limit states are in Figure 4.6. The output is divided into two sections.

**Table 4.4. Results of CPGA-R with the Example 1 input from the RCPGA manual.**

```

CPGA-R ASM Analysis Output 12/11/2012 7:40:27 AM

Time to completion = 00:00:43 Total number of CPGA runs = 443

Return Status States:

  Unaffected means that the limit state is unaffected by all of the variables.

  Computed means that the limit state was reached in the variable space.

  Extreme means that the limit state was not found within 8 standard deviations of
the mean.

Limit State BETA Failure Prob. Return Status
-----
Translation X = 0.110 3.4985665E-01 3.6322466E-01 Computed

Design Point
-----
Card ID Index Variable Value Directional Cosine
-----
LOAD 01 px -39.7869550057912 0.737367350205002
LOAD 01 pz 111.830889805245 0.604592528472047
LOAD 01 my 173.040729281488 0.120814090900201
Pile 01 X -5.04444948271573 0.254103940749335
Pile 02 X -2.50941699079941 0.107668045877356

Limit State BETA Failure Prob. Return Status
-----
Translation Z = 0.029 2.0162977E-01 4.2010448E-01 Computed

```

Design Point

-----

Card ID Index Variable Value Directional Cosine

-----

LOAD 01 px -39.253514910467 -0.484345290939787

LOAD 01 pz 114.089038540607 -0.81755105797474

LOAD 01 my 173.572869896873 -0.100867990081267

Pile 01 X -4.97271857005927 -0.270613865834808

Pile 02 X -2.49411867698635 -0.116677722568372

Limit State BETA Failure Prob. Return Status

-----

Pile #0001 ALF 6.0760755E00 6.2171590E-10 Computed

Design Point

-----

Card ID Index Variable Value Directional Cosine

-----

LOAD 01 px -39.056096594625 -3.77388455360848E-02

LOAD 01 pz 141.532485034133 -0.780022198195576

LOAD 01 my 187.365128574415 -0.270439052801879

Pile 01 X -4.08795932555464 -0.300253166420285

Pile 02 X -1.77661777961133 -0.476289727617509

Limit State BETA Failure Prob. Return Status

-----

Pile #0001 CBF 4.5275097E00 2.9929468E-06 Computed

Design Point

-----

Card ID Index Variable Value Directional Cosine

-----

```

LOAD 01 px -45.7736261285423 0.93859100278118
LOAD 01 pz 103.945243937097 0.337036229455707
LOAD 01 my 172.104976136111 3.36542492596207E-02
Pile 01 X -5.13231740912199 5.84558588197023E-02
Pile 02 X -2.53402501971461 3.00634929594376E-02

```

Limit State BETA Failure Prob. Return Status

```

-----
Pile #0002 ALF =8.000000E00 0 1.000000E-16 0 Extreme

```

Design Point

```

-----
Card ID Index Variable Value Directional Cosine
-----

```

```

LOAD 01 px -39.4 0.291427906800489
LOAD 01 pz 113.1 -0.769433813892922
LOAD 01 my 173.4 -0.175295781335943
Pile 01 X -5 -0.540643862560158
Pile 02 X -2.5 -4.12117676536306E-03

```

Limit State BETA Failure Prob. Return Status

```

-----
Pile #0002 CBF 4.4383974E00 4.5387028E-06 Computed

```

Design Point

```

-----
Card ID Index Variable Value Directional Cosine
-----

```

```

LOAD 01 px -45.3069045520247 0.887273894297676
LOAD 01 pz 102.555669825237 0.395964959926241
LOAD 01 my 169.459514796039 0.104452727508188
Pile 01 X -5.42804246593377 0.192888289794857

```

```
Pile 02 X -2.59824795030526 8.85467243017117E-02

*****

* Final Results *

*****

The greatest probability of failure occurs for the limit state: Translation Z =
0.029

The greatest probability of failure was 42.01E00%
```

The first two lines of the CPGA-R output file give the run status of the program, including the date and time of the analysis and the amount of time required to perform it. Also, the total number of individual CPGA runs is reported. This is the number of runs required to perform the analysis and determine the probability of unsatisfactory performance for each limit state.

The next four lines of the output file are a legend describing the return status of each limit state. The three return statuses are:

- **Unaffected:** Limit states that are uncorrelated with the input data can be defined. In these cases, changing the variables does not make a CPGA run approach that limit state. Therefore, the probability of unsatisfactory performance is either 100% or 0%, depending on whether the limit state is exceeded or not met, respectively, at the mean values for the variables.
- **Computed:** If the limit state approaches 0.0 and is computable within eight standard deviations for all its variables, the computed probability of unsatisfactory performance is reported.
- **Extreme:** It is possible for a variable to be defined with a mean and standard deviation that will not converge to a design point that is within eight standard deviations of the mean. In this case, the probability of unsatisfactory performance approaches 100% or 0%. Therefore, the probability of unsatisfactory performance is reported as either 100% or 0%, depending on whether the limit state is exceeded or not met, respectively, at the mean values for the variables.



Each limit state's results are given in the next section of output. The first line defines the limit state. For instance, the second limit state for the output in Table 4.4 is the pile cap translation in the  $Z$  direction, which is limited to a deflection of no more than 0.029 in. For this limit state, the distance all the variables moved from the mean is given by beta, which is approximately 0.2016. The probability of unsatisfactory performance is reported at the Failure Prob. This number falls on a scale of 0.0 to 1.0. For the same limit state of  $Z$  deflection, the failure probability is 0.4201 (42.01%). Because the value can be computed from the given variables within eight standard deviations, the return status is given as computed.

Beneath the probability of unsatisfactory performance values are the computed values for the design point. The design point is the closest point to the mean origin where the limit state has a value of 0.0. The card ID, index, and variable are used to identify the specific data that is varying for each variable. The value gives the actual value in the variable space of the design point. This value can be computed by taking the beta value from the probability of unsatisfactory performance line, multiplying it by the directional cosine value, and adding the product to the variable mean.

The design point and the directional cosine vector are given so the user can determine which variables have the greatest effect on the limit state.

The final results section presents the limit state with the highest probability of unsatisfactory performance. This limit state is the state most likely to be exceeded. The probability for that limit state is restated in percentile format.

#### **4.2.2 Latin Hypercube output and Importance Sampling with Latin Hypercube output**

The output format for the simulation methods Latin Hypercube and Importance Sampling are much simpler than for ASM, which returns information about the final state and location of the design point and each probability of unsatisfactory performance ( $P_u$ ) for each limit state. The simulation methods have the same header information, describing the run and giving the time and date. Also given is the number of simulation runs performed.

The rest of the output gives the probability of unsatisfactory performance in a decimal value and the coefficient of variation for that probability of

unsatisfactory performance. The probability of unsatisfactory performance applies to all the limit states.

Tables 4.5 and 4.6 show output values for the Latin Hypercube method and the Importance Sampling combined with Latin Hypercube, respectively.

**Table 4.5. Results of CPGA-R with Example 1 input for a Latin Hypercube run.**

<pre> CPGA-R Latin Hypercube Analysis Output 12/12/2012 10:02:54 AM  Time to completion = 00:20:56 Total number of CPGA runs = 10000  Probability of unsatisfactory performance = .7767 with a coefficient of variation of : 5.3618876398803E-03 </pre>
---

**Table 4.6. Results of CPGA-R with Example 1 input for an Importance Sampling run.**

<pre> CPGA-R Importance Sampling Output 12/12/2012 10:29:44 AM  Time to completion = 00:19:57 Total number of simulation runs = 10000  Probability of unsatisfactory performance = .76812434296304 with a coefficient of variation of : 5.95567106216815E-03 </pre>
---

### 4.3 Inconsistencies for ASM calculations in 1997 RCPGA

In the original RCPGA formulation of the ASM algorithm (Ayyub et al. 1997), as many as 2,000 variables could be defined. Also, limits could be established for pile cap displacement and rotation, as well as failure mechanisms at each pile, the Axial Load Factor (ALF) and Combined Bending Factor (CBF). A test problem for RCPGA was established with a five-variable vector and with six limit states (two for pile cap motion, and ALF and CBF for two piles). The variables established for the example were for the  $X$  and  $Z$  forces,  $Y$  moment acting on the pile cap, and displacements in the  $X$  direction for two of the five piles (Figure 4.5).

The example problem and results from the original RCPGA program are in Figure 4.3. The CPGA input file for this five-pile problem is in Table 4.1. Figure 4.4 shows the placement of the piles according to the original CPGA input (in the CPGA-R interface).

The probabilistic input for the variables in Figure 4.3 for the original RCPGA software is in Table 4.7. Figures 4.5 and 4.6 show the same input as it would be entered into the GUI for CPGA-R.

**Table 4.7. Reliability input for variables in the RCPGA software.**

```

Example 1 RCPGA
A3,1X,A5,1X,A1,2(1X,D12.6),2(1X,I4)
1.00D-03 1.00D-04
5 name Code mean sigma Cont1 Cont2
NOR oad s -39.4 1.5 1 1
NOR oad s 113.1 6.0 1 3
NOR oad s 173.4 8.5 1 5
NOR X s -5.0 .5 1
NOR X s -2.5 .25 2
1
1
2
1
2
2
1, 0.11
3, 0.29D-01

```

The RCPGA output is in Table 4.8. The greatest probability of unsatisfactory performance in the summary of reliability results at the end of the file is 41.65% at the limit state of a displacement of 0.029 in the *Z* direction.

**Table 4.8. Output from RCPGA ASM method.**

```

ID = Example 1 RCPGA
Total number of random variables = 5
**** The input data ****
-x=rv- -name- ----mean-- --stdv-- --Distr- -cont1- -cont2-
X( 1) oad -.394000D+02 .150000D+01 NOR 1 1
X( 2) oad .113100D+03 .600000D+01 NOR 1 3
X( 3) oad .173400D+03 .850000D+01 NOR 1 5
X( 4) X -.500000D+01 .500000D+00 NOR 1 0
X( 5) X -.250000D+01 .250000D+00 NOR 2 0
**** The result ****
*****
Limit state number (1-axial or 2-combined)= 1
Pile number = 1
The i (iteration) = 1
x=rv. --sigmaEN--- ---meanEN--- ---alpha---- -----dp-----
X( 1) .150000D+01 -.394000D+02 -.682647D-01 -.386341D+02
X( 2) .600000D+01 .113100D+03 -.940074D+00 .155290D+03
X( 3) .850000D+01 .173400D+03 -.334067D+00 .194640D+03
X( 4) .500000D+00 -.500000D+01 .000000D+00 -.500000D+01
X( 5) .250000D+00 -.250000D+01 .000000D+00 -.250000D+01
The beta (safety index) = .747992D+01
The i (iteration) = 2
x=rv. --sigmaEN--- ---meanEN--- ---alpha---- -----dp-----
X( 1) .150000D+01 -.394000D+02 -.682647D-01 -.386341D+02
X( 2) .600000D+01 .113100D+03 -.940074D+00 .155290D+03
X( 3) .850000D+01 .173400D+03 -.334067D+00 .194640D+03
X( 4) .500000D+00 -.500000D+01 .000000D+00 -.500000D+01
X( 5) .250000D+00 -.250000D+01 .000000D+00 -.250000D+01
The beta (safety index) = .747992D+01
Probability of unsatisfactory performance(Pu)= .371925D-13
*****
Limit state number (1-axial or 2-combined)= 1
Pile number = 2

```

```

The i (iteration) = 1
x=rv. --sigmaEN--- ---meanEN--- ---alpha---- -----dp-----
X( 1) .150000D+01 -.394000D+02 .346426D+00 -.465596D+02
X( 2) .600000D+01 .113100D+03 -.914641D+00 .188712D+03
X( 3) .850000D+01 .173400D+03 -.208377D+00 .197804D+03
X( 4) .500000D+00 -.500000D+01 .000000D+00 -.500000D+01
X( 5) .250000D+00 -.250000D+01 .000000D+00 -.250000D+01
The beta (safety index) = .137780D+02
The i (iteration) = 2
x=rv. --sigmaEN--- ---meanEN--- ---alpha---- -----dp-----
X( 1) .150000D+01 -.394000D+02 .346426D+00 -.465596D+02
X( 2) .600000D+01 .113100D+03 -.914641D+00 .188712D+03
X( 3) .850000D+01 .173400D+03 -.208377D+00 .197804D+03
X( 4) .500000D+00 -.500000D+01 .000000D+00 -.500000D+01
X( 5) .250000D+00 -.250000D+01 .000000D+00 -.250000D+01
The beta (safety index) = .137780D+02
Probability of unsatisfactory performance(Pu)= .000000D+00
*****
Limit state number (1-axial or 2-combined)= 2
Pile number = 1
The i (iteration) = 1
x=rv. --sigmaEN--- ---meanEN--- ---alpha---- -----dp-----
X( 1) .150000D+01 -.394000D+02 .939962D+00 -.457995D+02
X( 2) .600000D+01 .113100D+03 .339470D+00 .103855D+03
X( 3) .850000D+01 .173400D+03 .350899D-01 .172046D+03
X( 4) .500000D+00 -.500000D+01 .000000D+00 -.500000D+01
X( 5) .250000D+00 -.250000D+01 .000000D+00 -.250000D+01
The beta (safety index) = .453881D+01
The i (iteration) = 2
x=rv. --sigmaEN--- ---meanEN--- ---alpha---- -----dp-----
X( 1) .150000D+01 -.394000D+02 .939962D+00 -.457995D+02
X( 2) .600000D+01 .113100D+03 .339470D+00 .103855D+03
X( 3) .850000D+01 .173400D+03 .350899D-01 .172046D+03
X( 4) .500000D+00 -.500000D+01 .000000D+00 -.500000D+01
X( 5) .250000D+00 -.250000D+01 .000000D+00 -.250000D+01
The beta (safety index) = .453881D+01
Probability of unsatisfactory performance(Pu)= .282858D-05
*****
Limit state number (1-axial or 2-combined)= 2
Pile number = 2
The i (iteration) = 1
x=rv. --sigmaEN--- ---meanEN--- ---alpha---- -----dp-----
X( 1) .150000D+01 -.394000D+02 .903609D+00 -.455639D+02
X( 2) .600000D+01 .113100D+03 .413949D+00 .101805D+03
X( 3) .850000D+01 .173400D+03 .110170D+00 .169141D+03
X( 4) .500000D+00 -.500000D+01 .000000D+00 -.500000D+01
X( 5) .250000D+00 -.250000D+01 .000000D+00 -.250000D+01
The beta (safety index) = .454760D+01
The i (iteration) = 2
x=rv. --sigmaEN--- ---meanEN--- ---alpha---- -----dp-----
X( 1) .150000D+01 -.394000D+02 .903609D+00 -.455639D+02
X( 2) .600000D+01 .113100D+03 .413949D+00 .101805D+03
X( 3) .850000D+01 .173400D+03 .110170D+00 .169141D+03
X( 4) .500000D+00 -.500000D+01 .000000D+00 -.500000D+01
X( 5) .250000D+00 -.250000D+01 .000000D+00 -.250000D+01
The beta (safety index) = .454760D+01
Probability of unsatisfactory performance(Pu)= .271312D-05
*****
Displacement number (for DX,DY,DZ,RX,RY,RZ) = 1
The i (iteration) = 1
x=rv. --sigmaEN--- ---meanEN--- ---alpha---- -----dp-----
X( 1) .150000D+01 -.394000D+02 .767160D+00 -.398189D+02
X( 2) .600000D+01 .113100D+03 .629020D+00 .111726D+03
X( 3) .850000D+01 .173400D+03 .125695D+00 .173011D+03
X( 4) .500000D+00 -.500000D+01 .000000D+00 -.500000D+01
X( 5) .250000D+00 -.250000D+01 .000000D+00 -.250000D+01
The beta (safety index) = .364057D+00
The i (iteration) = 2
x=rv. --sigmaEN--- ---meanEN--- ---alpha---- -----dp-----
X( 1) .150000D+01 -.394000D+02 .767160D+00 -.398189D+02
X( 2) .600000D+01 .113100D+03 .629020D+00 .111726D+03

```

```

X( 3) .850000D+01 .173400D+03 .125695D+00 .173011D+03
X( 4) .500000D+00 -.500000D+01 .000000D+00 -.500000D+01
X( 5) .250000D+00 -.250000D+01 .000000D+00 -.250000D+01
The beta (safety index) = .364057D+00
Probability of unsatisfactory performance(Pu)= .357908D+00
*****
Displacement number (for DX,DY,DZ,RX,RY,RZ) = 3
The i (iteration) = 1
x=rv. --sigmaEN--- ---meanEN--- ---alpha---- -----dp-----
X( 1) .150000D+01 -.394000D+02 -.506854D+00 -.392396D+02
X( 2) .600000D+01 .113100D+03 -.855545D+00 .114183D+03
X( 3) .850000D+01 .173400D+03 -.105556D+00 .173589D+03
X( 4) .500000D+00 -.500000D+01 .000000D+00 -.500000D+01
X( 5) .250000D+00 -.250000D+01 .000000D+00 -.250000D+01
The beta (safety index) = .210931D+00
The i (iteration) = 2
x=rv. --sigmaEN--- ---meanEN--- ---alpha---- -----dp-----
X( 1) .150000D+01 -.394000D+02 -.506854D+00 -.392396D+02
X( 2) .600000D+01 .113100D+03 -.855545D+00 .114183D+03
X( 3) .850000D+01 .173400D+03 -.105556D+00 .173589D+03
X( 4) .500000D+00 -.500000D+01 .000000D+00 -.500000D+01
X( 5) .250000D+00 -.250000D+01 .000000D+00 -.250000D+01
The beta (safety index) = .210931D+00
Probability of unsatisfactory performance(Pu)= .416471D+00
*****
***Summary of Reliability Results for Piles**
-Pile- -LimitState- -Beta- ---Pu---
1 1 .747992D+01 .371925D-13
2 1 .137780D+02 .000000D+00
1 2 .453881D+01 .282858D-05
2 2 .454760D+01 .271312D-05
*****
***Summary of Reliability Results for Displacements**
-Displacement- ---Beta--- ---Pu---
1 .364057D+00 .357908D+00
3 .210931D+00 .416471D+00

```

The output of the CPGA-R software, given the same values and limit states, is in Table 4.4. The greatest probability of unsatisfactory performance was given for the limit state of a displacement of 0.029 in the Z direction, but the value was 42.01%.

Looking at the probabilities for exceeding the pile cap displacement limits, the values for RCPGA are different from the probabilities for exceeding the pile cap displacement limits in CPGA-R. Because the CPGA-R probabilities for unsatisfactory performance were higher than RCPGA's and both programs' design points generated values for the displacements at the limit state values, it seemed likely that CPGA-R was generating more accurate values.

The difference came to light when the Ayyub et al. (1997) design points for RCPGA were examined in detail and it was revealed that the X positions of the two piles, which were specified as variables in the vector, were not changing. In Table 4.8, for each iteration of each limit state, the alpha values for the variables X(4) and X(5) are always 0.0, so the design point

values (*dp*) for those variables are always the same as the mean values for those variables (*meanEN*). This must have been a result of a logical mistake in the coding for the 1997 RCPGA. When the CPGA-R example file was rewritten to not include the displacements of the two piles (Figures 4.7 and 4.8), the limit states for the deflection of the pile caps had the same probability as the runs in the original RCPGA example. This is shown by the greatest probability of unsatisfactory performance in Table 4.9, which has the same value (41.65%) for the same limit state (0.029-in. displacement in the *Z* axis).

**Table 4.9. Results of CPGA-R with Example 1 input from the RCPGA manual, modified to remove the pile translation variables.**

```

CPGA-R ASM Analysis Output 12/11/2012 7:44:53 AM

Time to completion = 00:00:16 Total number of CPGA runs = 175

Return Status States:

  Unaffected means that the limit state is unaffected by all of the
  variables.

  Computed means that the limit state was reached in the variable space.

  Extreme means that the limit state was not found within 8 standard
  deviations of the mean.

Limit State BETA Failure Prob. Return Status
-----
Translation X = 0.110 3.6405653E-01 3.5790796E-01 Computed

Design Point
-----

Card ID Index Variable Value Directional Cosine
-----
LOAD 01 px -39.8189342752799 0.767159750896063
LOAD 01 pz 111.726006249378 0.629020329475259
LOAD 01 my 173.011037935066 0.125695432343139

```

Limit State BETA Failure Prob. Return Status

-----  
Translation Z = 0.029 2.1093092E-01 4.1647062E-01 Computed

Design Point

-----  
Card ID Index Variable Value Directional Cosine

-----  
LOAD 01 px -39.2396331976045 -0.50685409896392

LOAD 01 pz 114.182765138042 -0.855544820115319

LOAD 01 my 173.589251975613 -0.10555559263876

Limit State BETA Failure Prob. Return Status

-----  
File #0001 ALF =8.000000E00 0 1.000000E-16 0 Extreme

Design Point

-----  
Card ID Index Variable Value Directional Cosine

-----  
LOAD 01 px -39.4 -6.82646597049929E-02

LOAD 01 pz 113.1 -0.940074032361122

LOAD 01 my 173.4 -0.334066984174823

Limit State BETA Failure Prob. Return Status

-----  
File #0001 CBF 4.5388135E00 2.8313107E-06 Computed

Design Point

-----  
Card ID Index Variable Value Directional Cosine

```
LOAD 01 px -45.7994689101363 0.939962080832129
LOAD 01 pz 103.855249690723 0.339470152113608
LOAD 01 my 172.046233905082 3.50899190893674E-02
```

Limit State BETA Failure Prob. Return Status

-----

```
File #0002 ALF =8.000000E00 0 1.000000E-16 0 Extreme
```

Design Point

-----

```
Card ID Index Variable Value Directional Cosine
```

-----

```
LOAD 01 px -39.4 0.346425982664289
LOAD 01 pz 113.1 -0.914640838619028
LOAD 01 my 173.4 -0.208377481665756
```

Limit State BETA Failure Prob. Return Status

-----

```
File #0002 CBF 4.5475952E00 2.7157633E-06 Computed
```

Design Point

-----

```
Card ID Index Variable Value Directional Cosine
```

-----

```
LOAD 01 px -45.5638718967269 0.903608989990676
LOAD 01 pz 101.805176880779 0.413948565198998
LOAD 01 my 169.141436014531 0.110169771615093
```

```
*****
* Final Results *
*****
```



```
The greatest probability of failure occurs for the limit state: Translation  
Z = 0.029
```

```
The greatest probability of failure was 41.65E00%
```

An addition to the ASM code used in CPGA-R, as opposed to the original RCPGA, has been a software check that makes the user aware that certain limit states might be unaffected by a selected variable vector. In this case, varying any or all the variables in a vector will not make the  $f(\vec{X})$  function approach 0.0. In RCPGA, the onus was placed on the user to choose limit states that would be affected by any or all variables in vector  $\vec{X}$ . In CPGA-R, all limit states are tested and unaffected variables are reported to the user.

## **5 Summary, Conclusions, and Future Research**

### **5.1 Summary and conclusions**

The report has addressed the creation of a validated reliability solution for pile placement using the pile group layout analysis software CPGA. This work, which follows the published research for the 1997 RCPGA software, has aimed to create a portable library of reliability routines that can be used with base CASE library software to introduce reliability analyses for a range of engineering problems such as pile layout and design. The routines followed the common reliability methods discussed in the RCPGA contractual report (Ayyub et. al. 1997) to establish the theory and limitations of the methods.

When the theory was examined, shortcomings in the logic for the original 1997 RCPGA software came to light and these problems were remedied in the new CPGA-R software. It also was recognized that, while the ASM method could give accurate results for limit states with a linear response surface, it is not accurate for cases in which the response surface is nonlinear, which can be a result of the nature of the system response curve or by having a response curve based on a selection of multiple limit states. However, simulation methods such as Latin Hypercube and Importance Sampling with Latin Hypercube can cover this weakness because they are area-based methods. Using the ASM method to provide a location for the secondary distribution function for Importance Sampling with Latin Hypercube is a particularly efficient and accurate method to measure reliability for CPGA problems.

In creating the additions to the CPGA GUI for CPGA-R, weaknesses in the original CPGA GUI were addressed first to help the user understand the input model. Routines then were added to extend the program's reliability analysis capabilities. These routines allowed the user to enter variable and limit state information in a manner that was consistent with the original CPGA user interface. Means to store and load this information was built into the GUI.

Also added were GUI methods to view the output of reliability analyses. Because reliability studies with multidimensional variables and multiple limit states can be abstract, significant effort was placed in making the output readable and, where possible, viewable. The authors of this report anticipate Corps district engineers will deal with multi-variable CPGA analysis problems. This means the results for  $N$  variables will be generated in  $N$ -variable space. This is difficult to visualize. To help provide a visualization of the reliability results for the ASM and simulation methods used in CPGA-R, several two-variable problems were analyzed and discussed in Chapter 4. The intent was to present graphically the reliability results generated by the ASM and simulation analyses and to relay a visual understanding of the reliability results. Chapter 4 and other parts of this report aimed to make the process clearer.

## 5.2 Future research

Reliability analysis is needed for major rehabilitation studies resulting in approach wall rehabilitations and/or extensions. Example reliability analyses discussed in Chapter 4 show the deformation limit state is generally the dominant one for the batter pile problem.

Lateral deformation of a batter pile group is dominated by the value specified for the axial stiffness in the CPGA input. The axial pile stiffness is expressed as (Hartman et al. 1989; Ebeling et al. 2012):

$$b_{33} = C_{33} \frac{AE}{L} \quad (5.1)$$

where

- $b_{33}$  = axial pile stiffness;
- $C_{33}$  = constant that accounts for the interaction between the soil and the pile;
- $A$  = cross-sectional area of the pile;
- $E$  = modulus of elasticity of the pile;
- $L$  = length of the pile.

The term  $AE/L$  is the elastic stiffness of the pile acting as a short column with no soil present. The authors of this report recognize the deformations are dominated by the soil, not the compression of the pile. The  $C_{33}$  term may be interpreted as a scale factor of the axial stiffness of the pile to

account for the actions of the soil along the surface and tip of the pile. The coefficient ( $C_{33}$ ) accounts for the stiffness of the soil-pile system in its entirety.

The original 1989 CPGA guidelines for design purposes (Hartmann et al. 1989) give a compression pile  $C_{33}$  term, which typically ranges from 1.0 and 2.0. There appears to be a relationship between  $C_{33}$  and pile length. Longer piles tend to have higher values of  $C_{33}$  than shorter ones.

Long-term loading, cyclic loading, pile group effects, and pile batter can affect  $C_{33}$ . In sand, long-term loading has little effect on the value of  $C_{33}$ ; however, consolidation in clay due to long-term loading can reduce  $C_{33}$ .

The value of  $C_{33}$  for single piles can be calculated using:

$$C_{33} = \frac{\Delta}{\delta} \quad (5.2)$$

where

$$\Delta = \frac{PL}{AE},$$

$\delta$  = axial movement of the pile head due to axial load  $P$ ;

$P$  = allowable axial design load for the pile.

More research will be conducted to provide data for defining a database of samples for key variables (i.e., the  $C_{33}$  term) used in the deterministic or reliability analysis of a cluster of in-line batter piles of flexible approach walls. Finite element modeling of 3D Soil-Structure Interaction may be used to help develop this database (especially the  $C_{33}$  term). Research will be conducted to determine soil interactions along the pile and at the batter pile tip, for defining simplified methods of design under the condition when the batter pile plunges into the soil because of loading. Results will be used to summarize the generated database and discuss the application of a reliability-based engineering procedure analyzing a flexible approach wall impact structure founded on clustered pile groups with batter piles, using CPGA-R and resulting in a minimum depth of pile embedment. This minimum depth of pile embedment will enable engineers to build cost-effective, reliable flexible approach walls.

## References

- Ang, A. H-S., and W. H. Tang. 1984. *Probability concepts in engineering planning and design, Volume II: Decision, risk, and reliability*. New York: John Wiley & Sons.
- Ayyub, B. M., Eloiseily, K., Patev, R. C., and M. A. Leggett. 1997. *Reliability assessment of pile groups (RCPGA)*. WES Technical Report for Contracts, DACW39-96-K-0046. Vicksburg, MS: US Army Engineer Waterways Experiment Station.
- Baecher, G. B., and J. T. Christian. 2003. *Reliability and statistics in geotechnical engineering*. New York: John Wiley & Sons.
- Castello, R. R. 1980. Bearing capacity of driven piles in sand. Ph.D. thesis, Texas A&M Univ.
- Dawkins, W. P. 1978. Pile head stiffness matrices (unpublished). Vicksburg, MS: US Army Engineer Waterways Experiment Station.
- Ditlevsen, O. 1981. *Uncertainty modeling with applications to multidimensional civil engineering systems*. New York: McGraw-Hill.
- Ebeling, R. M., Strom, R. W., White, B. C., and K. Abraham. 2012. *Simplified analysis procedures for flexible approach wall systems founded on groups of piles and subjected to barge train impact*. ERDC/ITL TR-12-3. Vicksburg, MS: US Army Engineer Research and Development Center.
- Hartman, J. P., J. J. Jaeger, J. J. Jobst, and D. K. Martin. 1989. *User's guide: Pile group analysis (CPGA) computer program X0080*. ITL-89-3. Vicksburg, MS: US Army Engineer Waterways Experiment Station.
- Hasofer, A. M., and N. C. Lind. 1974. Exact and invariant second moment code format. *Journal of the Eng. Mech. Division, ASCE*, 100(EM1).
- Hrennikoff, A. 1950. Analysis of pile foundation with batter piles. *Transactions, American Society of Civil Engineers* 115(2401).
- Lemaire, M. 2009. *Structural reliability*. New York: John Wiley & Sons.
- Melchers, R. E. 2001. *Structural reliability analysis and prediction*. New York: John Wiley & Sons.
- Mosher, R. L. 1984. *Load transfer criteria for numerical analysis of axially loaded piles in sand, Part 1: Load-transfer criteria*. Technical Report K-84-1. Vicksburg, MS: US Army Engineer Waterways Experiment Station.
- Nowak, A. S., and K. R. Collins. 2000. *Reliability of structures*. Boston: McGraw-Hill.
- Nowak, A. S., and K. R. Collins. 2013. *Reliability of structures, 2<sup>nd</sup> ed.* Boca Raton, FL: CRC Press, Taylor and Francis Group.

- O'Neill, M. W. 1964. Determination of the pile-head, torque-twist relationship for a circular pile embedded in a clay soil. MS thesis, Univ. of Texas.
- Rackwitz, R., and B. Fiessler. 1976. Note on discrete safety checking when using non-normal stochastic model for basic variables. Loads Project Working Session, MIT, Cambridge, MA, pp. 489-494.
- Rackwitz, R., and B. Fiessler. 1978. Structural reliability under combined random load sequences. In *Computer and Structures*, 9:489-494. Oxford: Pergamon Press.
- Rosenblatt, M. 1952. Remarks on a multivariate transformation. *Annals of Mathematical Statistics* 23(3):470-472.
- Saul, W. E. 1968. Static and dynamic analysis of pile foundations. *Journal of the Structural Division, ASCE*, 94(ST5):5936 (proceeding paper).
- Scott, F. S. 1981. *Foundation analysis*. Englewood Cliffs, NJ: Prentice-Hall.
- Semple, R. M., and W. J. Rigden. 1984. Shaft capacity of driven pile in clay. In *Analysis and design of pile foundations*, ed. J. R. Meyer, 59-79. American Society of Civil Engineers.
- Stoll, U. W. 1972. Torque shear test of cylindrical friction piles. *Civil Engineering, American Society of Civil Engineers*, 42:63-65.
- Swiler, L. P., and G. D. Wyss. 2004. *A user's guide to Sandia's Latin Hypercube sampling software: LHS UNIX library/standalone version*. Albuquerque, NM: Sandia National Laboratories.
- Terzaghi, Z., and R. B. Peck. 1967. *Soil mechanics in engineering practice*. New York: Wiley.
- USACE. 1991. *Design of pile foundations*. EM 11110-2-2906. Washington, DC: US Army Corps of Engineers.
- USACE. 2011. *Risk and reliability engineering for major rehabilitation studies*. EC 1110-2-6062. Washington, DC: US Army Corps of Engineers.

# Appendix A: Skin Friction and Tip Capacities of Piles

## A.1 Introduction

The skin friction capacity and limiting tip resistance of a pile founded in sand or in clay can be determined using one of the procedures outlined in this appendix.

## A.2 Skin friction and tip capacities of piles (USACE 1991)

The skin friction and tip capacity of a pile founded in different materials (i.e., sand or clay) can be determined using one of the relationships in this section. This material was presented first in USACE (1991).

### A.2.1 Pile capacity

Pile capacity should be computed by an experienced designer who is familiar with the various types of piles, how piles behave when loaded, and the soil conditions that exist at the site.

#### A.2.1.1 Axial pile capacity

The axial capacity of a pile can be represented by:

$$Q_{ult} = Q_s + Q_t \quad (A.1)$$

$$Q_s = f_s A_s \quad (A.2)$$

$$Q_t = q A_t \quad (A.3)$$

where:

$Q_{ult}$  = ultimate pile capacity;

$Q_s$  = shaft resistance of the pile due to skin friction;

$Q_t$  = tip resistance of the pile due to end bearing;

$f_s$  = average unit skin resistance;

$A_s$  = surface area of the shaft in contact with the soil;

$q$  = unit tip-bearing capacity;

$A_t$  = effective (gross) area of the tip of the pile in contact with the soil.

1. Piles in cohesionless soil

- a) Skin friction: For design purposes, the skin friction of piles in sand increases linearly to an assumed critical depth ( $D_c$ ), then remains constant below that depth. The critical depth varies between 10 to 20 pile diameters or widths ( $B$ ), depending on the relative density of the sand. The critical depth is assumed as:

$D_c = 10B$  for loose sands;

$D_c = 15B$  for medium dense sands;

$D_c = 20B$  for dense sands.

The unit skin friction acting on the pile shaft can be determined by:

$$f_s = K\sigma_v \tan\delta \quad (\text{A.4})$$

$$\sigma_v = \gamma' D \text{ for } D < D_c \quad (\text{A.5})$$

$$\sigma_v = \gamma' D_c \text{ for } D \geq D_c \quad (\text{A.6})$$

$$Q_s = f_s A_s \quad (\text{A.7})$$

where:

$K$  = lateral earth pressure coefficient ( $K_c$  for compression piles and  $K_t$  for tension piles);

$\sigma_v'$  = effective overburden pressure;

$\delta$  = angle of friction between the soil and the pile;

$\gamma'$  = effective unit weight of soil;

$D$  = depth along the pile at which the effective overburden pressure is calculated.

Values of  $\delta$  are in Table A.1.

Table A.1. Values of  $\delta$ .

Pile Material	$\delta$
Steel	0.67 $\phi$ to 0.83 $\phi$
Concrete	0.90 $\phi$ to 1.0 $\phi$
Timber	0.80 $\phi$ to 1.0 $\phi$



Values of  $K$  for piles in compression ( $K_c$ ) and piles in tension ( $K_t$ ) are in Table A.2. Tables A.1 and A.2 present ranges of values of  $\delta$  and  $K$  based on experience in various soil deposits. These values should be selected for design based upon experience and pile load tests. It is not intended for the designer to use the minimum reduction of the  $\phi$  angle while using the upper range  $K$  values.

Table A.2. Values of  $K$ .

Soil Type	$K_c$	$K_t$
Sand	1.00 to 2.00	0.50 to 0.70
Silt	1.00	0.50 to 0.70
Clay	1.00	0.70 to 1.00

Note: The above do not apply to piles that are prebored, jetted, or installed with a vibratory hammer. Picking  $K$  values at the upper end of the above ranges should be based on local experience.  $K$ ,  $\delta$ , and  $N_q$  values back-calculated from load tests may be used.

For steel H-piles,  $A_s$  should be taken as the block perimeter of the pile and  $\delta$  should be the average friction angles of steel against sand and sand against sand ( $\phi$ ). Table A.2 contains general guidance to be used, unless the long-term engineering practice in the area indicates otherwise. Under-prediction of soil strength parameters at load test sites has at times produced back-calculated values of  $K$  that exceed the values in Table A.2. It also has been found both theoretically and at some test sites that the use of displacement piles produces higher  $K$  values than does the use of nondisplacement piles. Values of  $K$  that have been used satisfactorily, but with standard soil data in some locations, are in Table A.3.

Table A.3. Common values for corrected  $K$ .

Common Values for Corrected $K$				
Soil Type	Displacement Piles		Nondisplacement Piles	
	Compression	Tension	Compression	Tension
Sand	2.00	0.67	1.50	0.50
Silt	1.25	0.50	1.00	0.35
Clay	1.25	0.90	1.00	0.70

Note: Although these values may be used in some areas, they should not be used without validating them.

- b) End bearing: For design purposes, the pile-tip bearing capacity can be assumed to increase linearly to a critical depth ( $D_c$ ), then to remain constant. The same critical depth relationship used for skin friction can be used for end bearing. The unit tip bearing capacity can be determined by:

$$q = \sigma_v' N_q \quad (\text{A.8})$$

where:

$$\sigma_v' = \gamma' D \text{ for } D < D_c \quad (\text{A.9})$$

$$\sigma_v' = \gamma' D_c \text{ for } D \geq D_c \quad (\text{A.10})$$

For steel H-piles,  $A_t$  should be the area within the block perimeter. A curve to obtain the Terzaghi and Peck (1967) bearing capacity factor  $N_q$  (among values from other theories) is in Figure A.1. To use the curve, one must obtain measured values of the angle of internal friction ( $\phi$ ), which represents the soil mass.

- c) Tension capacity: The tension capacity of piles in sand can be calculated using the  $K$  values for tension from Table A.2:

$$Q_{ult} = Q_{s_{tension}} \quad (\text{A.11})$$

## 2. Piles in cohesive soil

- a) Skin friction: Although called skin friction, the resistance is due to the cohesion or adhesion of the clay to the pile shaft.

$$f_s = c_a \quad (\text{A.12})$$

$$c_a = \alpha c \quad (\text{A.13})$$

$$Q_s = f_s A_s \quad (\text{A.14})$$

where:

$c_a$  = adhesion between the clay and the pile;

$\alpha$  = adhesion factor;

$c$  = undrained shear strength of the clay from a Q test.

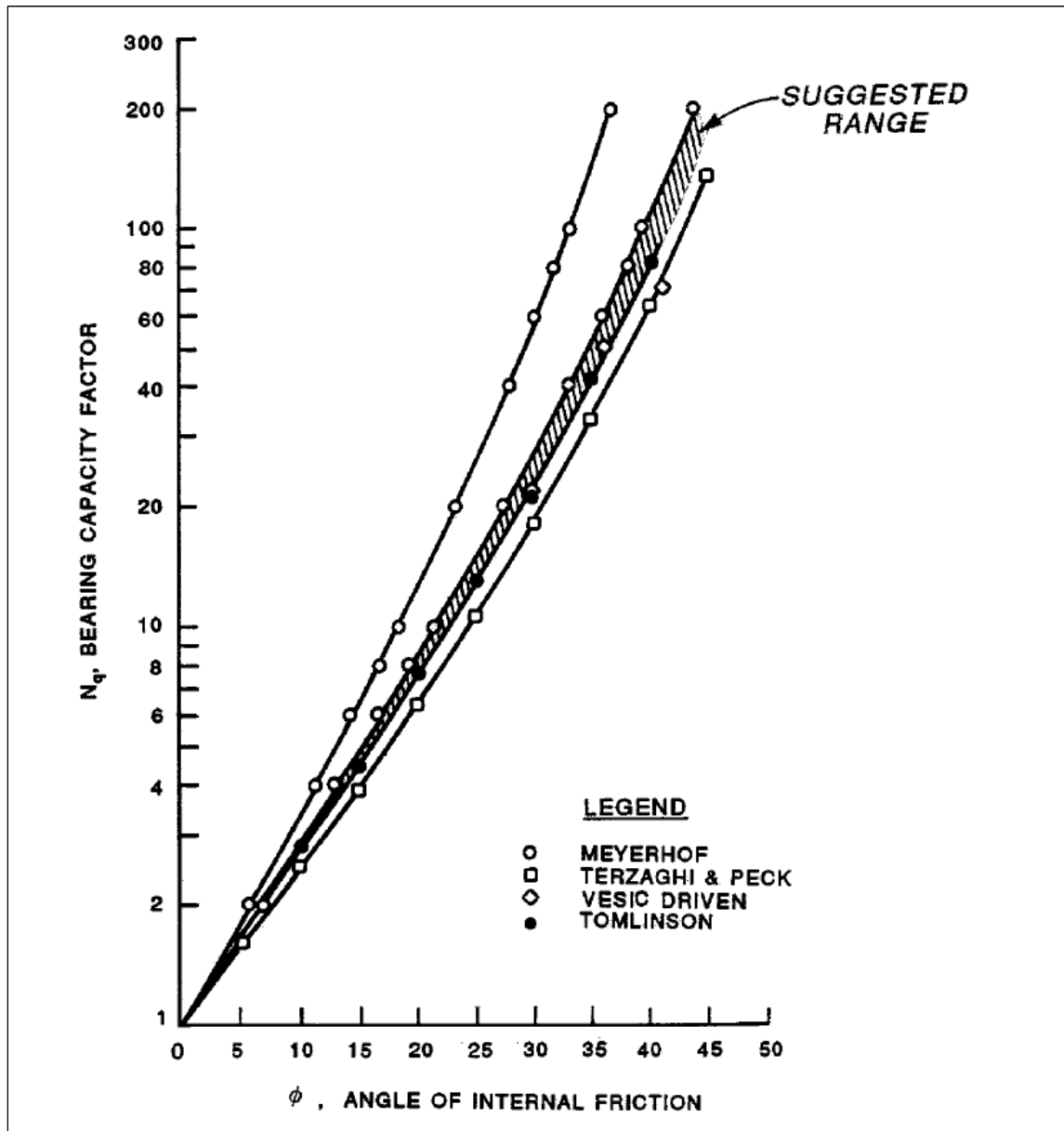


Figure A.1. Bearing capacity factor.

The values of  $\alpha$  as a function of the undrained shear are in Figure A.2a.

An alternate procedure, developed by Semple and Rigden (1984), to obtain values of  $\alpha$  (which is especially applicable for long piles) is in Figure A.2b, where:

$$\alpha = \alpha_1 \alpha_2 \tag{A.15}$$

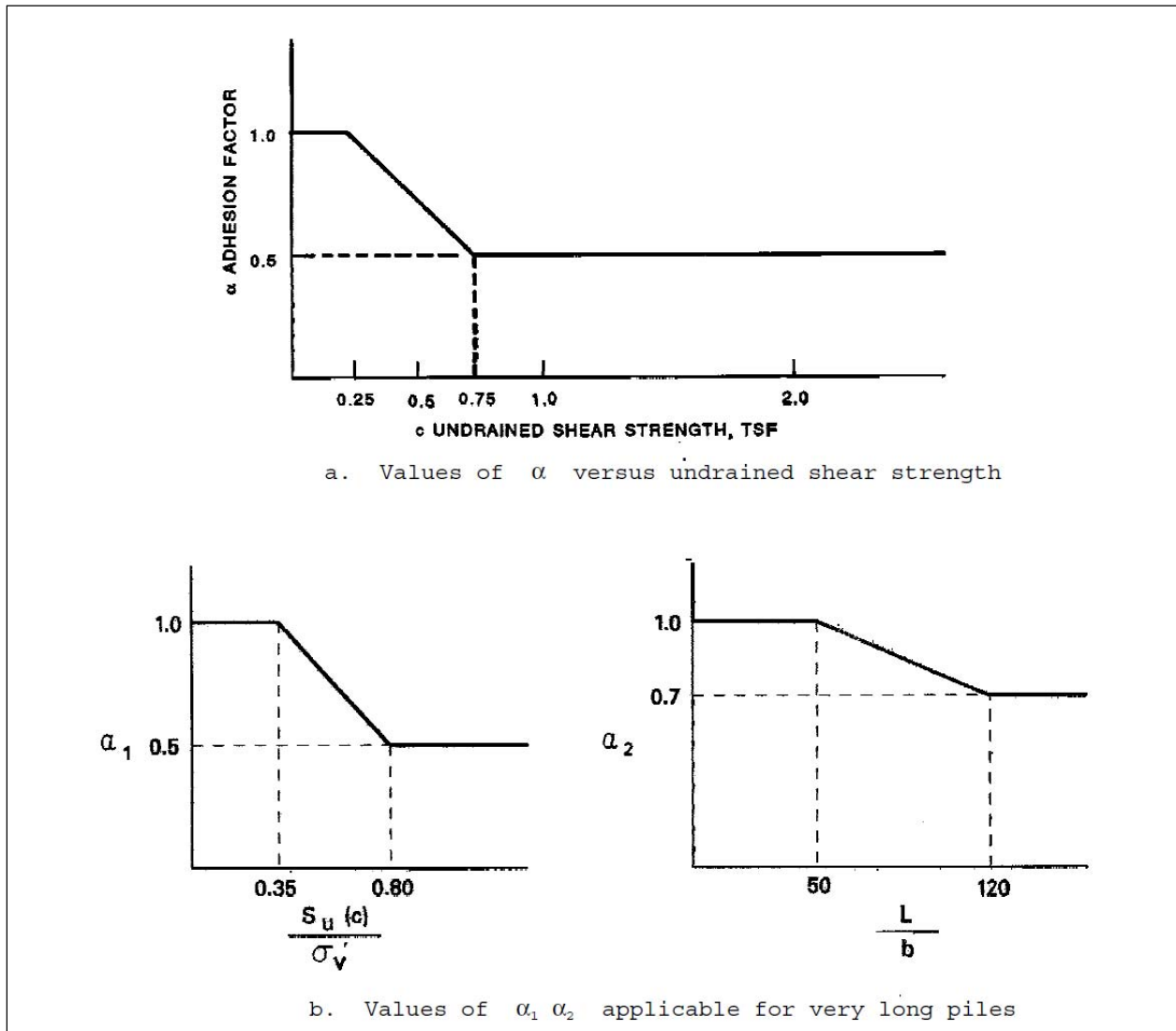


Figure A.2. (a) Values of  $\alpha$  vs. undrained shear strength and (b) values of  $\alpha_1 \alpha_2$  applicable for long piles.

and

$$f_s = \alpha c \tag{A.16}$$

b) End bearing: Determine the pile unit tip-bearing capacity for piles in clay by:

$$q = 9c \tag{A.17}$$

$$Q_t = A_t q \tag{A.18}$$

However, the movement necessary to develop the tip resistance of piles in clay soils might be several times larger than that required to develop the skin friction resistance.

- c) Compression capacity: Find the ultimate compression capacity by combining the skin friction capacity and the tip-bearing capacity:

$$Q_{ult} = Q_s + Q_t \quad (\text{A.19})$$

- d) Tension capacity: Compute tension capacity of piles in clay by:

$$Q_{ult} = Q_s \quad (\text{A.20})$$

- e) The pile capacity in normally consolidated clays (cohesive soils) also should be computed in the long-term *S* shear strength case. That is, develop an *S* case shear strength trend, as discussed previously, and proceed as if the soil is drained. The computational method is identical to that presented for piles in granular soils, and to present the computational methodology would be redundant. However, the shear strengths in clays in the *S* case are assumed to be  $\phi > 0$  and  $C = 0$ .

Some commonly used *S* case shear strengths in alluvial soils are in Table A.4.

Table A.4. S case shear strength.

S Case Shear Strength		
Soil Type	Consistency	Angle of Internal Friction ( $\phi$ )
Fat clay (CH)	Very soft	13° to 17°
Fat clay (CH)	Soft	17° to 20°
Fat clay (CH)	Medium	20° to 21°
Fat clay (CH)	Stiff	21° to 23°
Silt (ML)		25° to 28°

Note: The designer should perform testing and select shear strengths. These general data ranges are from tests on specific soils in site-specific environments and might not represent the soil in question.

### 3. Piles in silt

- a) Skin friction: The skin friction on a pile in silt is a two-component resistance to pile movement contributed by the angle of internal friction ( $\phi$ ) and the cohesion ( $c$ ) acting along the pile shaft. That portion of the resistance contributed by the angle of internal friction ( $\phi$ ) is, as with the sand, limited to a critical depth of ( $D_c$ ), below which the frictional portion remains constant; the limit depths are stated below. That portion of the resistance contributed by the cohesion might require limit if it is sufficiently large (Figures A.2a and b). The shaft resistance can be computed by:

$$f_s = K\gamma' D \tan\delta + \alpha c \quad (\text{A.21})$$

where ( $D \leq D_c$ )

$$Q_s = A_s f_s \quad (\text{A.22})$$

where:

$Q_s$  = capacity due to skin resistance;

$f_s$  = average unit skin resistance;

$A_s$  = surface area of the pile shaft in contact with soil;

$K$  = see Table A.2;

$\alpha$  = see Figures A.2a and b;

$D$  = depth below ground up to limit depth  $D_c$ ;

$\delta$  = limit value for shaft friction angle from Table A.1.

- b) End Bearing: The pile tip-bearing capacity increases linearly to a critical depth ( $D_c$ ) and remains constant below that depth. The critical depths are:

$D_c = 10 B$  for loose silts;

$D_c = 15 B$  for medium silts;

$D_c = 20 B$  for dense silts.

The unit and bearing capacity can be computed by:

$$q = \sigma_v' N_q \quad (\text{A.23})$$

$$\sigma_v' = \gamma' D \text{ for } D < D_c \quad (\text{A.24})$$

$$\sigma_v' = \gamma' D_c \text{ for } D \geq D_c \quad (\text{A.25})$$

$$Q_t = A_t q \quad (\text{A.26})$$

where:

$N_q$  = Terzaghi bearing capacity factor, Figure A.1;

$\sigma_v'$  = vertical earth pressure at the tip with limits;

$A_t$  = area of the pile tip, as determined for sands.

- c) Compression capacity: By combining the two incremental contributors, skin friction and end bearing, the ultimate capacity of the soil/pile can be computed by:

$$Q_{ult} = Q_s + Q_t \quad (\text{A.27})$$

- d) Tension capacity: Compute tension capacity by applying the appropriate value of  $K_t$  from Table A.2 to the unit skin friction equation above.

$$Q_{ult} = Q_{s_{tension}} \quad (\text{A.28})$$

- e) When designing pile foundations in silty soils, consider selecting a conservative shear strength from classical  $R$  shear tests. Also, test piles need to be considered a virtual necessity, and pile length might have to be increased in the field.
4. Piles in layered soils: Piles most frequently are driven into a layered soil stratigraphy. For this condition, the preceding methods of computation can be used on a layer-by-layer basis. The end-bearing capacity of the pile should be determined from the properties of the layer of soil in which the tip is founded. However, when weak or dissimilar layers of soil exist within approximately 5 ft or eight pile tip diameters, whichever is larger, of the tip founding elevation, the end-bearing capacity will be affected. It is necessary to compute this effect and account for it when assigning end-bearing capacity. In computing the skin resistance, the contribution of each layer is computed separately, considering the layers above as a

surcharge and applying the appropriate reduction factors for the soil type within that increment of pile shaft.

- a) Skin friction: The skin friction contributed by different soil types can be computed incrementally and summed to find the ultimate capacity. Consider the compatibility of strain between layers when computing the unit skin resistance.

$$Q_s = \sum_{i=1}^N f_{s_i} A_{s_i} \quad (\text{A.29})$$

where:

$f_{s_i}$  = unit skin resistance in layer  $i$ ;

$A_{s_i}$  = surface area of pile in contact with layer  $i$ ;

$N$  = total number of layers.

- b) End bearing: The pile tip bearing should be computed based on the soil type in which the tip is founded, with limits near layer boundaries mentioned above. With the overlying soil layers as surcharge, use:

Sand or silt:

$$q = \sigma_v' N_q \quad (\text{A.30})$$

$$\sigma_v' = \gamma' D \text{ for } D < D_c \quad (\text{A.31})$$

$$\sigma_v' = \gamma' D_c \text{ for } D > D_c \quad (\text{A.32})$$

$$Q_t = A_t q \quad (\text{A.33})$$

Clay:

$$q = 9c \quad (\text{A.34})$$

$$Q_t = A_t q \quad (\text{A.35})$$



- c) Compression capacity: By combining the skin resistance and end bearing, compute the ultimate capacity of the soil/pile by:

$$Q_{ult} = Q_s + Q_t \quad (\text{A.36})$$

- d) Tension capacity: Compute tension capacity by applying the appropriate values of  $Kt$  from Table A.2, as appropriate for granular soils, to the incremental computation for each layer, then combining to yield:

$$Q_{ult} = Q_{s_{tension}} \quad (\text{A.37})$$

5. Point-bearing piles: In some cases, the pile will be driven to refusal on firm, good-quality rock. Therefore, the capacity of the pile is governed by the structural capacity of the pile or the rock capacity.

#### A.2.1.2 Pile group capacity

The pile group capacity for piles in cohesionless and cohesive soils is:

1. Piles in cohesionless soil: The pile group efficiency  $\eta$  is defined as:

$$\eta = \frac{Q_{group}}{NQ_{ult}} \quad (\text{A.38})$$

where:

$Q_{group}$  = ultimate capacity of a pile group;

$N$  = number of piles in a group;

$Q_{ult}$  = ultimate capacity of a single pile.

The ultimate group capacity of driven piles in sand is equal to or greater than the sum of the ultimate capacity of the single piles. Therefore, in practice, the ultimate group capacity of driven piles in sand not underlain by a weak layer should be taken as the sum of the single pile capacities ( $\eta = 1$ ). For piles jetted into sand,  $\eta$  is less than 1. For piles underlain by a weak layer, the ultimate group capacity is the smaller of the sum of the single pile ultimate capacities or the capacity of an equivalent pier with the geometry defined by enclosing the pile

group (Terzaghi and Peck 1967). The base strength should be that of the weak layer.

2. Piles in cohesive soil: The ultimate group capacity of piles in clay is the smaller of the sum of the single pile ultimate capacities or the capacity of an equivalent pier (Terzaghi and Peck 1967). The ultimate group capacity of piles in clay is given by the smaller of:

$$Q_{group} = NQ_{ult} \quad (A.39)$$

$$Q_{group} = 2(B_g + L_g)D\bar{c} + \left[ 5 \left( 1 + \frac{D}{5B_g} \right) \left( 1 + \frac{B_g}{5L_g} \right) \right] c_b L_g B_g \quad (A.40)$$

where:

$$N_c = 5 \left( 1 + \frac{D}{5B_g} \right) \left( 1 + \frac{B_g}{5L_g} \right) \leq 9 \quad (A.41)$$

and:

$B_g$  = width of the pile group;

$L_g$  = length of the pile group;

$D$  = depth of the pile group;

$\bar{c}$  = weighted average of undrained shear strength over the depth of pile embedment ( $\bar{c}$  should be reduced by  $\alpha$  from Figure A.2);

$c_b$  = undrained shear strength at the base of the pile group.

This equation applies to a rectangular section only. It should be modified for other shapes.

### A.3 Skin friction and tip capacities of piles (Castello 1980)

The skin friction capacity of a pile founded in sand can be determined using the procedure recommended by Mosher (1984), who investigated load-transfer criteria of axially loaded piles in sand. One of the products from his investigation was a pair of charts attributed to the research of Castello (1980) for skin friction capacity and for pile tip capacity. These charts were identified as Figures 76 and 77 in the Mosher report and are reproduced in this report as Figures A.3 and A.4. Mosher's evaluations of

the field data show the average standard error of the unadjusted values for side resistance are 25%. A second chart in the Mosher report is similar to Figure A.3 but was developed using adjustments for residual stresses, as presented by Castello. However, the average standard error was higher: 32%. This second chart is not in this report due to its higher error.

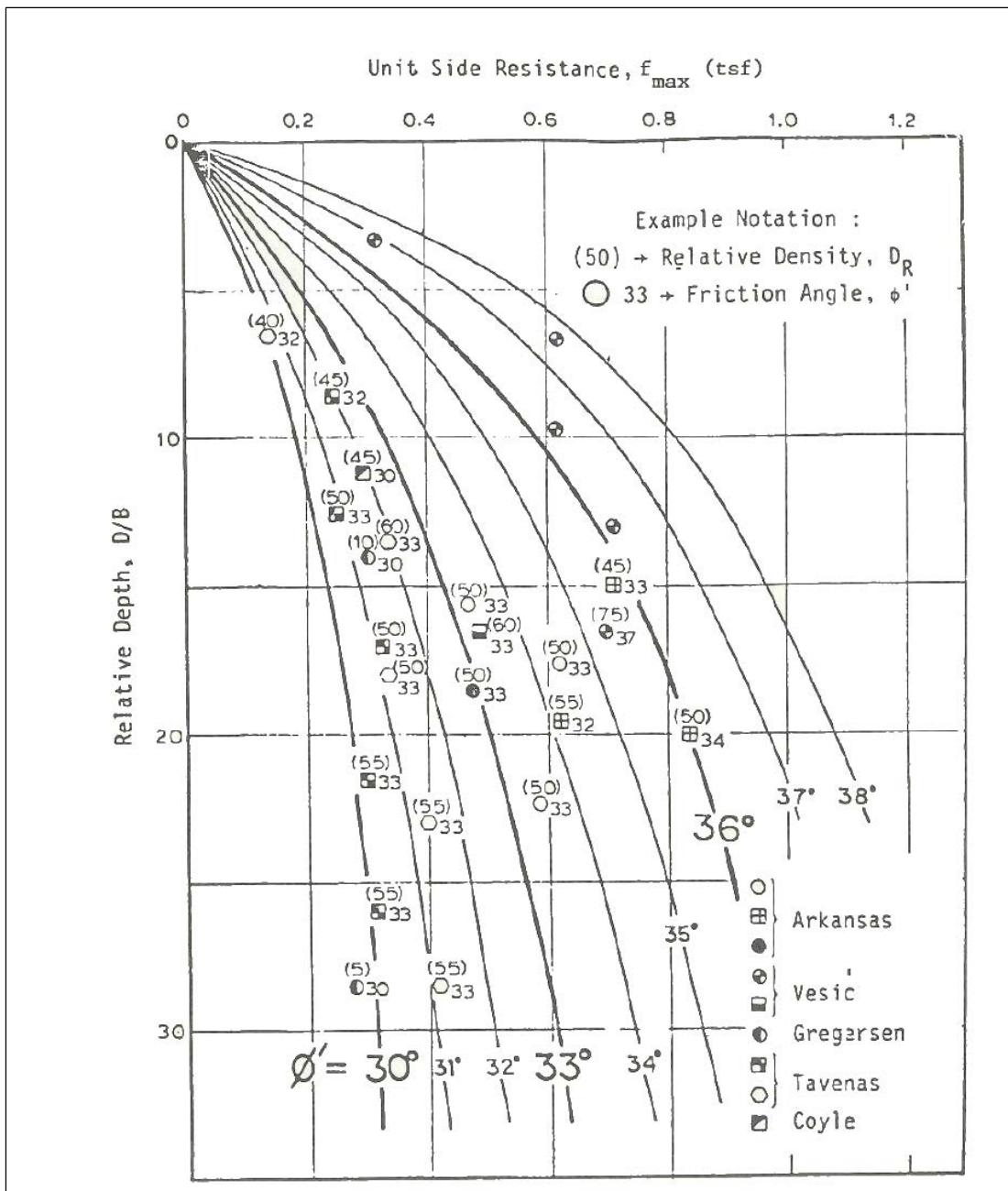


Figure A.3. Unit side resistance for piles in sand vs. relative length (Mosher 1984).

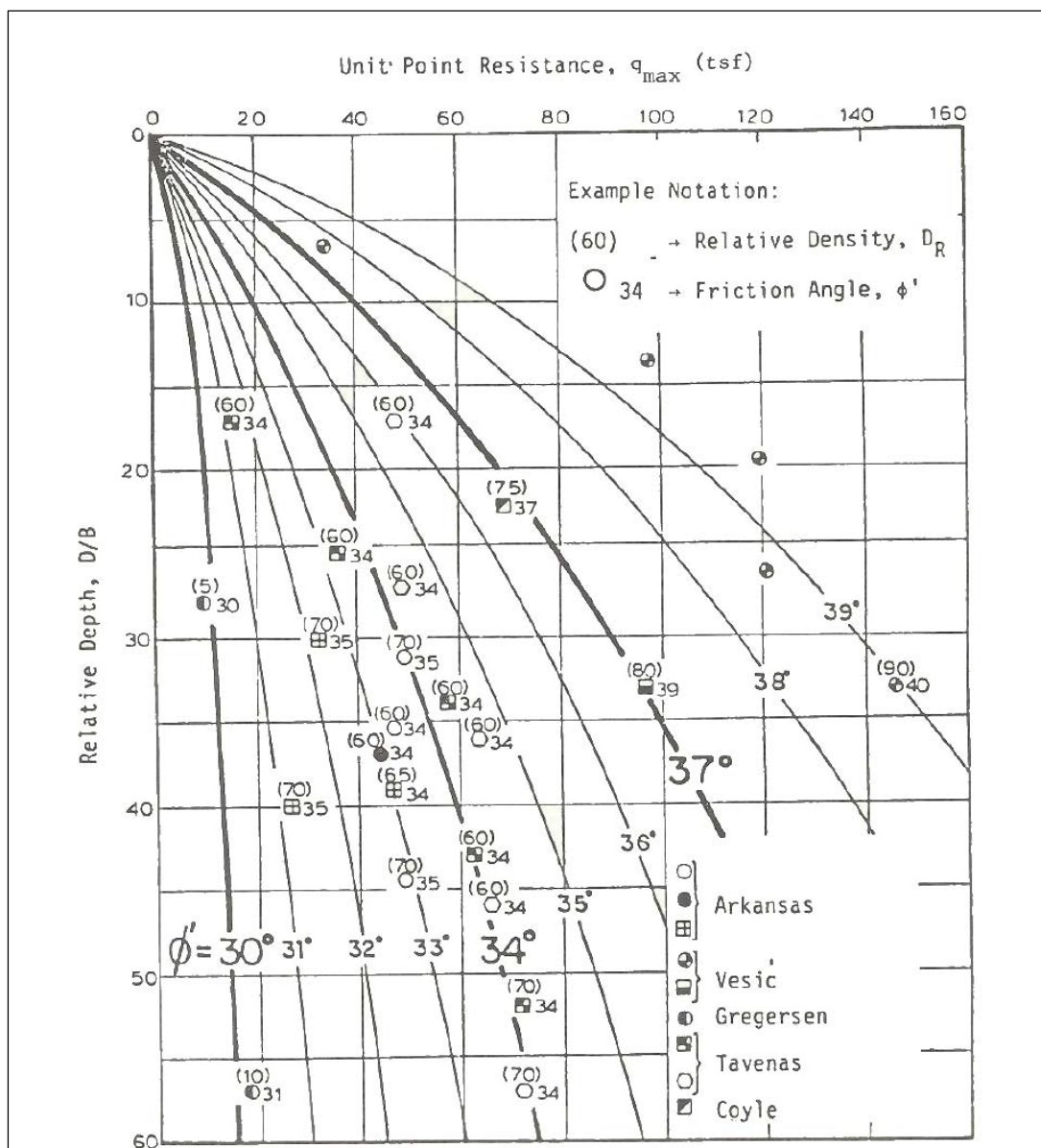


Figure A.4. Unit tip resistance for piles in sand vs. relative length (Mosher 1984).

To determine the skin friction capacity curve of a pile founded in sand, using Figure A.3 requires knowledge of the effective angle of internal friction ( $\phi'$ ) for the sand, the embedded length ( $D$ ), and the diameter of the pile ( $B$ ). The curve will proceed from a relative depth of zero to the relative depth of pile tip determined by dividing the embedded length of the pile by the diameter of the pile. The value of skin friction capacity (or unit side resistance – with units of tsf) for a specified depth of embedment is determined by finding where the current relative depth intersects the curve for the angle  $\phi'$ , which is parabolic with depth. It is possible to approximate this parabolic curve with a piecewise linear definition for the

skin friction capacity curve. Interval relative depth values along the pile are determined by dividing the interval depth of embedment by the diameter of the pile. At these regular relative depth intervals, the skin friction capacity can be determined from the figure, as described above. The results are more accurate with an increasing number of intervals between the mudline and the total depth of embedment of the pile.

To determine the unit tip resistance of a pile founded in sand, using Figure A.4 requires knowledge of the effective angle of internal friction ( $\phi'$ ) for the sand, the embedded length, and the diameter of the pile. The length of pile embedded in sand is normalized by the pile diameter. It is called the relative depth. For this relative depth and a specified value of  $\phi'$ , the unit tip resistance (in units of tsf) is obtained by intersecting the unit tip resistance value the appropriate curve for  $\phi'$  in Figure A.4. Thus, the unit tip resistance of a pile founded in sand is established.

# Appendix B: CPGA-R Probability Density Function (PDF) Distributions and Their Properties

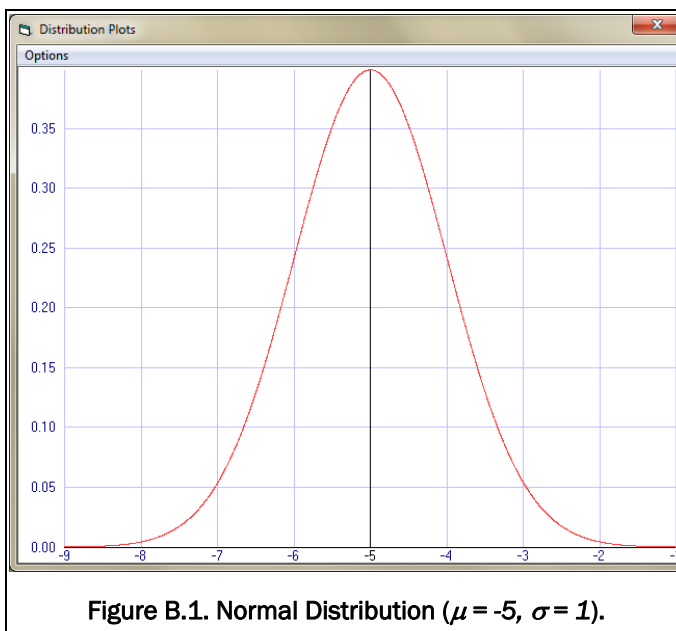
## B.1 Introduction

Six PDF distributions are used for reliability in CPGA-R: Normal, Bounded Normal, the Log-Normal, the Bounded Log-Normal, Uniform, and Triangular. The following sections give:

- the function,  $f(x)$ , for determining the probability at any point,  $x$ , on the distribution;
- the range that the distribution covers;
- the mean value of the distribution;
- the variance ( $\sigma^2$ ) of the distribution. Variance is the square of the standard deviation ( $\sigma$ ).

## B.2 PDF distributions

### B.2.1 Normal Distribution



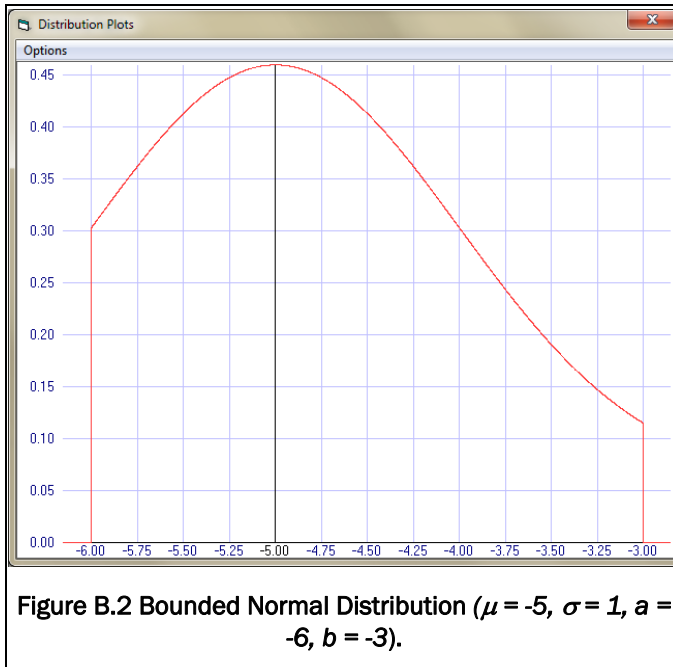
$$f(x) = \frac{1}{\sigma\sqrt{2\pi}} e^{-\frac{(x-\mu)^2}{2\sigma^2}}$$

$$\text{Range} = (\mu - 5\sigma, \mu + 5\sigma)$$

$$\text{Mean} = \mu$$

$$\text{Variance} = \sigma^2$$

### B.2.2 Bounded Normal Distribution



$$f(x) = \frac{1}{\sigma\sqrt{2\pi}} e^{-\frac{(x-\mu)^2}{2\sigma^2}} + \frac{Z}{b-a}$$

Range = (a, b)

Mean (discussed below)

Variance (discussed below)

where  $a$  is the start of the bounded region and  $b$  is the end of the bounded region.  $Z$  is the area of the curve outside of the bounded region (not shown).

The mean and variance can no longer be calculated with a simple equation, but must be solved numerically. The CDF for the curve is calculated by a finite differences method. The mean is given by  $E(x) = \sum_{i=1}^n x_i f(x_i)$ .

The variance is given by  $Var(x) = \sum_{i=1}^n f(x_i)(x_i - \mu)^2$ . For CPGA-R the curve is broken into 100 discrete steps, and  $f(x_i)$  is given at the center of the interval.

### B.2.3 Log-Normal Distribution

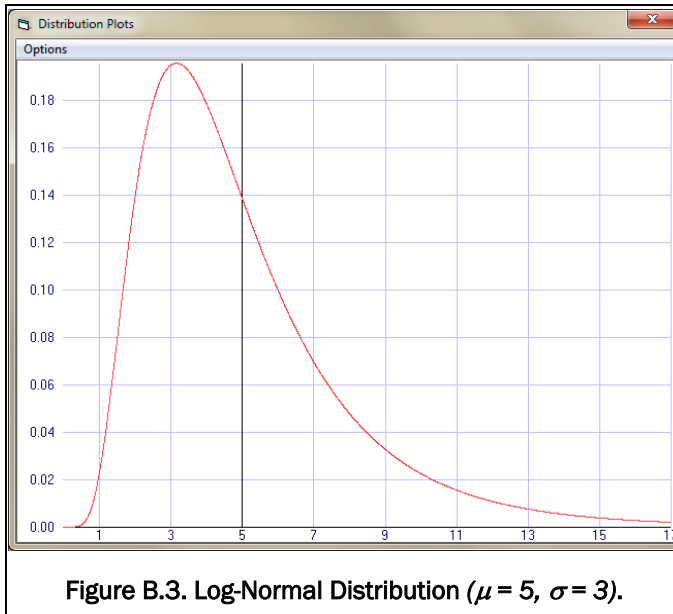


Figure B.3. Log-Normal Distribution ( $\mu = 5, \sigma = 3$ ).

$$f(x) = \frac{1}{x\sigma\sqrt{2\pi}} e^{-\frac{\ln(x)}{2\sigma^2}}$$

Range =  $(0, \mu + 5\sigma)$

Mean =  $e^{\left(\mu + \frac{\sigma^2}{2}\right)}$

Variance =  $e^{2\mu + \sigma^2} (e^{\sigma^2} - 1)$

### B.2.4 Bounded Log-Normal Distribution

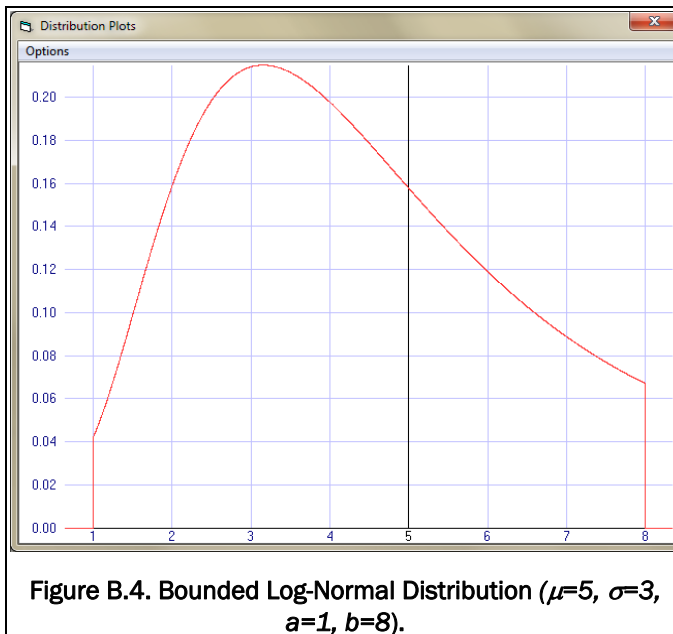


Figure B.4. Bounded Log-Normal Distribution ( $\mu=5, \sigma=3, a=1, b=8$ ).

$$f(x) = \frac{1}{x\sigma\sqrt{2\pi}} e^{-\frac{(\ln_x - \mu)^2}{2\sigma^2}} + \frac{Z}{b - a}$$

Range =  $(a, b)$

Mean (discussed below)

Variance (discussed below)

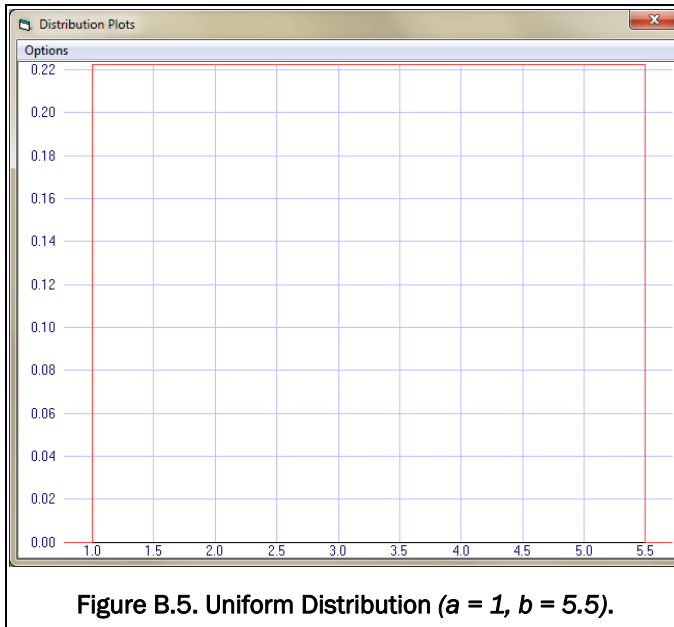
where  $a$  is the start of the bounded region and  $b$  is the end of the bounded region.  $Z$  is the area of the curve outside of the bounded region (not shown).

The mean and variance can no longer be calculated with a simple equation, but must be solved numerically. The CDF for the curve is calculated by a finite differences method. The mean is given by  $E(x) = \sum_{i=1}^n x_i f(x_i)$ .



The variance is given by  $Var(x) = \sum_{i=1}^n f(x_i)(x_i - \mu)^2$ . For CPGA-R the curve is broken into 100 discrete steps, and  $f(x_i)$  is given at the center of the interval.

### B.2.5 Uniform Distribution



$$f(x) = \frac{1}{b-a}$$

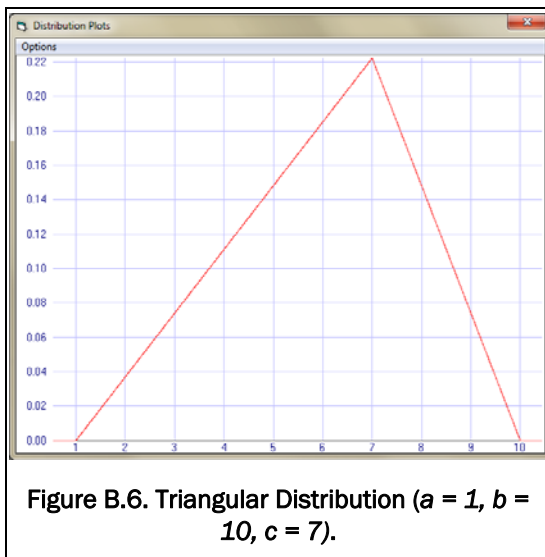
$$\text{Range} = (a, b)$$

$$\text{Mean} = \frac{a+b}{2}$$

$$\text{Variance} = \frac{(b-a)^2}{12}$$

where  $a$  is the start of the region and  $b$  is the end of the region.

### B.2.6 Triangular Distribution



$$f(x) = \begin{cases} \frac{2(x-a)}{(b-a)(c-a)} & \text{if } a \leq x \leq c \\ \frac{2(b-x)}{(b-a)(b-c)} & \text{if } c < x \leq b \end{cases}$$

$$\text{Range} = (a, b)$$

$$\text{Mean} = \frac{a+b+c}{3}$$

$$\text{Variance} = \frac{a^2+b^2+c^2-ab-ac-bc}{18}$$

where  $a$  is the start of the triangular region and  $b$  is the end of the triangular region. The peak point of the triangle is given by  $c$ , where  $a \leq c \leq b$ . Right triangular regions can be created by setting  $c$  to the same value as  $a$  or  $b$ .

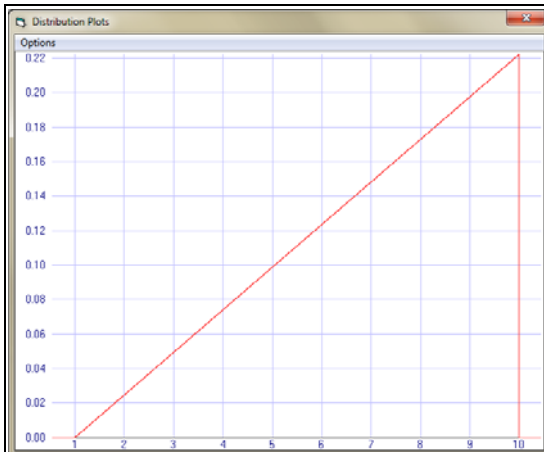


Figure B.7. Right Triangular Distribution ( $a = 1$ ,  
 $b = 10$ ,  $c = 10$ ).

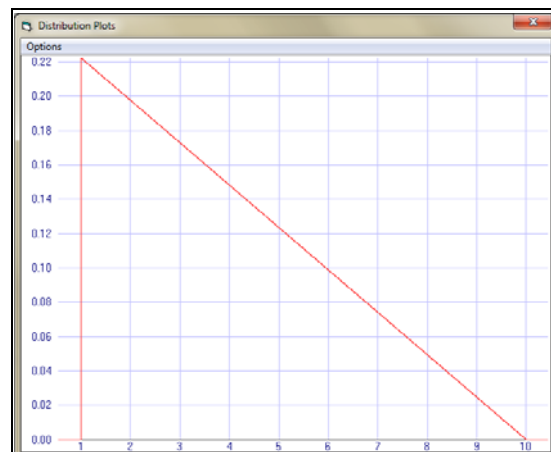


Figure B.8. Right Triangular Distribution ( $a = 1$ ,  
 $b = 10$ ,  $c = 1$ ).

## Appendix C: .PGR File Format

### C.1 Introduction

To store the reliability information that is keyed into CPGA-R, a file format has been added to the original CPGA. This new and complementary format stores the information necessary to perform a reliability analysis for a CPGA file. While this file is created as a sister file for a specific CPGA input file, each file is separate.

The .PGR file format:

Card 1 – Header:

“CPGA-R”

This card is the reliability file header. If the file does not feature this header, it is not correct and, therefore, will not be read as a reliability file.

Card 2 – CPGA path:

“<path>”

This card contains the fully defined path for the sister CPGA file with which the reliability file is associated. Opening the .PGR file in CPGA-R will load the sister file at the same time. Because fully defined paths can have spaces in their names, the file path should be in quotation marks.

Card 2 – Number of variables:

NUMVARS

This card contains only the single integer value giving the number of variables that are going to be defined below.

Card 3 – Variable data (repeated NUMVARS times):

DATATYPE

DATAID

DATACONSTITUENTID

DISTDATA1

DISTDATA2

DISTDATA3

DISTDATA4

DISTTYPE

This card is repeated for as many variables specified in Card 2.

DATATYPE is a string variable that describes the table of data in CPGA that contains the variable. This variable is one of:

- Pile;
- PROP;
- SOIL;
- BIJ;
- TENSION;
- ALLOW;
- DLS;
- ASCPCP;
- UNSUP;
- PMAXMOM;
- FUNSMOM;
- LOAD.

These correspond exactly according to the cards found in a CPGA file.

DATAID is either an integer pile number or the title of a row in the data table specified by data type.

DATACONSTITUENTID is the name of the specific element of the CPGA table that is being referenced. For instance, if LOAD is the DATATYPE, then *px* is the constituent force in the *x* direction for the specified load.

These different constituent elements are the different parts of the data tables stored in the CPGA data file:

DISTDATA1

DISTDATA2

DISTDATA3

DISTDATA4

DISTTYPE

The distribution type determines the data stored for each of the four DISTDATA floating point values. The DISTTYPE variable is a string variable with one of the following:

- Normal;
- Bounded Normal;
- Log-Normal;
- Bounded Log-Normal;
- Uniform;
- Triangle.

The distribution data for Normal is:

- DISTDATA1 = mean value;
- DISTDATA2 = standard deviation.

The distribution data for Bounded Normal is:

- DISTDATA1 = mean value;
- DISTDATA2 = standard deviation;
- DISTDATA3 = lower-bound  $x$  value;
- DISTDATA4 = upper-bound  $x$  value.

The distribution data for Log-Normal is:

- DISTDATA1 = mean value;
- DISTDATA2 = standard deviation.

The distribution data for Bounded Log-Normal is:

- DISTDATA1 = mean value;
- DISTDATA2 = standard deviation;
- DISTDATA3 = lower-bound  $x$  value;
- DISTDATA4 = upper-bound  $x$  value.

The distribution data for Uniform is:

- DISTDATA1 = lower-bound  $x$  value;
- DISTDATA2 = upper-bound  $x$  value.

The distribution data for Triangle is:

- DISTDATA1 = lower-bound  $x$  value;
- DISTDATA2 = peak  $x$  value;
- DISTDATA3 = upper-bound  $x$  value.

Card 4 – Number of correlations:

NUMCORRS

This card contains only the single integer value giving the number of correlations that are going to be defined below.

Card 5 – Correlation data (repeated NUMCORRS times):

VARID1

VARID2

CORRELATIONCOEFFICIENT

This card, which is repeated, contains two integer variables (VARID1 and VARID2) that are indexes of the list of variables defined with Cards 2 and 3 above. These values should be different, and the pair should not be repeated. These two variables will be correlated to a certain degree, defined by the floating point value CORRELATIONCOEFFICIENT, which must fall between 0 and 1.

Card 6 – Pile cap limits:

DISPLACEMENTX

DISPLACEMENTY

DISPLACEMENTZ

ROTATIONX

ROTATIONY

ROTATIONZ

This card gives the displacement limits for the pile cap in a CPGA analysis. If the pile cap is shifted higher than these limits, then the structure is assumed to have failed in some fashion. These variables are floating point value or “\*” if that limit does not matter.

# REPORT DOCUMENTATION PAGE

*Form Approved*  
*OMB No. 0704-0188*

Public reporting burden for this collection of information is estimated to average 1 hour per response, including the time for reviewing instructions, searching existing data sources, gathering and maintaining the data needed, and completing and reviewing this collection of information. Send comments regarding this burden estimate or any other aspect of this collection of information, including suggestions for reducing this burden to Department of Defense, Washington Headquarters Services, Directorate for Information Operations and Reports (0704-0188), 1215 Jefferson Davis Highway, Suite 1204, Arlington, VA 22202-4302. Respondents should be aware that notwithstanding any other provision of law, no person shall be subject to any penalty for failing to comply with a collection of information if it does not display a currently valid OMB control number. **PLEASE DO NOT RETURN YOUR FORM TO THE ABOVE ADDRESS.**

<b>1. REPORT DATE (DD-MM-YYYY)</b> September 2013		<b>2. REPORT TYPE</b> Final		<b>3. DATES COVERED (From - To)</b>	
<b>4. TITLE AND SUBTITLE</b>  Simulation and Advanced Second Moment Reliability Analyses of Pile Groups Using CPGA-R: Formulation, User's Guide, and Example Problems				<b>5a. CONTRACT NUMBER</b>	
				<b>5b. GRANT NUMBER</b>	
				<b>5c. PROGRAM ELEMENT NUMBER</b>	
<b>6. AUTHOR(S)</b>  Robert M. Ebeling, Barry C. White, and Moira T. Fong				<b>5d. PROJECT NUMBER</b>	
				<b>5e. TASK NUMBER</b>	
				<b>5f. WORK UNIT NUMBER</b>	
<b>7. PERFORMING ORGANIZATION NAME(S) AND ADDRESS(ES)</b>  Information Technology Laboratory US Army Engineer Research and Development Center 3909 Halls Ferry Road Vicksburg, MS 39180-6199				<b>8. PERFORMING ORGANIZATION REPORT NUMBER</b>  ERDC/ITL TR-13-2	
<b>9. SPONSORING / MONITORING AGENCY NAME(S) AND ADDRESS(ES)</b>  Headquarters, US Army Corps of Engineers Washington, DC 20314-1000				<b>10. SPONSOR/MONITOR'S ACRONYM(S)</b>  HQUSACE	
				<b>11. SPONSOR/MONITOR'S REPORT NUMBER(S)</b>	
<b>12. DISTRIBUTION / AVAILABILITY STATEMENT</b> Approved for public release; distribution is unlimited.					
<b>13. SUPPLEMENTARY NOTES</b>					
<b>14. ABSTRACT</b> More than 50% of the US Army Corps of Engineers' locks and their approach walls have continued past their economic lifetimes. As these structures wear out, they must be retrofitted, replaced, or upgraded with a lock extension. Innovative designs must be considered for Corps hydraulic structures, particularly flexible approach walls, and new tools for evaluating these designs must be developed. The Computer-Aided Structural Engineering (CASE) computer program CPGA performs basic pile group analyses using Saul's method. It is intended to be a simple program to aid in the rapid pile group analysis/design of the Corps hydraulic structures that are founded on groups of piles. The analysis uses the stiffness method, with the pile cap assumed to be rigid and the piles assumed to be linearly elastic. Soil resistance to pile movement may be included.  Probabilistic data generated during a reliability analysis of Corps hydraulic structures is formally used in risk and reliability engineering for major rehabilitation studies. Reliability studies deal with the demand on a system and the capacity of the system to respond to that demand. Both the demand and capacity can contain uncertainty, so the interaction of demand and capacity also will be uncertain. A reliability index can be determined for the uncertain interaction, and the probability of unsatisfactory performance can be determined from the reliability index.  This report deals with the extension of CPGA to include the generation of probabilistic data and application of risk-based methods to the analysis of the Corps pile group-founded hydraulic structures. The software is named CPGA-R, with the R referring to the new reliability analysis capability. CPGA-R uses both Advanced Second Moment (ASM) and Importance Sampling Simulation reliability analyses techniques.					
<b>15. SUBJECT TERMS</b> Pile groups CPGA		CPGA-R Reliability Advanced Second Moment (ASM)		Barge train impact Flexible lock approach wall Risk	
<b>16. SECURITY CLASSIFICATION OF:</b>			<b>17. LIMITATION OF ABSTRACT</b>	<b>18. NUMBER OF PAGES</b>  134	<b>19a. NAME OF RESPONSIBLE PERSON</b>
<b>a. REPORT</b>  Unclassified	<b>b. ABSTRACT</b>  Unclassified	<b>c. THIS PAGE</b>  Unclassified			<b>19b. TELEPHONE NUMBER (include area code)</b>